

SSC-425

**FATIGUE STRENGTH AND
ADEQUACY OF WELD REPAIRS**



This document has been approved
For public release and sale; its
Distribution is unlimited

SHIP STRUCTURE COMMITTEE
2003

SHIP STRUCTURE COMMITTEE

RADM Thomas H. Gilmour
U. S. Coast Guard Assistant Commandant,
Marine Safety and Environmental Protection
Chairman, Ship Structure Committee

Mr. W. Thomas Packard
Director,
Survivability and Structural Integrity Group
Naval Sea Systems Command

Mr. Joseph Byrne
Director, Office of Ship Construction
Maritime Administration

Mr. Thomas Connors
Director of Engineering
Military Sealift Command

CONTRACTING OFFICER TECHNICAL REP.
Lieutenant Eric M. Cooper / Ms. Dinah Mulligan
U.S. Coast Guard R & D Center

Dr. Donald Liu
Senior Vice President
American Bureau of Shipping

Mr. Gerard A. McDonald
Director General, Marine Safety,
Safety & Security
Transport Canada

Dr. Neil Pegg
Group Leader - Structural Mechanics
Defence Research & Development Canada - Atlantic

EXECUTIVE DIRECTOR
Lieutenant Eric M. Cooper
U. S. Coast Guard

SHIP STRUCTURE SUB-COMMITTEE

AMERICAN BUREAU OF SHIPPING

Mr. Glenn Ashe
Mr. Yung Shin
Mr. Phil Rynn
Mr. William Hanzalek

MARITIME ADMINISTRATION

Mr. Chao Lin
Mr. Carlos Setterstrom
Mr. Richard Sonnenschein

NAVAL SEA SYSTEMS COMMAND

Mr. Jeffery E. Beach
Mr. Edward E. Kadala
Mr. Allen H. Engle
Mr. Charles L. Null

UNITED STATES COAST GUARD

Mr. Rubin Sheinberg
Mr. Robert Sedat
Commander Ray Petow

DEFENCE RESEARCH & DEVELOPMENT ATLANTIC

Dr David Stredulinsky
Mr. John Porter

MILITARY SEALIFT COMMAND

Mr. Joseph Bohr
Mr. Rick A. Anderson
Mr. Michael W. Touma

TRANSPORT CANADA

Mr. Jacek Dubiel

CANADIAN COAST GUARD

Mr. Daniel Gauvin

Member Agencies:

*American Bureau of Shipping
Defence Research Establishment Atlantic
Maritime Administration
Military Sealift Command
Naval Sea Systems Command
Society of Naval Architects & Marine Engineers
Transport Canada
United States Coast Guard*



**Ship
Structure
Committee**

Address Correspondence to:

Executive Director
Ship Structure Committee
U.S. Coast Guard (G-MSE/SSC)
2100 Second Street, SW
Washington, D.C. 20593-0001
Ph: (202) 267-0003
Email: ecooper@comdt.uscg.mil

**SSC – 425
SR – 1398**

August 2003

FATIGUE STRENGTH AND ADEQUACY OF WELD REPAIRS

Fatigue cracks can be an expensive nuisance in commercial ships such as tankers and bulk-carriers, requiring weld repairs that often crack again within a short period of time. Experimental research was conducted to develop procedures for effective and reliable repairs appropriate for fatigue-prone details in commercial ships, and to develop simple and reliable methods to estimate the residual fatigue life of these repairs.

The tests were conducted on large-scale structural components, including:

- a) girder featuring unloaded attachments (five specimens)
- b) tee joint with load bearing attachments (two specimens)
- c) simplified model of longitudinal/transverse web frame connection (five specimens)
- d) complex model of longitudinal/transverse web frame connection (two specimens)

Fatigue cracks were repaired with various techniques shown to be effective including arc-gouging and welding (vee-and-weld), adding doubler plates, hole drilling, and hammer peening- either alone or in some combination. Fatigue tests were conducted at constant-amplitude stress ranges of realistically low magnitude resulting in lives on the order of a million cycles. Guidelines and examples are presented for the evaluation of the most suitable repair technique for various types of cracks and for the design and execution of these repairs.

The fatigue life (N), usually referred to as the residual life of the repair, was found to be independent of the fatigue load cycles applied to the detail prior to repair, (i.e. the clock on the residual life is essentially reset to zero by the repair). The residual life calculations presented in this report may be used to determine whether a repair may be considered permanent or whether it will eventually be necessary to cut out and completely restore a whole panel. The data should lead to safer, more reliable, and ultimately less expensive repairs for ships and other welded structures.

A handwritten signature in black ink, appearing to read 'T. H. Gilmour'.

T. H. GILMOUR
Rear Admiral, U.S. Coast Guard
Chairman, Ship Structure Committee

Technical Report Documentation Page

1. Report No. SSC - 425		2. Government Accession Number		3. Recipient's Catalog No.	
4. Title and Subtitle FATIGUE STRENGTH AND ADEQUACY OF WELD REPAIRS SR-1398				5. Report Date 29 May 2003	
				6. Performing Organization Code	
7. Author(s) Robert J. Dexter, Robert J. FitzPatrick, and David L. St. Peter				8. Performing Organization Report No. SR-1398	
9. Performing Organization Name and Address University of Minnesota Department of Civil Engineering 122 CivE, 500 Pillsbury Dr. S.E. Minneapolis, MN 55455-0116			10. Work Unit No. (TRAI5)		
			11. Contract or Grant No. DTMA1C99207		
12. Sponsoring Organization Name and Address Ship Structure Committee U. S. Coast Guard (G-MSE/SSC) 2100 Second Street, SW Washington, D.C. 20593-0001				13. Type of Report & Period Covered Final Report	
				14. Sponsoring Agency Code G-M	
15. Supplementary Notes Sponsored by the Ship Structure Committee. Jointly funded by its member agencies.					
16. Abstract (MAXIMUM 200 WORDS) Fatigue tests were performed on large-scale models of ship structural components. Cracks that formed in these test specimens were repaired using various techniques and the residual fatigue lives of these repairs were then determined by continuing the tests. The repair weld details are associated with lower-bound S-N curves for simple and reliable calculation of the residual life. Guidelines are presented for the evaluation of the most suitable repair technique for various types of cracks and for the design and execution of the most effective repair techniques. This research should facilitate rational and efficient design of more reliable weld repairs as well as scheduling for critical inspections.					
17. Key Words Ship, repair, fatigue, crack, weld			18. Distribution Statement Distribution unlimited, available from: National Technical Information Service Springfield, VA 22161 (703) 487-4650		
19. Security Class (This Report) UNCLASSIFIED		20. Security Class (This Page) UNCLASSIFIED		21. No of Pages	22. Price

Form DOT F 1700.7 (8/72) Reproduction of form and completed page is authorized.

CONVERSION FACTORS
(Approximate conversion of common U.S. Customary units
used for ship structures to metric or SI units)

To convert from	To	Function	Value
LENGTH			
inches	Meters	divide by	39.3701
inches	Millimeters	multiply by	25.4000
feet	Meters	divide by	3.2808
VOLUME			
cubic feet	cubic meters	divide by	35.3149
cubic inches	cubic meters	divide by	61,024
SECTION MODULUS			
inches ² feet	centimeters ² meters	multiply by	1.9665
inches ² feet	centimeters ³	multiply by	196.6448
inches ³	centimeters ³	multiply by	16.3871
MOMENT OF INERTIA			
inches ² feet ²	centimeters ² meters ²	divide by	1.6684
inches ² feet ²	centimeters ⁴	multiply by	5993.73
inches ⁴	centimeters ⁴	multiply by	41.623
FORCE OR MASS			
long tons	Tonnes	multiply by	1.0160
long tons	Kilograms	multiply by	1016.047
pounds	Tonnes	divide by	2204.62
pounds	Kilograms	divide by	2.2046
pounds	Newtons	multiply by	4.4482
PRESSURE OR STRESS			
pounds/inch ²	Newtons/meter ² (Pascals)	multiply by	6894.757
kilo pounds/inch ²	mega Newtons/meter ² (mega Pascals)	multiply by	6.8947
pounds/inch ²	kg/cm ²	divide by	14.2232
kg/cm ²	mega Pascals	multiply by	0.098065
BENDING OR TORQUE			
foot tons	meter tons	divide by	3.2291
foot pounds	kilogram meters	divide by	7.23285
foot pounds	Newton meters	multiply by	1.35582
ENERGY			
foot pounds	Joules	multiply by	1.355826
STRESS INTENSITY			
kilo pounds/inch ² inch ^{1/2} (ksi ^{1/2} /in)	mega Newton MNm ^{3/2}	multiply by	1.0998
J-INTEGRAL			
kilo pound/inch	Joules/mm ²	multiply by	0.1753
kilo pound/inch	kilo Joules/m ²	multiply by	175.3
TEMPERATURE			
Degrees Fahrenheit	Degrees Celsius	subtract & divide by	32 1.8

ACKNOWLEDGMENT

This research was performed in the Department of Civil Engineering at the University of Minnesota. The authors are deeply indebted to Paul Bergson, manager of the Structural Engineering Laboratory, Tim Miller, undergraduate research assistant and welder, and many others for their assistance with the experiments. As a subcontractor, Gibbs & Cox provided specific expertise in ship structure design and maintenance and determined the geometry and loading conditions of the test specimens. Dr. Robert Sielski, formerly of Gibbs & Cox, and Chris Potter performed most of this work. The Ship Structure Committee sponsored the project and the authors appreciate the patience and guidance of the Project Technical Committee, particularly Rickard Anderson of the Military Sealift Command.

TABLE OF CONTENTS

LIST OF TABLES.....	vii
LIST OF FIGURES	viii
EXECUTIVE SUMMARY	xiii
1.0 INTRODUCTION	1
2.0 BACKGROUND	5
2.1 Fatigue Design and Assessment Procedures.....	5
2.1.1 Nominal Stress Range Approach.....	6
2.1.2 Hot-Spot Stress Range Approach	8
2.1.3 Variable Amplitude Loading	10
2.2 Repair Techniques	12
2.2.1 Surface Crack Repairs.....	13
2.2.2 Through-Thickness Crack Repairs	16
2.3 Fatigue-Sensitive Details in Ships	19
3.0 EXPERIMENTAL PROCEDURES AND RESULTS.....	27
3.1 Simplified Model of Attachment	27
3.1.1 Test Setup.....	28
3.1.2 Static Calibration	28
3.1.3 Fatigue Test Procedure	28
3.1.4 Repair Techniques	29
3.1.5 Results.....	31

3.2	Complex Model of Bracket Attachment.....	34
3.2.1	Test Setup.....	34
3.2.2	Static Calibration	35
3.2.3	Fatigue Test Procedure	35
3.2.4	Repair Techniques	36
3.2.5	Results.....	38
3.3	Simplified Model of Longitudinal/Transverse Web Frame Connection	39
3.3.1	Test Setup.....	39
3.3.2	Static Test and Finite Element Model.....	40
3.3.3	Fatigue Test Procedure	42
3.3.4	Results.....	43
	3.3.4.1 Stop Hole Repairs	43
	3.3.4.2 Weld Repairs and Hammer Peening.....	45
3.4	Complex Model of Longitudinal/Transverse Web Frame Connection.....	48
3.4.1	Test Setup.....	48
3.4.2	Static Test and Finite Element Model.....	49
3.4.3	Fatigue Test Procedure	50
3.4.4	Results.....	50
4.0	SUMMARY.....	129
4.1	Attachments and Bracket Details.....	129
4.2	Longitudinal/Web-Frame Connection	131
5.0	CONCLUSIONS.....	133
6.0	RECOMMENDATIONS.....	135

APPENDIX A—Draft ASTM Standard Procedure for Repairing Fatigue Cracks in Ships A-1

APPENDIX B—Design Examples for Fatigue Crack Repairs.....B-1

REFERENCESC-1

LIST OF TABLES

Table 2.1	AASHTO/Eurocode 3/BS 7608 cross-reference for S-N curves.....	21
Table 3.1	Simple attachment specimen stress comparison.....	54
Table 3.2	Repair information table for simple attachment specimen 1	55
Table 3.3	Repair information table for simple attachment specimen 2	56
Table 3.4	Repair information table for simple attachment specimen 3	57
Table 3.5	Repair information table for simple attachment specimen 4	58
Table 3.6	Repair information table for simple attachment specimen 5	59
Table 3.7	Repair information table for complex attachment specimens.....	60
Table 3.8	Typical chemistry composition for steel used in web frame specimens.....	61
Table 3.9	Typical strain gage results for simplified web frame specimens.....	61
Table 3.10	Summary of cracks and repairs on simplified web frame specimen 1	62
Table 3.11	Summary of cracks and repairs on simplified web frame specimen 2	63
Table 3.12	Summary of cracks and repairs on simplified web frame specimen 3	64
Table 3.13	Summary of cracks and repairs on simplified web frame specimen 4	65
Table 3.14	Summary of cracks and repairs on simplified web frame specimen 5	66
Table 3.15	Measured stress ranges in complex web frame specimens.....	67
Table 3.16	Summary of cracks and repairs on full scale web frame specimen 1	68
Table 3.17	Summary of cracks and repairs on full scale web frame specimen 2	68

LIST OF FIGURES

Figure 2.1	Nominal stress S-N curves used in AASHTO, AISC, AWS, and AREMA specifications.....	22
Figure 2.2	BS 7608 nominal S-N curves.....	23
Figure 2.3	Stress regions approaching a welded joint.....	24
Figure 2.4	Fatigue-sensitive details found in ship structures	24
Figure 2.5	Bracket connection of girder to bulkhead detail	25
Figure 2.6	Longitudinal/transverse web frame connection	26
Figure 2.7	Longitudinal passing through a transverse web frame in a tanker ship.....	26
Figure 3.1	Drawing of simplified attachment model	69
Figure 3.2	Simple attachment specimen before testing.....	70
Figure 3.3	Simple attachment specimen in test setup	70
Figure 3.4	Simple attachment specimen test setup.....	71
Figure 3.5	Clamped roller connection.....	72
Figure 3.6	Strain gage layout	72
Figure 3.7	Stress distribution through the depth of the beam with actuator in tension.....	73
Figure 3.8	Typical cracks in simple attachment specimens (enhanced by dye penetrant) at the point defined as “failure”	74
Figure 3.9	Preemptive hammer peening the weld toe.....	74
Figure 3.10	Access hole for backside repairs.....	75
Figure 3.11	Single sided weld repair with backing bar.....	75
Figure 3.12	Single sided weld repair with backing bar removed.....	76
Figure 3.13	The web side of a two-sided weld repair	77
Figure 3.14	The attachment side of a two-sided weld repair with hammer peening	77
Figure 3.15	S-N curve for original detail and preemptive hammer peening.....	78
Figure 3.16	S-N curve for simple attachment specimen repairs	79
Figure 3.17	Simple attachment specimen doubler plate repair	80
Figure 3.18	Area of specimen with inadequate access to attachment for weld repairs.....	81
Figure 3.19	Mean life of the logarithmic life of different repair types and original detail at 100 MPa stress range	82

Figure 3.20	Complex bracket attachment specimen	83
Figure 3.21	A complex attachment specimen	84
Figure 3.22	Complex attachment brackets	85
Figure 3.23	Complex attachment test setup	86
Figure 3.24	Drawing of test setup	87
Figure 3.25	Clamped roller support connection	88
Figure 3.26	Drawing of strain gage layout	89
Figure 3.27	Strain gradient along the vertical stem of the tee	90
Figure 3.28	Linear strain distribution through the depth of the horizontal girder	91
Figure 3.29	A typical crack at the top of the bracket in the complex attachment specimen	92
Figure 3.30	Weld repair of crack not yet through-thickness without termination holes	92
Figure 3.31	Weld repair of typical through-thickness crack with termination holes drilled to larger diameter after the weld is complete	93
Figure 3.32	Weld repair with ground termination holes	93
Figure 3.33	Weld ground after repair	94
Figure 3.34	Weld that has been hammer peened after repair	94
Figure 3.35	Doubler plates welded to reinforce detail	95
Figure 3.36	S-N curve for complex attachment specimen	96
Figure 3.37	Repairs mean value of logarithmic life	97
Figure 3.38	Simplified longitudinal/web frame connection specimen drawing	98
Figure 3.39	Simplified longitudinal/web frame connection specimen drawing (side view)	98
Figure 3.40	Typical connection detail	99
Figure 3.41	Simplified web frame specimen test setup	99
Figure 3.42	Photo of simplified web frame specimen in test fixture	100
Figure 3.43	Strain gage layout for simplified web frame specimens	101
Figure 3.44	Stress gradient approaching cutout radius at detail D	101
Figure 3.45	Finite element model of simplified web frame specimen	102
Figure 3.46	Finite element results for simplified web frame specimen	103
Figure 3.47	Typical saw cut and tack weld used to initiate cracks at cutouts	104
Figure 3.48	Typical crack in web frame growing out of a cutout	104
Figure 3.49	Typical stop hole repair in web frame	105

Figure 3.50	S-N curve showing the fatigue data for different sized stop hole repairs.....	105
Figure 3.51	Repair of a crack in the web frame using a 24 mm stop hole and fully tensioned high-strength bolt.....	106
Figure 3.52	Stop hole performance for 25 mm cracks in 345 MPa steel.....	106
Figure 3.53	Performance of stop hole repairs relative to equation	107
Figure 3.54	Crack forming in lug after stop hole repair.....	107
Figure 3.55	Repair failures at other radius at cutout C	108
Figure 3.56	130 mm long crack after failure of 76 mm stop hole.....	108
Figure 3.57	130 mm long crack after weld repairing.....	109
Figure 3.58	130 mm long crack repaired using bolted doubler plates after weld repairing....	109
Figure 3.59	Weld repair in cracked lug plate (original crack shown in Fig. 3.54)	110
Figure 3.60	S-N curve showing performance of weld repairs	110
Figure 3.61	Crack forming in web frame-longitudinal connection.....	111
Figure 3.62	Drawing of section through web frame at connection to longitudinal.....	111
Figure 3.63	Weld repair at web frame-longitudinal connection	112
Figure 3.64	Crack forming in bottom hull at cutout.....	112
Figure 3.65	S-N curve showing life of original and repaired bottom hull detail at cutout	113
Figure 3.66	S-N curve comparing repairs made to different types of steel.....	114
Figure 3.67	Full scale longitudinal/web frame connection specimen drawing (front view)...	115
Figure 3.68	Full scale longitudinal/web frame connection specimen drawing (side view)....	115
Figure 3.69	Full scale web frame specimen test setup (front view).....	116
Figure 3.70	Full scale web frame specimen test setup (side view)	116
Figure 3.71	Photo of full scale web frame specimen in test fixture.....	117
Figure 3.72	Strain gage layout for full scale web frame specimens.....	118
Figure 3.73	Finite element model of full scale web frame specimen.....	118
Figure 3.74	Finite element results for full scale web frame specimen showing hot-spot at longitudinal-web frame weld	119
Figure 3.75	S-N curve showing life of original and repaired complex specimen 1	120
Figure 3.76	S-N curve showing life of original and repaired complex specimen 2.....	121
Figure 3.77	Typical crack in web frame at edge of longitudinal	121
Figure 3.78	76 mm stop hole in web frame (specimen 1).....	122

Figure 3.79	Stop hole repairs in specimen 2	122
Figure 3.80	Crack along back of longitudinal at connection to web frame (specimen 1).....	123
Figure 3.81	Vee-and-weld repair along back of longitudinal (specimen 1).....	123
Figure 3.82	Bracket added to stiffen connection (specimen 1).....	124
Figure 3.83	Crack propagating from stop hole into flat bar stiffener (specimen 1).....	124
Figure 3.84	First weld repair of cracked flat bar stiffener (specimen 1).....	125
Figure 3.85	Complete failure of flat bar stiffener (specimen 1).....	125
Figure 3.86	Failure of added bracket (specimen 1).....	126
Figure 3.87	Ineffective 14 mm stop holes in flat bar stiffener (specimen 2)	126
Figure 3.88	Doubler welded to flat bar stiffener (specimen 2)	127
Figure 3.89	Additional bracket (specimen 2).....	127

EXECUTIVE SUMMARY

Fatigue cracks can be an expensive nuisance in commercial ships such as tankers and bulk-carriers, requiring weld repairs that often crack again within a short period of time. Experimental research was conducted at the University of Minnesota to develop procedures for effective and reliable repairs appropriate for fatigue-prone details in commercial ships, and to develop simple and reliable methods to estimate the residual fatigue life of these repairs. Gibbs & Cox, as a subcontractor, provided specific expertise in ship structure design and maintenance and determined the geometry and loading conditions of the test specimens

Four types of fatigue tests were conducted on large-scale structural components, including:

- a) girder featuring unloaded attachments (five specimens)
- b) tee joint with load bearing attachments (two specimens)
- c) simplified model of longitudinal/transverse web frame connection (five specimens)
- d) complex model of longitudinal/transverse web frame connection (two specimens)

Tests were conducted at constant-amplitude stress ranges of realistically low magnitude resulting in lives on the order of a million cycles. The fatigue life (N) is defined as the number of cycles until the development of a through-thickness crack greater than 50 mm in length. Stress ranges (S) were determined using hand calculations and finite-element models of the specimens in combination with strain measurements made on the specimens. The fatigue lives were plotted in the S-N curve (log-log) format (where S is the stress range). The first two types of specimens were suitable for use of the nominal stress range for the fatigue S-N curves, whereas in the models of longitudinal/transverse web frame connection the hot-spot stress range was used. Note that there is typically an order of magnitude of variability of the fatigue lives in experiments at a particular stress range. Standard S-N curves from design specifications represent the lower bound to the expected fatigue lives, with 97.5 percent survivability. Similarly, the lower bounds to these experimental data were typically associated with one of the standard S-N curves or “fatigue categories”.

Fatigue cracks were repaired with various techniques shown to be effective including arc-gouging and welding (vee-and-weld), adding doubler plates, hole drilling, and hammer peening – either alone or in some combination. Guidelines and examples are presented for the evaluation of the most suitable repair technique for various types of cracks and for the design and execution of

these repairs. Repairs were made as needed and the testing continued with the same loading. Often multiple repairs were made at the same location.

In the case of the repairs, the fatigue life (N), usually referred to as the residual life of the repair, is defined as the number of cycles from the time the repair is made until the development of a through-thickness fatigue greater than 50 mm in length. The residual life of the repaired details was found to be independent of the fatigue load cycles applied to the detail prior to repair, i.e. the clock on the life is essentially reset to zero by the repair.

The calculations to estimate the residual life of various repair details use lower-bound S-N curves, similar to the design S-N curves for original (unrepaired) details. The future stress ranges must be estimated and converted to an equivalent constant-amplitude stress range in order to estimate the life of the detail. However, if:

- 1) the life of the original detail before cracking is known; and,

- 2) the loading can be assumed to be approximately the same after repair as before repair;

then the ratio of the life of the repaired detail to the life of the original detail (obtained from these experiments) can be readily used to estimate the residual life of the repaired detail. Note that in this case it is not necessary to estimate the future loading history, which greatly simplifies the analysis of the residual life of repairs.

The occurrence of the first fatigue crack at a particular detail in a ship may be an outlier, e.g. it may be from severe misalignment or weld defects unique to that one location. If the crack that occurs is not explained by unique circumstances, however, then it is an indicator that other details with similar stress ranges will also begin to develop cracks. Because of the inherent factor of ten variability in fatigue lives, these cracks will begin to manifest immediately, but may also take about ten times the life up to that point until they all crack. Thus the urgency in need to repair or retrofit other details that are yet uncracked must be judged, considering this variability. Similarly, the estimates of the residual life of these repairs is also a lower bound, and results up to ten times better can be expected.

The residual life calculations presented in this report may be used to determine whether a repair may be considered permanent or whether it will eventually be necessary to cut out and completely restore a whole panel. The data should lead to safer, more reliable, and ultimately less expensive repairs for ships and other welded structures.

1 INTRODUCTION

Fatigue is the formation of a crack due to cyclic elastic loading well within the design stress levels. Most dynamically loaded welded structures are explicitly designed for fatigue by checking the stress range at critical details under some fatigue design loading [1]. The stress range at the critical details is checked by comparison to an S-N curve that relates the life (N) to the stress range (S). Different S-N curves may be used depending on applicable codes or specifications.

Until recently, most ships were not explicitly designed for fatigue. Instead, the allowable peak stress was controlled in an attempt to indirectly avoid extensive fatigue cracking [8,9]. Consequently, many ships, particularly commercial bulk carriers and tanker ships, exhibit extensive fatigue cracking [10,11,12]. Among the details which exhibit cracking on ships are: 1) brackets at the intersections of girders with web frames or bulkheads; 2) the intersection of longitudinal stiffeners with transverse web frames or bulkheads; 3) hatch openings; 4) butt welds in hull plates, stiffeners, or girders; and 5) drain holes and weld-access holes in stiffeners and girders.

Because of the highly redundant nature of ship structure, these fatigue cracks are typically not a threat to structural integrity [8,13,14,15,16]. Therefore, the detection and repair of occasional fatigue cracks may be tolerated as a part of routine maintenance. Repairs are often made by arc-gouging a vee-shaped weld preparation along the length of the crack and welding. Other methods such as modifying the detail by adding soft toes, brackets, insert plates or doubler plates may also be used.

Unfortunately, fatigue cracks are frequently repaired without sufficient consideration of the performance subsequent to the repair. Poorly designed or executed repairs can lead to quick reinitiation of fatigue cracks at the location of the repair. In some cases individual ships have been reported to have thousands of cracks [10]. In these cases, the repair costs may be staggering. Therefore, there is a need for a method to assess the performance, primarily the remaining fatigue strength, of repair methods.

Ship Structure Committee project SR-1376 [37] was an initial effort to address this need. This study looked at full scale welded built-up I beams with a variety of butt welds in the flanges and weld-access holes in the webs. The tests establish the original fatigue strength of these details and the remaining fatigue strength after the cracked specimens are repaired several times in various

ways. The data showed that the repaired butt welds had a residual life that was equal to the life of original butt welds, i.e. that the repairs had essentially reset the clock on the fatigue life of the butt joint and that the life of the repaired joint was independent of the fatigue load cycles on the joint prior to repair. The S-N curves resulting from these tests provided a basis for calculations of the remaining fatigue life of butt joints after repair.

The research described in this report is follow-on to the research from SR-1376. Two of the other types of ship details that have exhibited cracking problems are investigated in the present research, including:

- 1) brackets and attachments at the intersections of orthogonal structure, such as girders intersecting with web frames or bulkheads; and;
- 2) the intersection of longitudinal stiffeners with transverse web frames or bulkheads.

Fatigue tests were carried out on replicate samples of both simplified and full-scale models of each detail. The specific objective of this research was to determine the fatigue strength of different repair techniques for each detail. These repair techniques included arc-gouging and welding (vee-and-weld), adding doubler plates, hole drilling, and hammer peening – either alone or in some combination.

Results from this project showed that the above repair methods can successfully be used on the type of details that were tested. The data can be used to evaluate the most suitable repair technique for various types of cracks and to determine whether a repair may be considered permanent.

It should be noted that the issue of repair weld quality is not addressed in this report. There is anecdotal evidence that the quality of repair welds in shipyards is not always as good as new construction. Of course, this is dependent on the particular shipyard and classification society. Quality problems with repair welds in service may account for the suspicion of lower fatigue strength for repair welds. The problem of repair weld quality must be solved through adequate quality control measures. Although the issue of repair weld quality is critical, it was not the intent of this research to study weld quality. It is believed that the weld quality issues can be separated from the issue of the inherent fatigue strength of the repair welds.

In this study, in order to get lower-bound quality repairs, previously unskilled welders (graduate research assistants) were minimally trained and then used to perform all repairs. Non-destructive testing was not used to screen out defects. The lower-bound quality repair welds

were not that much worse in fatigue than would be expected for welds produced by experienced welders with stringent non-destructive testing. The effect of weld quality is diminished in the poor details sometimes used in ship construction because the fatigue resistance is primarily determined by the geometrical stress concentration at the detail rather than by weld quality.

The following chapter provides additional background on fatigue and repair welding. Chapter 3 presents the test procedures and includes a discussion of each fatigue test's results. Finally, conclusions and recommendations are provided in Chapter 4. A draft ASTM standard for repairing fatigue cracks in ships is included in Appendix A. Appendix B contains detailed examples of specific repairs to illustrate the guidelines and the method for calculating residual life. Appendix C contains repair data for the test frame used in SSC project SR-1392.

2 BACKGROUND

Many aspects of designing ship structures for fatigue and repairing fatigue cracks are essentially the same as in other types of welded steel structures such as offshore platforms or even bridges. Therefore, this chapter first gives general background on fatigue design procedures. Different fatigue crack repair techniques and research in the literature on testing of repairs are then discussed. Finally, a discussion of typical fatigue-critical structural details in commercial ships is presented.

2.1 Fatigue Design and Assessment Procedures

Welded details in any structure can be analyzed using one of several techniques, including:

- a. Comparing nominal stress ranges obtained using ordinary strength of materials equations to standard S-N curves [1]
- b. Comparing hot-spot stress ranges obtained using finite-element analyses or predetermined stress concentration factors (SCF) to hot-spot S-N curves [17]

The S-N curve, which appears as a straight line on a log-log plot, relates the stress range (S) to the lower-bound life (N) derived from full-scale test data. The life is defined as the number of cycles to develop a through-thickness crack at least 50 mm in length. The lower-bound S-N curves represent the mean regression line minus two standard deviations of the log of N – such that 97.5 percent of the experimental data have lives exceeding the S-N curve. There is often considerable reserve life after the development of a through-thickness crack [18,19], but for design this conservative definition is appropriate.

The large heat input from welding causes expanding material to yield in compression upon heating which results in residual tensile stresses in the joined parts near the weld upon cooling. These tensile residual stresses are typically on the order of yield strength of the steel plating. This effect is built into the S-N curves, which are derived from full-scale test data containing realistic residual stresses [1].

Moreover because of these large residual stresses, any effect from the mean applied stress is negligible. In other words, even if part of the load cycle is in compression, it will not likely be enough to reduce the fatigue crack propagation since the stress at the joint will still be fluctuating in

tension. Therefore, the stress range is the only significant loading variable for fatigue of welded structures [1]. However, once the crack is propagating through base metal away from a weld, the tensile residual stresses will diminish and the effect of mean stress and any compressive residual stress will become important [18,19]. However, in the testing done in this study, full load reversal was used because dynamic loading of ship structures from wave action generally results in nearly complete load reversal.

2.1.1 Nominal-Stress-Range Approach

The modern nominal-stress fatigue-design procedure was developed for steel bridges through research sponsored by the American Association of State Highway and Transportation Officials (AASHTO) [2,20,21]. The nominal-stress approach is the simplest method of designing for fatigue. The procedure is based on designing for the nominal stress ranges, knowing the fatigue strength of structural details in terms of the nominal stress S-N curve. The nominal stress range is calculated using ordinary strength-of-materials equations for bending and axial load and does not include the effects of any stress concentrations such as geometric discontinuities or welds. Different S-N curves are used to evaluate the fatigue resistance of different details depending on the geometry of the detail. Each S-N curve represents a particular detail category, where details with similar fatigue strength are put in the same category. Since the stress range is based on the nominal stress, the effect of the stress concentration is reflected in the detail category empirically.

Each detail category has a constant-amplitude fatigue limit (CAFL). The CAFL is a stress range below which no fatigue cracks are expected to occur in tests conducted with constant-amplitude loading. These limits are shown as the horizontal lines on the right side of the S-N curves (Figure 2.1). If the loading has variable amplitudes, a more complex analysis must be used, which is discussed below.

The fatigue resistance of a given detail category is independent of the type of steel [1,20,21] and the welding process used [22,23]. The full-scale fatigue experiments are typically carried out in moist air and therefore reflect some degree of environmental effect or corrosion fatigue. Some design codes require a factor of two decrease in fatigue life when details are exposed to seawater as opposed to moist air. However, full-scale fatigue experiments in seawater at realistic service stress ranges do not show significantly lower fatigue lives [24], provided that corrosion is

not so severe that it causes pitting or significant section loss. The fatigue lives seem to be more significantly influenced by the stress concentration at the toe of welds and the initial discontinuities. Therefore, the lower-bound S-N curves in Figure 2.1 and the S-N curves generated in this research can be used for the design of details in any natural environmental exposure, even near salt spray. However, pitting or significant section loss from severe corrosion may become a fatigue critical condition and can lower that fatigue strength [25,26].

The fatigue design procedures developed for steel bridges are used throughout North America for a variety of welded structures, including the American Association of State Highway and Transportation Officials (AASHTO) bridge design specifications [2], the American Institute for Steel Construction (AISC) “Manual of Steel Construction” [3], the American Railway Engineering and Maintenance-of-Way Association (AREMA) “Manual for Railway Engineering” [4], and the American Welding Society (AWS) “Structural Welding Code” [5].

Figure 2.1 shows the S-N curves used in these design specifications. Category A represents base metal. Welded joints are considered longitudinal if the axis of the weld is parallel to the primary stress range. Continuous longitudinal welds are Category B details. A special Category B' was added to account for the lower fatigue strength of complete penetration longitudinal welds with permanent backing bars as well as partial penetration longitudinal welds. The termination of longitudinal fillet welds are more severe (Category E).

Category C includes transverse full-penetration groove welds (butt joints) subjected to non-destructive evaluation (NDE). Experiments show that groove welds that are not subject to NDE may contain large internal discontinuities and the fatigue strength is reduced as low as Category E [75]. Transverse groove welds with a permanent backing bar are reduced to Category D [1,6,37]. A weld access hole or drain hole less than 100 mm across with edges conforming to the ANSI smoothness of 1000 may be considered a Category D detail. Poorly executed cope holes must be treated as Category E details.

Attachments normal to flanges or plates are rated Category C if less than 51 mm long in the direction of the primary stress range, D if between 51 and 101 mm long, and E if greater than 101 mm long. Transverse stiffeners are treated as short attachments (Category C). The Category E', slightly worse than Category E, applies if the attachment plates or the flanges exceed 25 mm in thickness.

Eurocode 3 [7] and the British Standard 7608 [6] also use a nominal stress approach but they each have unique sets of S-N curves with different category labels. However, the end result of checking the stress range will be approximately the same regardless of which of these sets of S-N curves is used, since all of these design specifications are empirical and are calibrated with the same database of full-scale test results. Thus none of these sets of S-N curves has any inherent advantages or will estimate the fatigue life of a detail more accurately than any other set of S-N curves. The American Bureau of Shipping (ABS) guidelines [27], the U.K. Health and Safety Executive [28], and other groups in the marine industry use S-N curves from the British Standards (BS 7608) [6]. These S-N curves are shown in Figure 2.2. The BS 7608 S-N curves can be associated approximately with the AASHTO S-N curves so that knowledge of the fatigue strength of details in this specification can be translated to an equivalent AASHTO category. Seven of the 14 Eurocode curves, however, are precisely the same as the seven AASHTO curves. Table 2.1 cross-references the Eurocode 3 and BS 7608 S-N curves with the AASHTO S-N curves.

One major disadvantage of the nominal-stress approach is that computing the nominal stress can sometimes be difficult in complex stress fields, particularly in cases of complicated geometry analyzed using finite-element analysis. This is especially a problem with ship structures, which contain many complex details, some of which have not been properly tested to determine their detail category. However, when applicable, the nominal stress approach is generally preferred due to its ease of use.

2.1.2 Hot-Spot-Stress-Range Approach

The hot-spot-stress-range approach was developed for the design of tubular joints, but it is also now commonly used in the design of ship structures. The name is derived from the fact that noticeable heat is sometimes generated during fatigue testing in regions of highly localized stresses that often exceed the elastic limit [17]. The local stress at a point where a crack forms can be thought of as the superposition of three types of stress:

- The nominal stress caused by the global action of the remotely applied load, disregarding the stress concentrating effects of the joint or the weld.
- The geometric stress concentration caused by the local shape of the joint.

- The local stress concentration caused by the weld toe. This stress is strongly influenced by the weld shape and residual stresses, and is therefore highly variable.

A diagram of the different stress regions is shown in Figure 2.3.

The hot-spot approach involves using a baseline S-N curve associated with butt welds or fillet welds in a nominal stress field. The AASHTO Category C curve corresponds to an ordinary butt weld with reinforcement, and can be used as a hot-spot baseline curve. ABS uses the BS 7608 Category T curve, along with a correction factor based on the plate thickness [6], which is similar to the Category C curve. By using this baseline curve, the effect of the local stress concentration from the weld toe is included in the S-N curve. The hot-spot stress range used in the calculations includes only the first two components listed above, i.e. the nominal stress times the geometric stress concentration factor (SCF).

As in the nominal-stress approach, the fatigue strength is independent of type of steel and welding process. Although the experimental evidence cited earlier [24] indicates that corrosion should not have an effect at realistic service load histories, it is common in specifications for offshore structures to put a factor of 2.0 on life as a penalty for the detail being in a seawater environment. This issue remains controversial, but the perceived corrosion effect is based on test data where the stress ranges are much larger than in service. When the stress ranges are very high and unrealistic, some of the positive effects of corrosion are negated, such as accumulation of corrosion product in the crack causing crack closure, leaving only the negative effects.

In order to determine the proper magnitude of hot-spot stress, one can either determine the SCF from finite element analysis (which is the only option when in the design stage) or measure the stress directly by placing strain gages in the direction of the primary stress range as close as possible to the weld toe in a test specimen or prototype of the detail. One problem that is encountered when applying this principle is that the stress gradients are very steep in the vicinity of the weld. Because of these high gradients, the maximum stress computed or measured will be sensitive to the mesh size or strain-gage length [31].

Compounding this problem is the fact that methods for evaluating the maximum stress vary. An objective evaluation of these various methods was conducted to determine a method of application that is appropriate for ship foundation details with large eccentricity [32]. Most of the methods involve some type of complex extrapolation of the stress from the gradient approaching the weld toe. A simple approach was found to be best: the hot-spot stress is conveniently defined as

the stress measured with a 3 mm strain gage placed as close as practically possible to the weld toe, i.e. centered about 5 mm from the weld toe. This definition of hot-spot stress range was found to adequately correlate the fatigue strength of the various details [32].

The main advantage of using the hot-spot stress range approach is the fact that it can be readily applied to a wide range of structural details. It is particularly useful in situations where the stress field is complex and difficult to compute a nominal stress, or where finite element modeling must be done anyway for strength design. The disadvantage lies mainly in the variability between different hot-spot stress definitions and varying baseline S-N curves. Another problem involves the constant-amplitude fatigue limit (CAFL). The hot-spot approach implies that all details will have a CAFL at the same number of cycles, while full-scale fatigue tests show that the CAFL occurs at different orders of magnitude of cycles for different categories (see Figure 2.1).

2.1.3 Variable-Amplitude Loading

Both the nominal and hot-spot S-N curves are based on constant-amplitude loading tests. In order to handle real applications, the lifetime history of the stress ranges must be characterized for the critical details. Typically Miner's rule is used to calculate an effective stress range from a histogram of variable stress ranges. Theoretically, this effective constant-amplitude stress range results in approximately the same fatigue damage for a given number of cycles as the same number of cycles of the variable-amplitude service history. The effective stress range, S_{Re} , [33] can be calculated as

$$S_{Re} = \sqrt[3]{\sum_i (\alpha_i S_{ri}^3)}$$

where:

α_i = Number of stress cycles with stress range S_{ri} divided by the
total number of stress cycles

Variable-amplitude fatigue tests conducted with various sequences in the variable-amplitude loading history have shown that Miner's Rule is reasonably accurate in most cases but can be unconservative with some load histories with unusual sequences. For this reason, some fatigue design specifications put a safety factor of 2.0 on life if Miner's Rule is used.

The AASHTO specifications compare the above effective stress range to the appropriate S-N curve for the detail being analyzed. No additional safety factor is used for Miner's Rule

since it is relatively accurate for truck loading on bridges. For large numbers of cycles, the AASHTO specification has another check which involves a stress range called the “fatigue-limit-state” stress range with an exceedance rate of approximately 1:10,000 cycles. This stress range is compared to the CAFL for the detail. If the fatigue-limit state stress range is less than the CAFL, then cracking is not expected at all during the useful life [33]. The idea is that most (all except 0.01 percent) of the stress ranges should be below the CAFL, but that occasionally the stress range can exceed the CAFL with no significant effect. Note that if the typical total life of a ship is about 100 million cycles, then 0.01 percent is about 10,000 cycles allowed above the CAFL. This approach is simple and conservative and if these conditions are met, a more refined analysis does not need to be performed.

The ABS SafeHull approach [27,34,35], which is used for the fatigue design of double hull tankers, bulk carriers, and containerships [34], calculates a peak stress range based on an assumed Weibull distribution of stress ranges. The allowable stress range is determined from S-N curves and corresponds to the fatigue strength at about 10,000 cycles. The standardized peak loadings were developed by ABS after analysis of a number of ships and deriving an appropriate shape parameter for a Weibull distribution to describe the fatigue-loading spectrum representing approximately 20 years operation in the North Atlantic. Weibull distribution approaches have been proposed in the past by Munse et al [36]. Note that it is much more difficult to predict the peak stress range than it is the 0.01 percent exceedance level stress range as in the AASHTO approach for long-life variable-amplitude fatigue. The greatest uncertainty is in the extreme tails of the stress range distribution.

The AASHTO S-N curves and detail categories are used in this report. They can be converted to equivalent British Standards S-N curves using Table 2.1, and then an allowable stress range can be determined for use with the ABS SafeHull approach.

2.2 Repair Techniques

In reviewing the literature for this project, it was determined that very little experimental fatigue test data exist for ship repairs. Ship Structure Committee Project SR-1376 tested butt welds and associated weld-access holes. Through-thickness cracks were weld repaired multiple times [37]. Other SSC reports [38,39] discuss the analysis of repairs of cracked details in ship structures, but this research was based on finite element models and did not include testing. These reports did, however, provide both repair ideas and a baseline to compare the experimental data from this project.

There is no guidance on the expected fatigue strength of ship repairs in various international rules and guidelines for construction of ships. Many of these, such as the American Welding Society (AWS) “Guide to Steel Hull Welding,” [40] have recommendations governing repair welds, but none discuss resultant fatigue strength of these repairs.

The Tanker Structure Co-operative Forum has published several books that show pictorials of the types of cracks that commonly occur in tankers and the suggested repairs [41,42,43]. These books were very helpful in identifying typical cracked details and the suggested repairs. However, these books do not address the expected fatigue strength of the repairs.

There were some fatigue test data for repairs made to other types of steel structures, particularly highway bridges. As discussed in the previous section, the fatigue resistance of a welded detail does not depend on the type of structure in which the detail is located, aside from the variation in stress range distribution and possible degradation of fatigue strength due to exposure to seawater and corrosion. It is expected that the effects of these latter factors can be accounted for in predicting the residual life of repaired details the same way these factors are treated in predicting the life of new details. Therefore the limited test data for details used in bridges and other types of steel structures are applicable to ship details as well.

Repair techniques can be categorized into three major categories: 1) surface crack repairs, 2) repair of through-thickness cracks, and 3) modification of the connection or the global structure to reduce the cause of cracking. The expensive option of substantial renewal of a panel of the structure is essentially similar to new construction and is presently accepted as a permanent repair. Therefore, substantial renewal of the structure is not discussed further.

2.2.1 Surface Crack Repairs

Surface crack repair techniques include grinding, gas tungsten arc (GTA) or plasma remelting of the weld toe, and impact treatments. These techniques can be used both as repairs and as improvement methods for the fatigue strength of uncracked welds. Many references provide data on the effect of these procedures as improvement techniques [44,45,46,47]. The improvement in fatigue strength can be attributed to one or a combination of the following: 1) improvements in the weld geometry and corresponding reduction in the stress concentration; 2) elimination of some of the more severe discontinuities from which the fatigue cracks propagate; or 3) reduction of tensile residual stress or the introduction of compressive residual stress [45]. In all cases, once the treatment is applied to the welds, the remaining fatigue life is at least as good as the life of the original detail when it was new, in other words there is no remaining effect of prior fatigue loading cycles. In most cases these treatments result in fatigue strength of the treated detail that is at least one fatigue “category” greater than the original detail, i.e, the next greatest S-N curve in the AASHTO set of S-N curves can be used to predict the residual life of the repaired detail. (The increment in fatigue strength between the British S-N curves is approximately the same.)

One study by Fisher et al. (NCHRP 206) [48] investigated the effectiveness of these three techniques to repair shallow surface cracks at the weld toe. These methods were applied to the ends of cover plates (flange doublers) in full-scale welded girders, but the results can be extended to any weld toe region subject to normal in-plane stresses, including most types of welded attachments and tubular joints.

Results for the grinding repairs were mixed, and this study therefore concluded that grinding away cracks was not a cost effective alternative. This grinding did not attempt to change the profile of the weld by grinding the entire weld surface, tapering, or feathering the weld toe. Therefore, the stress concentration of the weld toe was not significantly altered. More extensive grinding of such cover plate details has been shown to be effective, e.g. Graf [49] or Yamada and Albrecht [50]. However, such extensive grinding is considered overly expensive as a retrofit technique for bridges. In offshore structures with tubular joints, where the welds are very large, grinding is very effective at shaping the weld and enhancing fatigue strength by reducing the associated stress concentration factor.

GTA or plasma remelting of the weld toe involves remelting a small volume of the weld toe and the base metal. This is accomplished by manually moving the tungsten electrode at a constant rate along the weld toe. The GTA remelting process tends to remove slag intrusions as well as reduce the stress concentration at the weld toe [45]. The NCHRP 206 study looked at using GTA remelting as a repair procedure. Results were good provided the crack was fully removed by the GTA process. The report recommended that cracks up to 5 mm deep could be successfully repaired using this process. However, in order for this procedure to be effective, it requires greater operator skill and adequate penetration must be achieved.

Peening methods work mainly due to the introduction of compressive residual stress near the weld toe. Because the compressive residual stress lowers the effective tensile stress range on cracks and crack-like defects, it has been found to only be effective when conducted under dead load. In other words, the peening only has to be effective against live load. The reason for this is that once the dead load is applied, local compression induced by the peening may disappear. Therefore, peening is better suited as a retrofit technique than in new construction.

Air-hammer peening has been used successfully as a repair for shallow surface cracks. Experiments in NCHRP 206 demonstrated that a fatigue crack up to 3 mm deep in cover-plated details can be arrested by peening provided the stress range does not exceed 41 MPa. Peened beams with crack depths larger than 3 mm usually show no measurable increase in life. More than three decades of experience with hammer peening the end welds of cover plate attachments in bridges has shown this to be an inexpensive and effective technique, in most cases the repaired details or retrofit uncracked details will never crack in the remaining useful lifetime of the structure. For example, coverplate attachment end welds, both uncracked as well as with shallow surface cracks up to 3 mm deep, were hammer peened on the Yellow Mill Pond Bridges in Connecticut in the 1970's. These details withstood over 56 million truck traffic cycles over three decades before the bridges were replaced only because a wider bridge was needed [51].

Hausmann et al [52] studied the effect of air pressure and number of passes on the resulting deformation and associated residual stresses. Best results were obtained with lower pressures (below 280 kPa) and greater number of passes (up to six). A depth of plastically deformed grains greater than 0.5 mm was consistently obtained. The depth of compressive residual stress extends from two to four times the depth of plastically deformed grains.

Peening is also useful for improving the fatigue performance of welds without detectable fatigue cracks. Experiments have shown that the fatigue strength is increased by at least one detail category, i.e. the fatigue life is approximately doubled. Fatigue resistance of repair welds can also be improved by up to 175% by peening after repair welding [53]. The benefit of peening in the case of welds without detectable defects is also primarily due to residual stress. For example, Harrison [54] found that welds that were stress relieved after peening had no significant increase in fatigue life.

It might be expected that the peening operation would derive some benefit from blunting or eliminating many crack-like defects at the weld toe such as slag intrusions. However, the peening operation also introduces numerous lap-type defects. The depths of these defects range from 0.05 to 0.25 mm, i.e. the same order of depth as typical weld toe slag intrusions. Unfortunately, like the slag intrusions, these defects also serve as a site for crack initiation, thereby negating the benefit of blunting the weld toe defects. Even greater improvement is reportedly obtained when the peening operation is followed by light surface grinding, which apparently removes many of these lap-type defects.

A new method still under investigation is the use of ultrasonic impact treatment (UIT) to improve the fatigue strength of welds. The method involves deformation treatment of welds by impacts at ultrasonic frequency (roughly 27 kHz) on the weld toe surface. The process removes some material at the weld toe and also results in a residual stress field at the weld toe that is favorable to preventing crack initiation, similar to the effect of hammer peening. The tool is much easier to handle, and the noise generated is negligible compared to that of air hammer peening [55]. UIT has been shown to be even more effective than hammer peening at substantially improving the fatigue performance of welded joints [56], so it can be assumed that UIT will increase the fatigue strength of cover plate details and transverse stiffeners by at least one detail category [55]. However, the equipment is presently proprietary and the vendor must perform treatment services. Additional research into the effectiveness of the method on full-scale welded bridge girders is continuing

2.2.2 Through-Thickness Crack Repairs

The most common type of repair on ships is the repair of through-thickness cracks greater than 50 mm in length. Through-thickness cracks are typically repaired by arc-gouging a vee-shaped weld preparation along the crack path and then welding, usually using the shielded metal arc welding (SMAW) process with low-hydrogen electrodes.

There are a few studies looking at the fatigue resistance of repair welds [37,57,58,59]. These studies were either on plates or highway bridge girders with welded attachments. All generally concluded that at best, the fatigue resistance of a repair weld can only be as good as the original detail. Lower fatigue resistance will result from failure to completely remove the crack or from poor weld quality. If post-weld improvement techniques are used (peening, grinding, GTA remelting) then fatigue resistance is likely to increase.

Regarding ship structural details, project SR-1376 tested butt welds and associated weld-access holes and through-thickness cracks were weld repaired multiple times [37]. Results showed that as long as a crack is completely removed, a full-penetration repair weld completely restores the fatigue life of a cracked butt weld. Previous studies have shown that when stringent non-destructive testing is used original butt welds can be as good as Category C details. In this study, non-destructive testing was not used. Consequently the original butt welds were shown to be AASHTO Category D details. Surprisingly, the repair welds were also Category D, regardless of whether a two-sided or one-sided weld was used and whether the latter was made with or without a backing bar. The cyclic loading prior to a repair apparently has no effect on the fatigue life of the repair. Also, multiple cycles of repair (up to four) have no detrimental effect on the restored fatigue strength. Weld access holes were also shown to be Category D details.

Vee-and-weld repairs are most effective when used to repair a previous weld that cracked, i.e. they will usually not crack again until at least the time it took to crack the detail in the first place. A vee-and-weld repair in a plate where there was no weld before, however, is rarely effective, i.e. they will usually crack again in a time period less than the time it took to crack the detail in the first place [60]. In this case it is necessary to modify the detail, which is discussed below.

For through-thickness cracks that have not only propagated through the plate thickness but also away from the local stress concentration, hole drilling using either a drill bit or hole saw has proven to be an effective retrofit [61]. Holes essentially blunt the tip of the crack, reducing the stress concentration. The size of the hole must satisfy the relationship

$$\frac{\Delta K}{\sqrt{\rho}} \leq 10.5 \sqrt{\sigma_y}$$

where ρ is the radius of the hole, mm, ΔK is the stress intensity factor range. A simpler form of the above equation can be obtained by substituting for the stress intensity factor, K , and the hole radius, ρ

$$\Delta K = \Delta \sigma \sqrt{\pi a}$$

$$\rho = \frac{D}{2}$$

and solving for the minimum hole diameter, D in mm

$$D \geq \frac{S_R^2 a}{18 \sigma_y}$$

where S_R is the stress range (MPa) and a is the length of the crack (mm) for edge cracks (to the edge of the hole) and $2a$ is the total length of a two-ended crack (defined from the edges of the two holes at the two ends of the crack), and σ_y is the yield strength of the plate (MPa). If this relationship is not satisfied, the crack will most likely reinitiate from the edge of the hole. The validity of this retrofit has been studied in the laboratory on full-scale welded beams subjected to variable amplitude loading up to 90 million stress cycles.

Slightly better resistance to reinitiation can be obtained if bolts are inserted in the holes and tightened so as to introduce some local compression around the hole. Other methods attempt to cold work the hole to introduce some beneficial residual stress state around the hole and crack tip [62].

Hole drilling or sawing may also be used to isolate a fatigue crack so that it does not extend from a secondary component into the main girder. A large number of bridges have been retrofitted by installing saw-cut holes in the girder web. Stop-holes have been used successfully for cracks formed under distortion-induced stress ranges in bridge girders. For distortion induced cracks, stop-holes are more effective than weld repairs, since cracking relieves the distortion-induced stress ranges, thereby reducing the driving force for subsequent crack extension. Weld repairs restore the distortion-induced stress ranges and will crack again, typically more quickly than the original cracking.

Another technique that can be used to repair through-thickness cracks is doubler plates, or doublers. Typically cracks repaired using doublers are either large or have reached a critical length. Doublers are also typically used to restore a section that has been heavily damaged by corrosion.

Doublers can either be attached by welding or with high-strength bolts. From a fatigue resistance standpoint, the bolted doublers are always better than welded ones, because a high-strength bolted connection can be considered an AASHTO Category B detail, while a welded connection will be Category E or worse. However, bolted connections may require drilling a large number of holes and require access to both sides of the cracked surface, and therefore may not always be cost effective or even possible. A recent report for the Navy concluded that doubler plates were a viable permanent repair technique and that other details, such as the connection of longitudinals to bulkheads and web frames, would govern the fatigue life before the doubler plates would cause cracking [63].

Welded doubler plates are not typically used in highway bridges since a welded cover plate is an AASHTO Category E or E' detail. But in ship repairs, welded doublers are more common, primarily because the detail categories used in ships are much lower than in bridges. Typically, the crack tips are drilled out and a doubler is fillet welded over the cracked region. ABS rules consider doublers to be a temporary repair only, however, unless structural analysis shows that the repair will be structurally adequate. ABS also prohibits the use of doublers in any area that contains fuel oil or other flammables because the doubler could trap explosive gases [34,63].

When the stress range in a repaired region must be reduced for the repair to be effective, such as in a weld repair where there originally was no weld, then a design modification of some sort is required. This could involve adding a doubler plate(s) to increase the cross-sectional area. If the detail contains a sharp corner, then introducing a soft-toe or radius can reduce local stresses considerably. Another option may be to change the overall geometry of the connection to reduce stress in the joint. Care must be taken, however, to ensure that any design modifications do not become fatigue problems themselves.

2.3 Fatigue-sensitive details in ships

In project SR-1376, a literature search was conducted to determine the types of ship details which should be used for fatigue tests of weld repairs [37]. In addition, a survey was conducted of over 50 shipyards, ship owners, operators, regulators, surveyors, universities, consultants, and other agencies with an interest in ship repair in the U.S.A., Europe, and Asia. Previous Ship Structure Committee Reports were also reviewed and the results included in a project interim report [64]. Results indicated that the three details with highest priority for repair research were 1) brackets at the intersections of web frames and girders with bulkheads; 2) the intersection of longitudinal stiffeners with transverse web frames or bulkheads; and 3) butt welds in stiffeners and girders. An example of all three of these details can be seen in Figure 2.4, which is a photograph taken in the engine room of a containership.

Since butt welds were already covered in project SR-1376, this project focuses on the bracket connection of web frames and girders to bulkheads and the intersection of longitudinal stiffeners with transverse web frames or bulkheads. The first detail's most important feature is the bracket that connects the structural members. An example of this detail can be seen in Figure 2.5. This is a critical part because it is all that connects the 2 members together. A bracket usually consists of a built-up section or is cut from a rolled section, so that it can be welded to the two structural members. Usually there is a gap left between the members, making the precision of cutting them less important. The bracket also makes for less welding, which will help reduce the amount of warping seen in the members.

An example of the second detail is shown in Figures 2.6 and 2.7. At this detail, longitudinal stiffeners attached to the inner or outer hull must pass through a cutout in the transverse web frame. The longitudinals are typically angle or bulb sections, but may also be tee sections. Lug plates connecting the longitudinal to the web frame at the cutout generally are present to stiffen the connection. A vertical flat bar stiffener is usually present and may or may not be attached to the longitudinal.

Both of these details have been well documented as a nuisance location for cracking in tankers, containerships, and bulk carriers [41,43,66,67,68]. The first detail's cracks form at the end of the bracket in the girder or web frame. The cracks start in the weld toe of the bracket and propagate out into the structural member. These cracks are caused by the primary bending stresses

exerted on the ship through fluctuating wave pressures. Only a small bending stress is required to fatigue this detail, since it is a Category E' detail on the AASHTO S-N Curves.

The second detail can be treated as AASHTO Category C using the hot-spot stress range design approach. Cracks typically form in the web frame, initiating at the cutout. Additional cracks can form in the vertical stiffener, the longitudinal or possibly even in the hull plate. Some have suggested that the torsional distortion of the unsymmetric longitudinal causes an additional twisting moment that contributes to cracking. Finite element studies have looked at varying the cutout shape in order to relieve stresses at this location [69,70].

This problem is analogous to the fatigue cracking seen in orthotropic decking in steel bridges, where floor beams (ribs) pass through transverse diaphragms. Again, cracks usually form at the cutout, either in the ribs or the diaphragms. A study by Kaczinski et al [71] performed full-scale fatigue testing on orthotropic deck for the Williamsburg Bridge in New York. This study found that if the diaphragm is groove welded to the rib, AASHTO Category C resistance could be achieved. The study recommended that a larger cutout and thicker diaphragm would be most beneficial to improve fatigue resistance. This study also successfully used hammer peening and hole drilling to repair cracks that formed at the cutout in the diaphragm.

Table 2.1: Cross-reference for S-N curves (nearest curve at 2×10^6 cycles)

AASHTO	Eurocode 3	BS 7608
A	160	B
B	125	C
B'	100	D
C	90	D
D	71	F
E	56	G
E'	40	W

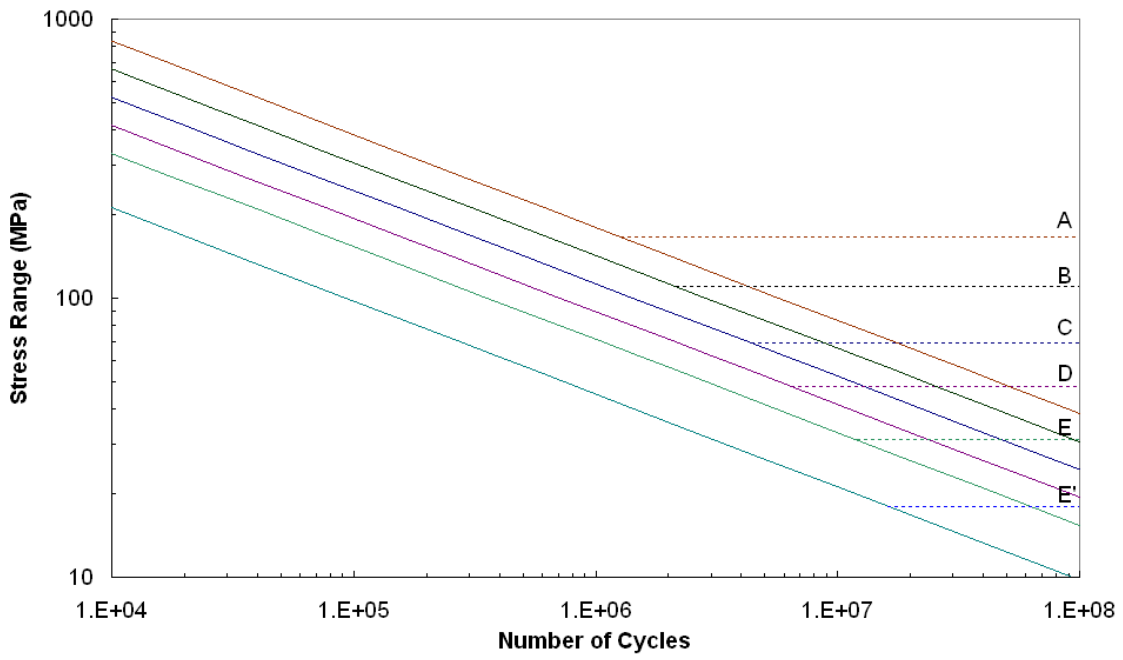


Figure 2.1: Nominal stress S-N curves used in AASHTO, AISC, AWS, and AREMA specifications

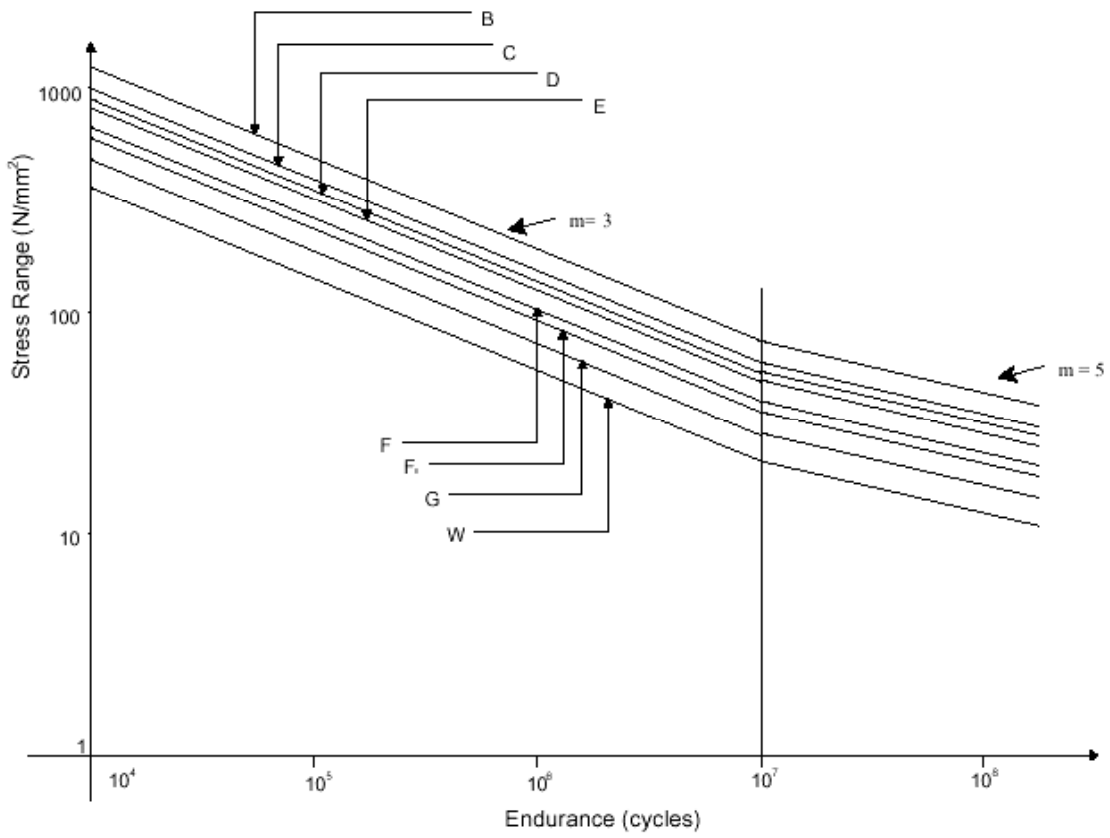


Figure 2.2: BS 7608 nominal S-N curves

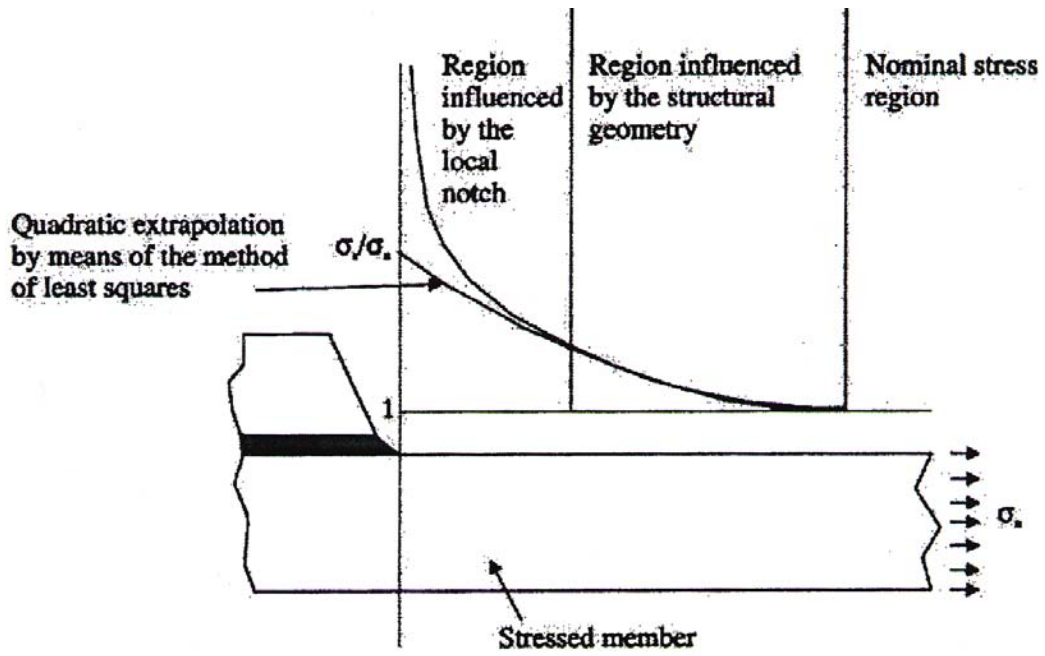


Figure 2.3: Stress regions approaching a welded joint [30]

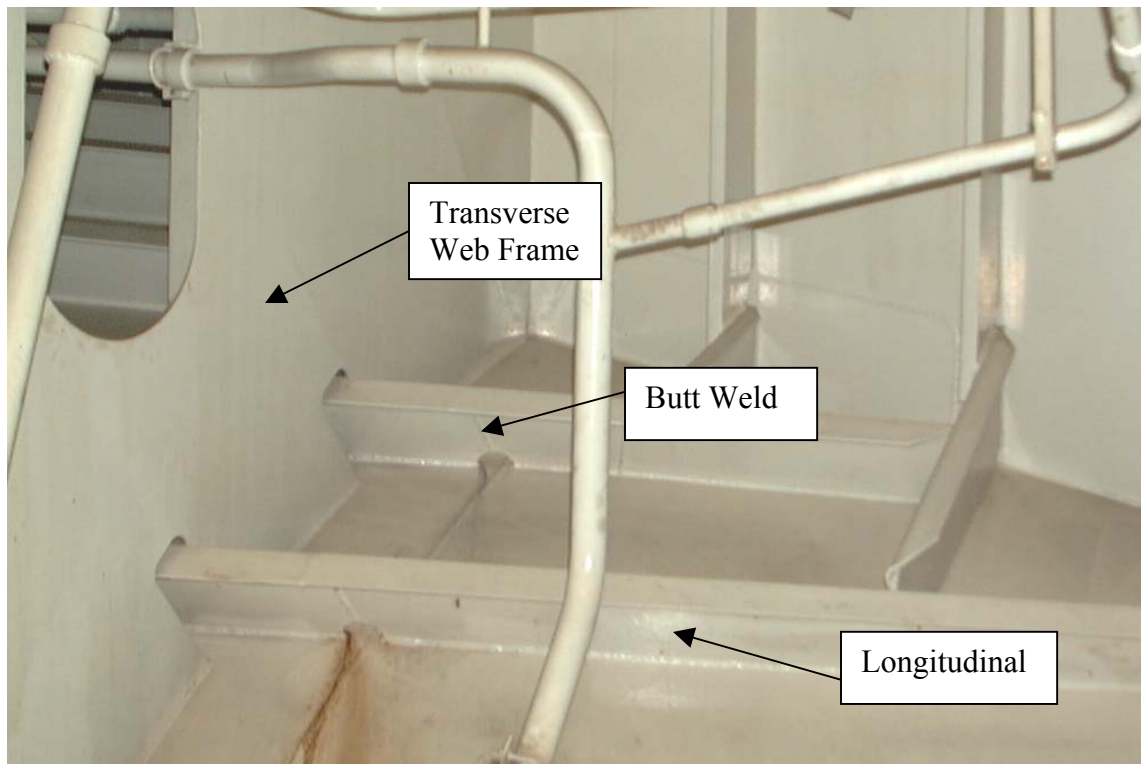


Figure 2.4: Fatigue-sensitive details found in ship structures [65]

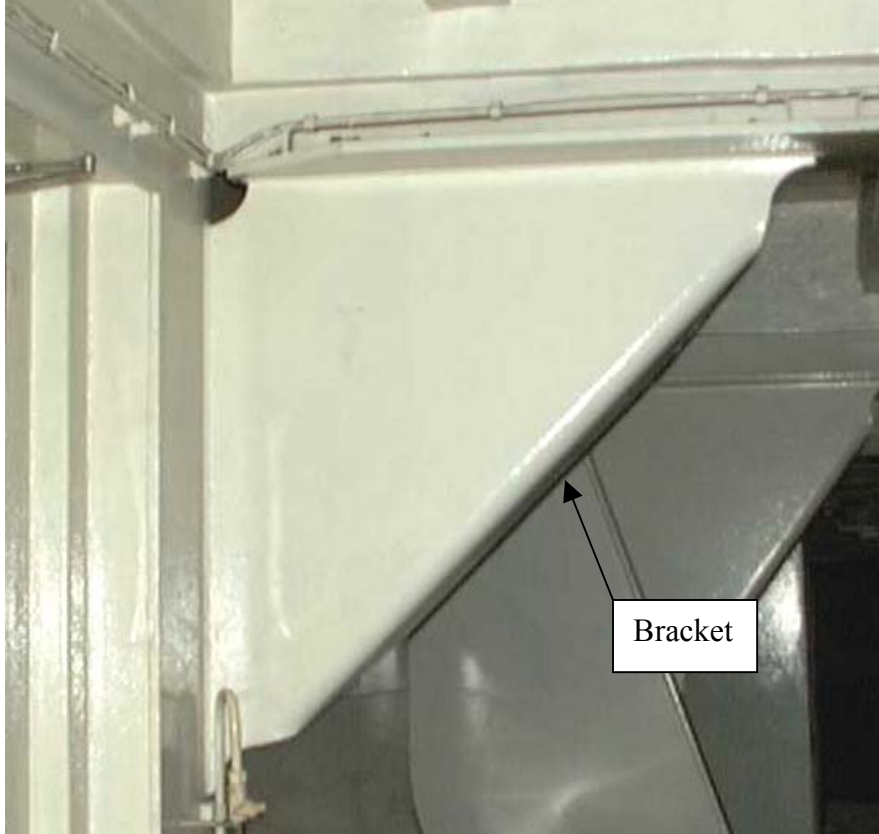


Figure 2.5: Bracket connection of girder to bulkhead detail [65]

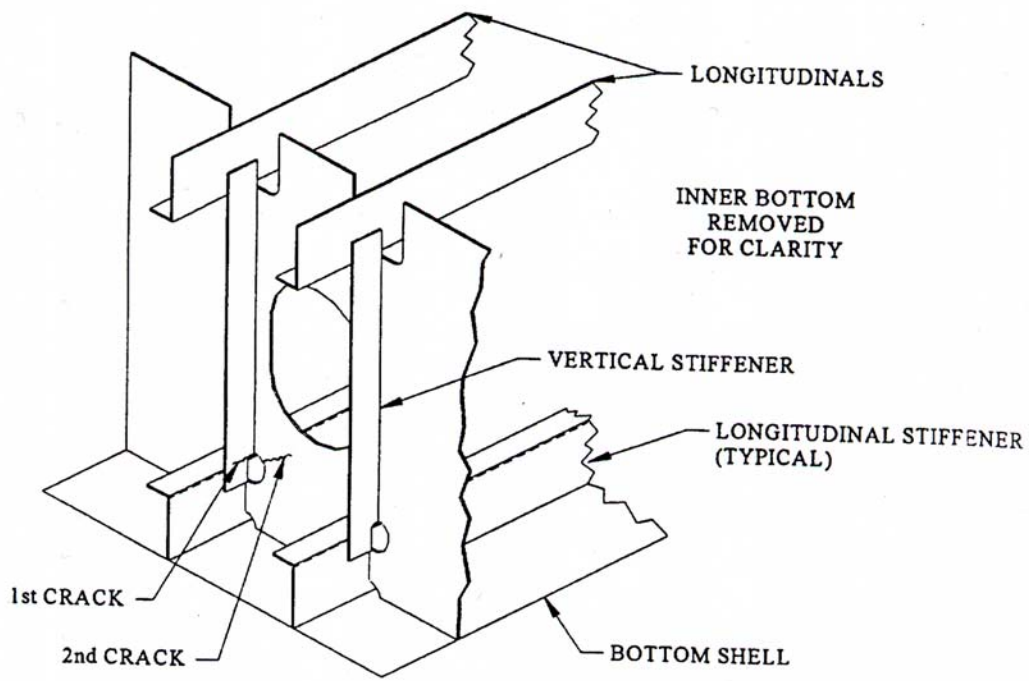


Figure 2.6: Longitudinal/transverse web frame connection [66]



Figure 2.7: Longitudinal passing through a transverse web frame in a tanker ship [65]

3 EXPERIMENTAL PROCEDURES AND RESULTS

This chapter presents the experimental/numerical research that was performed to develop reliable methods to estimate the residual fatigue life of typical weld repairs. Fatigue tests were conducted on realistic large-scale ship-structure models. Fatigue cracks were repaired with various techniques, including stop holes, vee-and-weld repairs, and doubler plates, and the testing continued. Fatigue life and stress-range data were recorded for both the original details and the repaired details. These data were plotted on S-N curves and compared to typical fatigue categories.

Four types of fatigue tests were conducted:

- a) simplified model of attachment (five specimens)
- b) complex model of bracket attachment (two specimens)
- c) simplified model of longitudinal/transverse web frame connection (five specimens)
- d) complex model of longitudinal/transverse web frame connection (two specimens)

Each of these experiments and the relevant analyses are discussed below.

3.1 Simplified Model of Attachment

As discussed in Section 2.3, a detail that has frequently had fatigue problems in commercial ships is the connection between orthogonal structures, either girders or web frames. The first type of specimen is a simple model of a girder with a non-load-bearing attachment detail. The simple-attachment specimen, shown in Figures 3.1 and 3.2, is a rolled wide-flange beam approximately 250 mm deep spanning 3050 mm between supports featuring eight 150 mm lengths of rolled tee-sections fillet welded to the flanges. Each WT6 x 9.5, rolled tee section simulates a transverse plate with a rib as in a typical attachment. The web of this tee section is 6 mm thick and the transverse flange of this tee section is 9 mm thick. The tee sections are spaced so that there is 305 mm of clear distance between each one, i.e. enough such that cracking and repair of one attachment detail should not affect any other.

3.1.1 Test Setup

The simple-attachment specimens were tested in four-point bending with the load being applied to the specimen 533 mm inside of the supports. The setup is shown in Figures 3.3 and 3.4. All of the tee sections were located in the region of constant bending moment between the load points and therefore are subjected to approximately equal stress ranges. Clamped rollers (as shown in Figure 3.5) were used at the supports and loading points to facilitate loading reversal and to make the supports behave like an ideal roller. The load is applied with a 350 kN-capacity servo-controlled hydraulic actuator through a spreader beam to the two load points.

3.1.2 Static Calibration

The simple-attachment specimens were tested statically to make sure they behaved as predicted by the primary bending stress equations. A schematic of the strain gage layout is shown in Figure 3.6. Table 3.1 shows the very good comparison between the measured stresses and the stress calculated using standard bending equations at the peak loads. In cases where the measured stress range is significantly less than the calculated stress range, the measured stress range is used when reporting or plotting the data. Figure 3.7 shows that the stress gradient through the beam depth is linear and that the neutral axis is at the midpoint in the beam, as expected.

3.1.3 Fatigue Test Procedure

A 220 kN sinusoidal cyclic load range (plus and minus 110 kN) was applied at a frequency ranging from 2 to 2.5 Hz. This induces a nominal bending stress range in the beam flange of 100 MPa at all the attachment details.

Visual inspection, aided by the dye penetrant technique, was used to find the cracks. A dye penetrant test involves using a cleaner to free the surface from dust, dirt, or debris. The surface is then sprayed with a red dye and given adequate time to allow the dye to seep into any cracks or surface defects. The dye is wiped clean after sufficient time and a developer is sprayed onto the area to assist the dye to weep out of any cracks it seeped into, and thereby exposing the crack. The penetrant makes the cracks show up in red against the white developer, as shown in Figure 3.8. The cleaner used in this technique was also frequently used by itself because it can be seen pumping in and out of the crack as the specimen cycles.

The number of cycles and size of the crack were recorded each time the specimen was checked. This was done until the cracks forming at the detail reached our criterion for failure. Failure is defined as the development of a through-thickness crack at least 50 mm in length along the weld toe. Long shallow surface cracks are often much longer than 50 mm along the weld toe before they propagate through the plate. Examples of cracks defined as failures at either end of the attachments are shown in Figure 3.8.

3.1.4 Repair Techniques

Various weld details were used to repair the cracks in the simple attachment specimens. In addition, hammer peening was used on some of the repair welds. On one specimen, all of the attachment details were hammer peened before the specimen was tested to determine the effect on the life of the original attachment details. All the likely crack initiation locations were hammer peened on this specimen, i.e. at weld toes on the weld returns on the end of the web and along the flange (as shown in Figure 3.9). Note that it is relatively easy to verify that the peening was performed correctly from the appearance of the weld toe. The chisel tool used for the peening hammer is about 13 mm wide and has a radius of about 3 mm at the tip. The air pressure used to run the hammer was normal shop air, from 420 to 450 kPa. All weld toes received four passes with the peening tool. This procedure was determined to be optimal by in a study by Knight [72].

All the weld repairs were begun by drilling a hole from 14 to 17 mm in diameter at the crack tip in the web of the beam. This was not done for the flanges because there is not room for a drill between the attachments and many cracks severed the flange. To allow for the possibility that the crack is longer than estimated using dye-penetrant testing, the hole is drilled with the center about 5 mm past the suspected location of the crack tip. Next, carbon air-arc gouging is used to create an access hole in the web of the rolled beam. The access holes were cut out as ovals, with the long side being about 50 mm long and the narrow distance being about 30 mm. The hole at the crack tip was used as the start point for the access holes, as shown in Figure 3.10.

Single sided weld repairs made in the flat position were used for the top flange of the specimens. The repair detail varied in whether or not the backing bar was removed and if hammer peening was added. The first step in a single sided weld repair after cutting the access hole is arc-gouging out the through-thickness crack to form a vee-shaped groove. Again, to be

sure to capture the full extent of the crack, gouging was extended to about 5 mm past of the penetrant mark. The backside (bottom side) of the gouge was ground smooth to allow a 6 mm thick backing bar to be tack welded to the specimen.

Welding was done using the shielded metal arc welding (SMAW) process with E7018 electrodes. The welders were graduate research assistants trained by certified welders but with minimal skill beforehand, a common skill level in repair shipyards in foreign countries. It was our intention to achieve lower-bound quality for the repair welds. Non-destructive testing was not used on the repair welds. Despite these conditions, the results are not that much worse than would be expected if welded by experienced welders under strict quality assurance. It is believed to be better to have more robust models for the life of these repairs and not to have to rely upon strict quality assurance. It is still prudent to require some degree of non-destructive testing and other quality assurance in developing specifications for repair welding, although it is comforting to know that if there are minor lapses in quality the results will not be worse than predicted using the models developed in this research.

The groove in the 13-mm thick flange was then filled with about 6 to 10 weld passes, depending on the width. A completed single-sided repair with backing bar is shown in Figure 3.11.

In cases where the backing bar was removed, it was removed either by pounding with a hammer or by arc-gouging. When gouging the backing bars it was important not to gouge too deeply because then a two sided repair must be completed to fix the gouging on the back side. A picture of a completed single-sided weld repair with the backing bar removed is shown in Figure 3.12.

Two-sided repair welds were made in the bottom flanges of the specimens and occasionally in the top flange. The first step in making a two-sided repair weld is gouging out the bottom side of the crack to form a vee-shaped groove about half of the thickness of flange. This groove is then welded in the overhead position using the SMAW process with E7018 electrodes. The groove usually takes 4 to 6 passes to fully fill it fully. The remainder of the crack and the root of the weld, about three-fourths the flange thickness, were arc-gouged from the flat position to form a vee-shaped groove on the topside of the weld repair. This side of the weld is then made in the flat position using the same electrodes. Filling this groove also took 4 to 6 passes. A completed two-sided weld repair is shown in Figure 3.13.

In cases where hammer peening was performed on repair welds, it was applied to the toes of the completed welds. A hammer peened weld repair is shown in Figure 3.14. Again, note that it is relatively easy to verify that the peening was performed correctly from the appearance of the weld toe. The hammer-peening procedure used on the repair welds was the same as described above for the new details.

3.1.5 Results

The data are plotted with standard AASHTO S-N curves in Figures 3.15 and 3.16. Results for each specimen are also presented in Tables 3.2-3.6. In the tables “1st” refers to cracks in the original specimen, “2nd” refers to cracks in the first repair weld, etc. The original attachment detail would be expected to be a Category E detail according to AASHTO fatigue design specifications. The cycles to failure for the original detail exceed the Category D S-N curve. This indicates that the fatigue resistance of this attachment detail is slightly better than estimated by AASHTO.

The specimens that were preemptively treated by hammer peening never cracked, although the number of cycles was greater than necessary to show these hammer-peened details would be at least as good as Category C. (It is not necessary to carry these tests out to greater number of cycles since most details on a ship are worse than Category C. Therefore performance at least as good as Category C is good enough for ships.) These results confirm previous observations that hammer peening increases the fatigue resistance of a detail by at least one category, as was discussed in Section 2.2.1. The ratio of the fatigue lives of one category to the next highest category is about two, so for practical purposes, if the loading history on the detail remains the same, the hammer-peened detail will last at least twice as long before cracking as the original detail without hammer peening.

Other studies show that if the hammer peening treatment is carried out as a retrofit even after most of the life of the original details is consumed, the clock is essentially reset and the remaining life will be at least twice the original life [48]. (The data on hammer peened repair welds discussed below also bear this out.) This means that if a cracking problem begins to develop after ten years, other similar details can be hammer peened and they would be expected to last another twenty years.

Consistent with the findings of Dexter and Kelly, these data also show that the fatigue life of a repair welded attachment detail is essentially reset, i.e. the previous cycles that the base metal has

undergone do not seem to affect the life of the repair weld, which acts essentially like a new weld with no prior fatigue damage [37]. In the study by Dexter and Kelly, the groove weld repairs were made at details which were also simply butt welds in flanges and webs with no attachment details [37]. Thus there was a one-for-one replacement of the welds and the life of the repair welds was comparable to the life of the original new groove welds.

In the present study, however, a groove weld repair is created at the attachment, which was previously only fillet welded. Therefore it would be expected that the remaining fatigue resistance of the weld-repaired detail would be degraded relative to the fatigue life of the original detail in new condition. Groove welds are susceptible to larger weld defects and higher residual stress than fillet welds, especially when welded under poor conditions common in repair shipyards (and simulated by our novice welders). The S-N data indicate that these repair welds are above the Category E' S-N curve. The Category E' S-N curve is one curve lower than the predicted curve for the original detail. So it can be concluded that a weld repair on a Category E detail will produce a detail which has the remaining life of at least a Category E' detail. For practical purposes, if the loading history on the detail remains the same, the weld repaired attachment detail will only last 33 percent as long as the original detail. Clearly, these types of weld repairs are not going to be considered permanent repairs.

The third simple-attachment specimen had the initial crack at the top, edge, west, flange grow until only about a quarter of the gross cross-sectional area remained. This large crack was repaired by welding two 6 x 203 x 152 mm doubler plates to the web after the cracked web and flange were weld repaired. The crack and repair are shown in Figure 3.17. The doubler plates added to the web also stiffened the attachment on the bottom side of the beam, making it so the bottom attachment did not crack. This is reported in the repair table for the third specimen, but will not be included in any of the other charts because it would skew the data. The doubler plates also affected the repair weld, by stiffening the section so that it did not crack either. This data will be included in all of the tables because it is a different type of repair.

The webs of the outer attachments are located very near the clamped roller connection for applying the load. As shown in Figure 3.18, there was not enough access at this location to remove slag and achieve reasonable weld quality. This lack of access was reflected in the relatively short fatigue life of many of these repairs. Since these data were affected by the lack of access they were not included in the S-N curves, although the data are still included in the Repair Tables for

reference. The log of the mean life of each type of repair are shown in Figure 3.19. This shows that one-sided and two-sided weld repairs have approximately the same fatigue life, with the two-sided welds fairing slightly better as expected. The lack of significant difference between one-sided and two-sided welds was also seen by Kelley and Dexter in SR-1376 [37].

The difference in life of first repairs and multiple repairs was also examined. It was expected that the fatigue life of a multiple repair would be degraded relative to original repairs. Figure 3.19 shows that there is a small loss of fatigue life with multiple repairs, especially for the one-sided welds, but not a significant one. The data include welds that were repaired up to four times. Four repairs is a practical limit due to many factors including weld magnetization, which was also noted as a factor by Kelly and Dexter [37] and by Pilarski and Dexter in SR-1392 [18].

A significant increase in the life of the repairs can be obtained by hammer peening the toes of the repair weld. The repairs that were hammer peened survived for the remainder of the specimen's life, considerably longer than any of the weld repairs. The number of cycles they were exposed to after repair and hammer peening was at least as good as the original detail or Category D. These tests could not be carried out for longer due to the fact that other cracks ended the useful life of the specimens. Nevertheless, these results show that hammer peening the weld repair at a non-load bearing attachment can at least restore the fatigue strength to Category D, which in most cases is good enough for a ship.

3.2 Complex Model of a Bracket Attachment

The second type of specimen tested in this project is also aimed at representing the intersection of orthogonal girders, however in these specimens the attachment is load bearing. The complex-attachment specimens, shown in Figures 3.20 and 3.21, were fabricated from rolled channel shapes about 450 mm deep, similar in size to what would be found on a tank ship. For typical ship structures, one of the flanges on the specimen would be a deck of side shell plate. Because of the asymmetry in the effective plate areas the plate compared to the area of the flange of the girder, there is significantly less stress in the plate. Cracking almost always occurs in or near the flange, and not at the plate. In these specimens, two separate girders and brackets are actually being tested simultaneously. The main components of the complex attachment specimen are a 3454 mm long girder, a 1892 mm long orthogonal girder, and two brackets all made from MC18 x 42.7 sections. The brackets join the two girders together through lap joints, but leave a 38 mm gap between the cross and stem of the tee. The brackets, shown in Figure 3.22, are also made from a MC18 x 42.7 section. The connection detail with two brackets is shown in Figure 3.22. This detail with a lap joint is expected to be a Category E' detail. Thus this specimen will provide an example of repairs to a very poor detail with very high initial misalignment and stress concentration.

3.2.1 Test Setup

The two complex-attachment specimens were tested side-by-side for symmetry. If tested separately there would be torsion in the non-symmetric channel sections unless they were loaded precisely through the shear center. The set up is shown in Figures 3.23 and 3.24. The complex-attachment specimens were tested with the load from a 156 kN servo-hydraulic actuator applied horizontally to the two webs of the channels. This arrangement gave maximum moment and stress range at the top ends of the brackets, and induced this bending moment into the horizontal girders as well. Because there are two ends of the horizontal girder attached to each vertical stem, the moment in the girders was only half the moment in the vertical stems.

As in the simple-attachment tests, clamped roller connections were used on the horizontal girder as shown in Figure 3.25. The connection to the actuator did not use rollers, but the actuator's swivel head allowed rotation. This connection provided more fixity than a purely pinned connection, as discussed below.

3.2.2 Static Calibration

The complex attachment specimens were tested statically to take strain gage measurements and make sure that the strain measurements compared well to the simple bending stress equations used to determine the nominal stress. The strain gage layout is shown in Figure 3.26. The strain gages were placed to show that the two specimens were sharing the load equally and to show the stress gradient in both the vertical stem of the tee and through the horizontal girders.

Again the simple bending stress equations were checked, and they compared well to the measured values. Figure 3.27 shows the strain gradients along the stem of the tee, this strain gradient deviates from linearity near the top because of the partial fixity in the connection at the top of the channel. The last gage near the bottom does not see all of the stress because this gage is located below the line where the brackets start. The stress distributions in the beam are linear and have the neutral axis near the middle of the beam, as seen in Figure 3.28.

3.2.3 Fatigue Test Procedure

The complex attachment specimens were tested with a sinusoidal load varying between 0.3 and 0.5 Hz with a maximum range of 120 kN on both specimens (plus and minus 60 kN). The nominal bending stress range in the channel section at the end of the bracket was 78 MPa for all specimens. The critical stress range changed to 71 MPa when doubler plates were added. This change is due to the movement of the critical point to the end of the doubler, which was further up the stem of the tee.

The complex attachment specimens were run and visually checked the same way as described above for the simple specimens. Dye penetrant was used to check for cracks in the same way as it was for the simple specimens.

The complex attachment specimens also had the time, number of cycles, and size of crack recorded each time the specimen was checked. These data were recorded for both the initial

cracks and the repair cracks. As in the simple specimen test the repair number and number of cycles were recorded with each new crack large enough to meet the criterion for failure (through thickness cracks greater than 50 mm in length). Most of the cracks in this test were allowed to grow beyond this criterion for failure, but a few of them were stopped early. The cracks that were not allowed to grow to through thickness were repaired when they were only surface cracks. This was done to see if there was an advantage to repair the cracks before they reach through thickness. The through-thickness cracks were allowed to grow to at least 180 mm long to allow the repair to be not too close to the edge of the bracket. A typical crack just before repair is shown in Figure 3.29.

3.2.4 Repair Techniques

The variations in weld repairs involved drilling out the weld start and terminations points, hammer peening, and adding doubler plates. For the repair welds on through thickness cracks, the crack tips were first drilled out. Then, after welding, the weld terminations were either drilled out or ground out (with a Dremel tool) of the hole drilled at the crack tip. The partial-thickness cracks did not have their start and termination points on the welds drilled out.

The weld repairs for the partial-thickness cracks were the simplest repairs. The first step for this type of repair was to arc-gouge out the crack into the form of a vee-shaped groove. An additional 6 mm on each side was arc-gouged outside of the dye-penetrant marking to ensure that the crack tips had been removed. The groove was arc-gouged deep enough that no signs of the crack could be seen during gouging and by visual inspection after gouging. It is very important to make sure that the entire crack is removed in this step, to ensure that the crack will not reinitiate prematurely. The final step in this repair was using the SMAW process with E7018 electrodes to fill in the gouged section, usually using 4 to 6 passes. A partial thickness repair is shown in Figure 3.30.

The through-thickness cracks were all repaired with two-sided weld repairs. The first step for repairing these was to drill out the crack tips with 6 to 13 mm diameter holes. The weld repair was then completed in the same manner as described for the two-sided repair of the simple specimen (Section 3.1.4). Once the welding was completed then the starting and termination points of the weld were ground flush and a 12 to 25 mm hole was drilled.

Two options were explored for the weld terminations when there was an existing hole from a previous repair. The first was to put a backing bar over the hole and fill it with a plug weld when the first gouge is welded. Then the normal repair can be completed with a slightly larger hole drilled to remove the weld termination (holes up to 29 mm were used). A through-thickness repair with drilled-out weld termination points is shown in Figure 3.31. The other option is running the repair weld out into the hole and then coming back and grinding the run out down later with a Dremel tool. A picture of a ground out hole is shown in Figure 3.32.

The first of three modifications tested for through-thickness vee-and-weld repairs was grinding down the weld and weld toe. After the weld repair is completed, the grinding is done by taking a disk grinder and smoothing out the weld, especially the weld toe. This should remove small surface imperfections on the weld and at the weld toe. A picture of a ground down weld repair is shown in Figure 3.33.

The second modification of through thickness vee-and-weld repairs is hammer peening. As discussed in section 3.1.4, it is applied to the toes of the repair welds. This gets more difficult to do the more times the location is repaired because of the multiple weld toes and sites for potential crack initiation. A picture of hammer peening done after multiple repairs on the complex-attachment specimen is shown in Figure 3.34.

The last modification of this detail is adding doubler plates. The doublers were welded to an individual flange, or to the flange and web on the outside of the channel sections. A picture of a doubler plate is shown in Figure 3.35. The doubler plates were added after the weld repair and hole drilling were completed. To add doubler plates all of the weld in the area of the plates was first ground flush. The flange doubler plates were notched with a disk grinder to allow the bracket and flange to remain separated from the repair. The doubler plates were welded to the specimens using SMAW with E7018 electrodes. The welds were placed all of the way around the doubler on the web and as far around the doubler on the flange as space would allow. The bracket blocked one side of the doubler from being welded to the flange. All of the doubler plates were 18 mm thick, between 76 mm and 102 mm wide and between 203 mm and 254 mm long.

3.2.5 Results

The results of the repairs on the complex-attachment specimens are shown in Figure 3.36, and Table 3.8. As expected, the original detail is Category E'. All of the different weld repairs came out at or below this category. The repairs with termination holes had a life of about 0.42 times the original detail, which is longer than the ones without termination holes. The life of the repairs without termination holes had a life of 0.30 times the original detail. Also, drilled termination holes produced a longer life than ground ones did. So, if a weld repair is used, both the beginning and termination points of the weld should be drilled out, if possible.

The two simplest modifications of the weld repairs were hammer peening and grinding. Grinding to clean up the defects on the welds exterior did not increase the life of the repair, but it made it much easier to find the next crack that occurred in that location. This is the same conclusion as noted in section 2.2.1 by Fisher et al in NCHRP 206[48]. In the simple-attachment specimen tests, hammer peening proved to be very effective. However, in these complex attachment tests, there was not enough access to hammer peen both sides of the specimen and hammer peening was not found to be that effective. Therefore hammer peening is limited to applications where there is adequate space and access. The unsatisfactory results from disc grinding were expected. Kirkhope et al. [44] in reviewing techniques for fatigue life improvement of welds found that disc grinding often leaves grinding marks that are normal to the stress direction in a transversely loaded weld, which serve as initiation sites for fatigue cracks. Their report discusses other techniques for fatigue life improvement, including hammer peening, which was used in this study. Kirkhope et al. conclude that weld toe burr grinding, TIG dressing, and hammer peening treatment are best suited for ship repair. Of these, hammer peening requires the least time in a repair environment, and gives the most consistent fatigue life improvement.

The doubler plate repair proved to be by far the best repair. The two doubler plate repair reached the category E' life, matching the original detail, and neither repair had any noticeable crack growth. The repair using just a doubler plate on the flange of the specimen proved to be better than just a weld repair, but it failed from distortional fatigue in the web. The second doubler plate added to the web keeps the termination hole from undergoing distortional fatigue stress. In addition to increasing the life at the repair location, the doubler plates moved the critical crack location farther up the stem of the tee to a lower stress location. A comparison of the logarithmic mean lives is shown in Figure 3.37.

3.3 Simplified Model of Longitudinal/Transverse Web Frame Connection

Five simplified models of the longitudinal/transverse web frame connection were fabricated as shown in Figures 3.38 and 3.39. The simplified transverse web frames were 1000 x 1337 x 8 mm plates with cutouts for longitudinal angle stiffeners in all four corners. Cutouts in the web frame were made by drilling 50 mm diameter holes to create the radius, then flame cutting up to the drilled holes and then grinding the flame-cut edges. The angle stiffeners were rolled sections of L8 x 6 x ½ (the numbers in this designation for angle sections represent the leg lengths and thickness in inches) that were 610 mm long. The angle stiffeners were also attached to a 610 mm wide plate, 9.5 mm thick, that was fillet welded along the top and bottom edges of the web frame (representing the hull or other stiffened longitudinal panel). The connection between the angle stiffener and the web frame is shown in detail in Figure 3.40. Two 1000 x 76 x 9.5 mm flat bar stiffeners were also welded to the web frame between the longitudinal stiffeners on each side.

The first three simplified models were fabricated out of A36 steel and the other two out of A572 Grade 50 steel. Previous studies [20,21] have shown that the fatigue strength of specific welded details is independent of the grade of steel, and this variation was intended to confirm those findings. Table 3.8 shows the chemical composition of the two grades of steel. Mill certifications showed an average yield strength of 347 MPa and an average ultimate strength of 485 MPa for the A36 steel. The A572 Grade 50 steel had an average yield strength of 446 MPa and an average ultimate strength of 515 MPa. All fabrication welding was done with the flux-cored arc welding (FCAW) process with E71T-1 wire and carbon dioxide gas shielding.

3.3.1 Test Setup

The simplified model experiment was designed to create constant shear throughout the web frame. This was done by loading the web frame as a cantilever, with a rigid connection to a supporting column. The simplified model test setup is shown in Figures 3.41 and 3.42. The shear loading simulates the loading in typical transverse web frames in tank ships which can create tension around some of the cutouts, generating cracks at these connections. No load was applied directly to the longitudinals in the simplified model, in order to isolate the effect of the shear stress on cracks forming at this detail.

At the fixed end of the specimen, L6 x 6 x ½ angles were used as shear connectors. Thick angle sections cut from W14 x 211 shapes served as rigid connection angles for absorbing the

bending stresses caused by the cantilever loading, in order to simulate a continuous hull. On the free end of the cantilever, L6 x 6 x ½ connection angles with welded endplates were bolted to the web frame. The endplates of these angles were then bolted to a spreader beam, which was in turn bolted to a 490 kN hydraulic actuator. Load was measured with a load cell just below the actuator swivel head. The actuator was run in load control using a computer-controlled servo-hydraulic system.

3.3.2 Static Test and Finite Element Model

Strain gages were installed on each specimen at predicted hot-spots (stress concentrations) to determine the actual stress ranges during an initial test on the uncracked specimen. The strain gages were oriented in the anticipated direction of the largest absolute value of the principal stress, which is also normal to the anticipated crack plane. During the static test, load was slowly cycled between 9.0 and 213 kN while strain readings were recorded by a personal computer-based data acquisition system. Stress was calculated from the uniaxial strain by multiplying by the elastic modulus (200 GPa). It is recognized that a small correction for the Poisson effect should be applied in areas where there is a multiaxial stress state, although this was not done for simplicity.

The typical strain gage layout for each specimen is shown in Figure 3.43, with each detail labeled A-D. This layout was determined after observing the actual cracking behavior of simple specimen #1. Predicted hot-spots included

1. along the edges of the cutouts near the radii,
2. in the bottom hull plate near the cutout at the fixed connection, and
3. in the lug plates near their welds.

At the radius for cutout D, three strain gages were placed in a line parallel to the tangent of the cutout at distances of 2.5, 9.5, and 17.5 mm from the edge, in order to determine the stress gradient approaching the cutout. These values are plotted in Figure 3.44. A strain gage rosette was placed at the very center of the web frame in order to determine the remote, or nominal, stress.

Initial test results are shown in Table 3.9 as the average stresses measured at each location at peak load. Given the complex geometry of these specimens, measured stress readings were essential in applying the hot-spot stress approach. Large stresses were experienced at the cutouts relative to the nominal stress in the web frame. High stresses were also seen in the bottom hull near the connection to the supporting column.

A finite element model of the web frame was created to be able to predict the stress at any point in the specimen. The commercial code ABAQUS/CAE 6.3 was used through the Supercomputing Institute at the University of Minnesota. The model used C3D8R, an 8-node, 3-dimensional element with reduced integration. These solid elements were found to work slightly better than thin shell elements. A mesh size approximately equal to the thickness of the web frame was used in regions near the cutouts. Welds were not explicitly modeled; rather, overlapping surfaces that were linked by welds were modeled as two rigidly connected surfaces. The mesh for the simplified model specimens is shown in Figure 3.45.

Because of the complexity of the specimen, not all parts were modeled. The flat bar stiffeners were omitted, as their inclusion did not affect the results significantly. A large bar section was added to the loaded end of the web frame to simulate the loading conditions. Also on the loaded side of the specimen, the longitudinal stiffeners were not attached to the hull plates. This gave results that were in much better agreement with the experimental results. Apparently, since there is no direct connection of the hull plates to the fixture on the loaded end of the cantilever, very little load goes into the hull plates at this location.

The hot-spot stress results are shown in Figure 3.46. Note that the areas around the radius in the upper left (detail A in Figure 3.43) and lower right cutout (detail D) are in tension, while these areas are in compression at the other cutouts. This pattern is expected due to the shear distortion tending to open these cutouts A and D and close the other cutouts B and C. The location with the greatest stress range is at the radius for cutout D, as was seen in the experimental results, with a stress range of approximately 240 MPa. The model was in good agreement with actual static test results, which gave a stress range of 204 MPa at this location. Other crack locations agreed fairly closely as well. This model was very helpful for determining stresses in regions where poor access prevented the attachment of strain gages.

3.3.3 Fatigue Test Procedure

All simplified model tests were conducted at a frequency of 1.5 Hz and with a mean load of 111.0 kN. Mean stress has little effect on fatigue strength, but results from a test with a high mean tensile stress can be considered conservative since the high mean tensile stress would be expected to decrease the fatigue life relative to fully reversed loading or zero mean stress. The load was cycled between 9.0 and 213.5 kN, giving similar stress ranges as measured in the initial static test. This stress range would be expected to produce cracks at the radii after approximately 400,000 cycles, based on AASHTO Category B resistance for typical flame cut edges. The specimens were run continuously, accumulating up to 130,000 cycles per day.

Specimens were visually inspected at regular intervals for cracks. The visual inspection included spraying a fast-drying cleaner solvent at the above-mentioned hot spots. In the presence of a crack, the cleaner would be observed pumping in and out of the crack while the remainder would dry on the surface. The cracks were often examined further using the complete dye penetrant procedure, as described in section 3.1. When a crack was observed, the date, time, location, number of cycles, and surface length was recorded. “Failure”, or the end of life, was considered to be the development of a through-thickness crack at least 50 mm long. If the crack were noticed before this failure criterion was met, the specimens would be visually inspected frequently until the failure criterion was met.

Although it was originally hoped that cracks would form naturally at the cutouts, the cracks that initially occurred formed at the attachment to the test fixture. The fatigue resistance at the radii may have been better than expected because of the use of a drilled hole to start the cutout and grinding the flame cut edges. Specimen 1 accumulated over 2.9 million cycles without any cracks occurring naturally at the cutouts. This is much larger than the lower bound predicted by the AASHTO Category A curve, which is 700,000 cycles. Since our objective was to test repairs of typical cracks, and the cracks commonly occur at the cutout in service, it was decided to induce cracking at the cutout radii by sawing a 19 mm long notch with a reciprocating saw at each cutout. A small tack weld was placed at the tip of the saw cut using an E7018 shielded-metal arc welding (SMAW) electrode.

3.3.4 Results

Tables 3.10-3.14 summarize the cracks and their repairs for each specimen. Repairs were made in situ, with all repairs being made in the vertical position. Repairs on the simple specimens consisted of stop holes, vee-and-weld repairs, hammer peening, and bolted doubler plates. All weld repairs were done by first arc gouging the crack out, then welding using the SMAW process with E7018 electrodes, as is typically done in ship repairs. After the repairs, the fatigue cycling was resumed. Some details were repaired more than once in order to keep the test running.

3.3.4.1 Stop Hole Repairs

Cracks in the web frame at the cutouts (Figure 3.48) were repaired using stop holes centered ahead of the crack at a distance equal to the radius of the stop hole (Figure 3.49). This was done to be sure that the crack tip was removed. The hole sizes were chosen so that the validity of the equation given in Chapter 2 could be verified. Various hole diameters ranging from 14 mm to 76 mm were tried to determine the effectiveness of each. On specimen 4, a high strength bolt was also inserted into the stop hole and fully tensioned to determine if the compression force from the bolt provided any benefit.

Figure 3.50 shows the performance of all stop holes in a tensile stress field on an S-N curve. All of these repairs plotted above the AASHTO Category C curve. This is better than expected, as typically drilled holes are considered a Category D detail. For the most part, the performance of the stop hole improved with increasing diameter. However, there is some scatter present which is typical of fatigue data.

By far the best performance came from the 24 mm stop hole with a fully tensioned 22 mm diameter high-strength A325 bolt (Figure 3.51) with a washer placed under both the head and the nut. The compressive force caused by the bolt tightening not only creates compressive residual stresses, but it creates an area of high friction between the washers which holds the two sides of the cracked plate together, acting almost as a small doubler. This repair never failed after 3 million cycles, although cracks did form in the washer on one side of the web frame, which indicates that the area was beginning to loosen up.

Figure 3.52 shows the stress range that the stop hole repairs were subjected to as a function of the hole diameter compared to the maximum stress range allowed by the equation for

survival, given a 25 mm initial crack and 345 MPa steel, and whether or not each repair survived. Repairs which “survived” are shown as runouts on Figure 3.50. The data show that the equation is conservative as one of the stop hole repairs was subjected to a stress range 40% greater than allowed by the equation and still survived. No cracks occurred at stress ranges below the allowable. The data show the equation is not excessively conservative, however, because some cracks did occur where the stress was only 33% greater than allowable

The data of all stop hole repairs is shown in Figure 3.53 in a different format: the actual hole diameter used versus the hole size required by the equation to prevent reinitiation. All data points below the 45-degree line should theoretically be failures, i.e. cracks reinitiated at the holes. All failures that did occur are below this line, but some of the surviving holes are also below the line, again indicating that the stop hole equation is conservative. One failure occurred when a hole diameter of 90 mm was predicted to be required and a 57 mm diameter hole size was used, indicating that the equation is not excessively conservative.

A phenomenon that should be noted is stress redistribution, or load shedding, at the cutout D due to cracking and hole drilling. Removing part of the web frame through hole drilling may have diverted more load through the lug plate which caused cracking there. Soon after the initial crack coming out of the cutout was repaired with a stop hole, the bottom of the lug plate would start to crack along the weld to the web frame (see Figure 3.53). This lug plate crack would then propagate a certain distance and then appear to arrest until the stop hole failed, then the lug would continue to crack. For the bolted stop hole repair, the lug was almost 80% fractured when the test was stopped. Therefore, the lug plays an essential role in prolonging the life of the repaired detail, and too large of a stop hole may divert too much load to the lug. As a result, follow-up repairs would require fixing or improving the lug.

Most of the repair failures occurred at detail D. This detail experienced the most severe tensile loading and therefore was most prone to cracking. The tensile stresses at detail A were roughly 30% lower compared to detail D. Two repair failures occurred at detail C after an initial crack formed on its own at the radius which was not saw cut, nearest the flat bar stiffener (Figure 3.55). The reason that repairs at details B and C did not fail is because they were in compressive stress fields. Small crack growth did occur at these two details out of the initial saw cuts, but once they were repaired they never cracked again. (Note that these data from cutouts B and C are not included in the plots, since they would not be considered a worst case). In a compressive

stress field, a hole as small as 6 mm was successful in preventing further crack growth. In fact, there is a good possibility that these cracks may have arrested on their own.

One final thing to keep in mind when determining proper stop hole size is the presence of previous holes. If one hole is drilled and fails, and then another hole is attempted ahead of the new crack tip, the new crack length, a , to consider is the distance from the crack tip all the way back to the original starting point, not just the distance to the edge of the first failed stop hole.

3.3.4.2 Weld Repairs and Hammer Peening

Weld repairs were also used on the simple specimens. In one case at detail D, where the original stop hole repair failed rather suddenly, a 130 mm crack had to be weld repaired before testing could continue (Figure 3.56). For this repair, a 9.5 mm hole was first drilled at the crack tip. Then the crack was air arc gouged to about 75% of the thickness of the web frame from one side followed by welding. Then other side of the web frame was back-gouged and welded also (Figure 3.57). This was followed by drilling out the weld termination with an 11 mm hole and grinding the weld smooth. Because the original material was base metal and this repair would certainly crack again quickly, two 305 mm x 250 mm x 9.5 mm doubler plates were bolted over the repair weld using eight 22 mm diameter A325 high strength bolts (Figure 3.58). This repair never failed, lasting over 500,000 cycles. The predicted life for a bolted doubler repair (Category D) at that stress range would be 150,000 cycles, so this repair was considered successful.

Some weld repairs were performed on the simple specimens to repair cracks in other places as well. The crack that formed in the bottom of the lug plate was vee-and-welded on specimen 2 (Figure 3.59). This weld repair was somewhat effective, as is shown in Figure 3.60, where it achieved approximately 45% of the life of the original lug plate. Both the original detail and the repair fell above the Category C curve as expected since the hot-spot stress range was used. This crack was not repaired on later specimens, to see the effect of the lug cracking on the stop hole repair in the web frame.

Another location that was weld repaired was at the back of the longitudinal angle where it connects to the web frame (Figure 3.61). A crack initiating at the weld root would always form here on the side without the flat bar stiffener. As shown in Figure 3.62, this crack was caused by a lack of fusion defect inherent in the connection. By fillet welding the longitudinal to the web

frame, an unfused gap will be present which serves as an initial crack. Repairing this detail by gouging and adding a new fillet weld (Figure 3.63) was found to be effective (103% of original life). This is likely because the crack was arc gouged partially into the web frame, resulting in a partial-penetration groove weld to the longitudinal. A deeper gouge and full groove weld, as done on specimen 5, improved the repair further to 107% of the original life. Hammer peening (refer to section 3.1 for a description of the procedure) the toes of the repair weld was also performed at this location, although it did not help much because cracking still occurred at the root.

Figure 3.60 also shows the performance of this detail and its repairs on an S-N curve. Both the original and the repairs were very close to the Category B curve, but Category C is recommended as a more conservative approximation. One data point is much lower than the others, sitting right on the Category C curve. The reason for the poorer performance of this repair is that the crack was welded without first arc gouging it. By not arc gouging, the crack was likely not fully removed, and thus reinitiated quickly.

Surface cracks were typically hammer peened, such as in the bottom hull plate at the cutout (Figure 3.64). As long as the crack was peened before it grew too deep (> 3 mm), the repair was effective. If not, the crack would reinitiate almost immediately. Results from peening repairs are shown on an S-N curve in Figure 3.65. The original detail plotted as Category C and the repair as Category D. Pre-peening this detail prior to testing prevented cracks at this location from ever forming on specimens 3 and 4, improving the detail to Category A. On specimen 5, the fabrication weld at this location was not fully wrapped around the web frame, making it impossible to peen the entire weld toe. As a result, a crack formed and had to be repaired by hole drilling. But the pre-peening still achieved Category A resistance, despite the fact that it failed. Peening was not effective on welds that failed at the root, such as in the “back of angle” cracks mentioned above.

Figure 3.66 shows a comparison of all repairs made on the two different types of steel. There is no noticeable difference between repairs made to A36 steel and those made to A572 steel. Both lie within the same scatterband. This confirms previous findings that fatigue is independent of the type of steel. It should be noted, however, that higher strength steels such as A514, HY-80, or HY-100 require special welding procedures in order to produce a defect-free weld. For these steels, minimum preheat and interpass temperatures must be provided per AWS

D3.5 [40] to prevent cold cracking. Undermatched electrodes should be used for steels with strengths of 480 MPa or greater in order to prevent excessive residual stresses.

All but one of the repairs, regardless of the type of steel, were better than Category C. This means that the repairs described herein can be considered to be at least as good as the original detail. In other words, the ratio of the life of the repair to the life of the original detail can be considered at least equal to 1.0. Depending on the type of repair used, this ratio can be as high as 11.1. Appendices A and B present procedures and examples of how to design typical repairs and how to calculate the resulting residual life.

3.4 Complex Model of Longitudinal/Transverse Web Frame Connection

The full-scale specimens are shown in Figures 3.67 and 3.68. They consisted of the same size web frame as the simple model described in the previous section, except with two cutouts instead of four. The longitudinals on these were the same size section, but 1524 mm long instead. The hull plate was also larger to match the longitudinals. The longitudinal-web frame connection was the same as that in the simple specimens (Figure 3.40), except that for the full-scale test, the cutouts were flame cut rather than drilled and ground smooth. Complex specimen 2 was further varied by removing the lug plate via torch cut. A flame-cut opening is more typical of actual ship details and typically has a lower fatigue strength than smoothed openings, on the order of AASHTO Category B. Every welded connection for the two specimens was made with 8 mm fillet welds, welding all parts continuously to structure. For the complex models, specimen 1 was fabricated out of A572 Grade 50 steel, and specimen 2 out of A36 steel. The material properties for the complex specimens were the same as those for the simplified test.

3.4.1 Test Setup

The test setup for the complex test is shown in Figures 3.69-3.71. The upper hull plate and longitudinal stiffener were loaded at the ends as two cantilevers. Loads from a 340 kN actuator were distributed using a 1525 mm long spreader beam and transferred to the specimen through clamped roller assemblies. The ends of the transverse web frame were rigidly attached to two columns spaced 2.0 m apart through 250 mm deep spacer beams, bolting with two L6 x 6 x ½ angles on each side. Load was measured with a load cell just below the actuator swivel head. The actuator was run in load control using a computer-controlled servo-hydraulic system.

The test was designed to simulate pulsating secondary hydrostatic pressure loads, which are transferred through the connection detail into the web frame in shear. The test was run with load reversal about zero, which is realistic for ship structures. Some experiments have shown that the ballast condition is more severe than the loaded condition in terms of fatigue damage for this detail [68]. This is because in the ballast condition, the hydrostatic pressure from the water-filled ballast tanks creates a mean tensile stress in the web frame normal to the hull plates. The effect of the mean stress, however, is small.

3.4.2 Static Test and Finite Element Model

Strain gages were installed on each specimen at predicted hot spots to determine the actual stress ranges during an initial test on the uncracked specimen. The hot spots were chosen based on the results of the finite element model discussed below. During this test, load was slowly cycled between -53.8 and 53.8 kN while strain readings were recorded by a personal computer-based data acquisition system. Stress was calculated from the uniaxial strain by multiplying by the elastic modulus (200 GPa). Again, no adjustments were made for the Poisson effect for simplicity.

The typical strain gage layout for each specimen is shown in Figure 3.72. Predicted hot spots included the weld connecting the longitudinal to the web frame and along the edges of the cutouts near their radii. Two strain gages were attached to the bottom side of the longitudinal on each side of the web frame. Strain gage rosettes were placed at three locations around the cutout in the web frame. Initial static test results are shown in Table 3.15 as the average stresses measured at each location at peak load. Note that the removal of the lug plate in specimen 2 caused larger stress ranges under the same amount of load. Given the complex geometry of these specimens, measured stress readings were essential in applying the hot-spot stress approach.

A finite element model of the complex specimen was created to be able to predict the stress at any point. The commercial code ABAQUS/CAE 6.3 was used through the Supercomputing Institute at the University of Minnesota. The model used C3D8R, an 8-node, 3-dimensional element with reduced integration. These solid elements were found to work slightly better than thin shell elements. A mesh size approximately equal to the thickness of the web frame was used in regions near the cutout. Welds were not explicitly modeled; rather, overlapping surfaces that were linked by welds were modeled as two rigidly connected surfaces. The mesh for the complex model specimens is shown in Figure 3.73. A load of 66.7 kN was applied to each end of the longitudinal (for a total load range of 133 kN). Some rotation caused by the lack of symmetry of the angle section occurred.

Results from the finite element model are shown in Figure 3.74. The hot spot in this case is at the weld between the back of the longitudinal stiffener and the web frame at the cutout on the side without the flat bar stiffener. Cracking is expected to begin at this weld, similar to the second case

of cracking seen in the simplified model test. The model predicts a local stress range of 300 MPa at this point. Of course this is a much higher stress than is typically seen in service, and for the actual testing a smaller load range of 108 kN was used. The actual loads used in the experiment were roughly 80% of those used in the model, which predicts that the actual hot spot stress ranges would also be 80% of those in the model.

Another hot spot is at the corners of the lug plate. The stresses here are due to the transfer of shear forces from the longitudinal into the web frame. Stresses are lower at this location, on the order of 200 MPa. Stresses in the web frame around the cutout are also lower. The highest stress here is only 170 MPa, which may cause cracking at high numbers of cycles, but this should be much later than cracks at the main hot spot. If the computer model results are reduced by a factor of 0.80 as discussed above, then results from the computer model agreed well with the readings obtained in the static test (see Table 3.15).

3.4.3 Fatigue Testing Procedures

Both complex model tests were conducted at a frequency of 2.0 Hz and with a mean load of 0.0 kN. No sawcuts were made in the complex specimens, as they were not needed to initiate cracks. The load was cycled between -53.8 and 53.8 kN, giving similar stress ranges as measured in the initial test. The specimens were run continuously, accumulating up to 170,000 cycles per day. Inspection and reporting procedures were identical to those used in the simplified model test.

3.4.4 Results

Table 3.16 summarizes the cracks and their repairs for the complex specimen. Repairs were made in situ, with all repairs being made in the vertical position. Repairs on the complex specimens consisted of stop holes, vee-and-weld repairs, hammer peening, and detail modification. All weld repairs were done by first arc gouging the crack out, and then welding using the SMAW process with E7018 electrodes. After the repairs, the specimens were returned to testing. Some cracks were repaired more than once in order to keep the test running.

The original detail can be considered to be AASHTO Category C, if hot-spot stresses are used in the analysis, as they are here. The actual test results showed the original detail to be much better than this, achieving Category A resistance for both specimens. Specimen 2 actually had a shorter life in terms of number of cycles, however the removal of the lug plate caused the stress

range to increase, and thus it still plotted as Category A. This high fatigue strength is not totally unexpected, however, since Category C represents a lower-bound 97.5% confidence limit. Also the test specimens likely represent a higher level of quality than would be expected in an actual ship, as a small specimen can be constructed with a lower probability of misalignment errors, defects, etc.

All of the cracks and their repairs for each specimen are shown on S-N curves in Figures 3.75 and 3.76. Every initial crack seemed to generate from the same general location. This occurred at the hot spot predicted by the computer model at the weld between the longitudinal and the web frame. The first crack formed in the web frame at the edge of the longitudinal on the side of the web frame without the flat bar stiffener (Figure 3.77). This crack initiated at the toe of the weld where it wraps around the web frame cutout. The crack propagated slowly in two directions: into the web frame and into the longitudinal. After propagating roughly 15 mm into the longitudinal, it seemed to arrest at that point, however it continued to propagate into the web frame and grew to a total length of about 50 mm, after which it was repaired using a 76 mm stop hole in specimen 1 (Figure 3.78), and a 38 mm stop hole in specimen 2 (Figure 3.79).

The stop hole repair was very effective, as no cracks ever reinitiated from the hole. According to the hole drilling equation, a 52 mm diameter hole was the minimum size required for specimen 1 and 150 mm for specimen 2. Since the 76 mm diameter hole used was much more than required, no reinitiation ever occurred, as expected, and the repair achieved at least 100% of the life of the original detail. This result is also consistent with other studies [70,71] that have suggested that an increased cutout size can reduce stresses in the web frame and prevent cracking. By drilling such a large hole near the cutout, the cutout effectively becomes much larger. In specimen 2 the stop hole was a bit undersized, however the repair did not fail. This could further illustrate that the hole drilling equation is conservative (as discussed in Section 3.3) and/or that the stress range decreases enough away from the cutout that the smaller hole works. Regardless of the reason, the stop hole repairs were effective, and lasted at least as long as the original detail.

At the same time, another crack was propagating the length of the weld connecting the longitudinal to the web frame in specimen 1, similar to cracks that occurred in the simplified model test (Figure 3.80). This crack initiated at the root of the longitudinal-web frame weld and grew to 145 mm. As in the simplified test, this crack was repaired by arc gouging the crack deep into the web frame and then groove welding the longitudinal to the web frame and reinforcing with an additional fillet weld. This was then followed with hammer peening the weld toes (Figure 3.81).

Unfortunately this repair was not as successful in the complex test as it was in the simplified test. The weld-repaired detail only achieved approximately 20 percent of the life of the original detail. The reason for the poorer performance is likely due to the fact that in the complex test the longitudinals received direct loading. In the simplified test, the only load present was shear in the web frame, but in the complex test, the longitudinals themselves were subject to both bending and torsion. As a result, stresses along the back of the longitudinal were higher, and the groove weld repair alone was not sufficient.

For the second repair of this crack, a 410 x 130 x 9.5 mm bracket was fillet welded to the longitudinal and web frame (Figure 3.82). This is similar to the repair suggested by the Tanker Structure Co-operative Forum [43] for this type of crack. The bracket helped to make the web frame more symmetric with respect to the flat bar stiffener present on the other side. It also moved the critical location outward on the longitudinal, away from the site of the previous crack. The resulting life of the bracket repair was much better, achieving 76% the life of the original detail (see Figure 3.75). This crack did not occur on specimen 2.

Another crack occurred at the flat bar stiffener where it connects to the longitudinal. After drilling the 76 mm stop hole (described above) in specimen 1, the crack was not repaired further, leaving an existing crack in the center of the longitudinal. Because of the stop hole, it could not propagate further into the web frame, but it was able to turn and begin propagating into the flat bar stiffener (Figure 3.83). Unfortunately the crack was not low enough to clear the longitudinal, so a stop hole could not be drilled, and instead a weld repair was attempted (Figure 3.84). This was ineffective, achieving 7 percent of the original life.

A second weld repair was then attempted in combination with the added bracket (described above). This weld repair plus detail modification was better, achieving 29 percent of the original life. After the second crack formed at the flat bar stiffener, the test was allowed to continue running until the crack from the flat bar stiffener propagated into the added bracket, causing complete failure of the detail (Figures 3.85 and 3.86).

The flat bar stiffener also cracked in specimen 2 at the same time as the initial web frame crack was propagating. Two 14 mm stop hole repairs were attempted, both of which were ineffective (see Figure 3.87). The hole drilling equation calls for at least a 150 mm stop hole, which is impossible on the 76 mm wide stiffener, and the repairs obviously did not work. Next a weld repair was attempted, removing as much of the crack as possible from the stiffener and web frame.

The repair weld was then ground smooth to allow for a 200 x 60 x 8 mm doubler plate to be welded to the flat bar stiffener (Figure 3.88). A 200 x 130 x 8 mm bracket was also welded to the opposite side of the web frame, connecting to the longitudinal (Figure 3.89). This was similar to the bracket repair performed on specimen 1.

Looking at the results on the S-N curves (Figures 3.75 and 3.76), the stop hole repairs in the web frame were most effective, achieving Category A resistance. The detail modification involving the added bracket was able to achieve Category B resistance, but was very close to the Category A line. The weld repairs were worse, and they can be conservatively estimated as Category D. The 14 mm stop holes were ineffective, achieving only Category E resistance. If the original detail is taken as Category C (as it is in design), then weld repairs and grossly undersized stop holes will not be able to achieve the same life as the original. However, drilling stop holes (per the equation) and/or adding a bracket can improve the repair to at least the same life as the original detail, possibly greater.

In retrospect, something should have been done to repair the crack at the center of the longitudinal left after drilling the stop hole in specimen 1. Not repairing this crack likely reduced the effectiveness of the repairs made at the other locations. Leaving a crack tip intact is never a good idea as it does not take much of a stress range for it to continue propagating. For the general case, crack tips should always be drilled out at a minimum and further repaired if necessary. In specimen 2, a better job was done of removing the crack, and the resulting repair reflected that improved strength.

No difference was noticed between repairs made to the two types of steel. The fatigue life of the original detail constructed of the lower strength steel was significantly less than that of high strength steel (roughly half), but this was more likely due to the removal of the lug plate. Adding the lug greatly reduces stresses at the hot spot by making the connection as a whole much stiffer. If the cracked detail in question has no lug plate, it is recommended that a lug be added in conjunction with whatever other repair strategy is taken, in order to further prolong the detail's life.

Table 3.1: Simple-attachment specimen stress comparison.

Items	Positive		Negative		
	Calculated	Measured	Calculated	Measured	
Load Span	111	112	111	111	KN
Stress 1	55	46	-55	-50	Mpa
Stress 2	18	16	-18	-15	Mpa
Stress 3	-23	-20	23	24	Mpa
Stress 4	-55	-46	55	52	Mpa
Stress 5	55	46	-55	-44	Mpa
Stress 6	55	47	-55	51	Mpa
Stress 7	28	25	-28	-27	Mpa

Table 3.2: Repair information table for simple-attachment specimen 1.

Legend	
1st letter=	Top or Bottom
2nd letter=	Edge or Center
3rd letter=	East or West
4th letter=	Web or Flange

Specimen 1

Crack	Number of Cycles	Stress Range	Metal that Cracked	Repair Metal	Notes	
1st BEEF	985987	100 MPa	Base	E7018	crack tip in web drilled out with a 14 mm hole, access hole gouged into web, top 3/4 of crack air-arc gouged out, gouge refilled with weld metal, weld root and remainder of crack gouged out from bottom side of flange, gouge refilled with weld metal, all weld toes are hammer-peened	set 1
1st BCEF	985987	100 MPa	Base	E7018		
1st BCWF	985987	100 MPa	Base	E7018		
1st BEWF	985987	100 MPa	Base	E7018		
1st TEEF	1051537	100 MPa	Base	E7018	crack tip in web drilled out with a 14 mm hole, access hole gouged into web , crack gouged out through-thickness, 6 mm thick backing bar welded to bottom of flange, gouge filled with weld metal, backing bar removed	set 2
1st TEEW	1051537	100 MPa	Base	E7018		
1st TCWW	1051537	100 MPa	Base	E7018		
1st BEEW	1051537	100 MPa	Base	E7018		
1st BCWW	1051537	100 MPa	Base	E7018	Repaired in the same manor as the 1st 4 cracks, except no hammer peening	
1st TCEF	1100156	100 MPa	Base	E7018	Same repair as for the top flanges as in set 2, but the backing bars were left in place	set 3
1st TCWF	1100156	100 MPa	Base	E7018		
1st TEWF	1100156	100 MPa	Base	E7018		
1st TCEW	1228237	100 MPa	Base	E7018	Same repair as for the top flanges as in set 2, but the backing bars were left in place	set 4
1st TEWW	1228237	100 MPa	Base	E7018		
2nd BEEW	176700	100 MPa	E7018	E7018		
1st BCEW	1228237	100 MPa	Base	E7018	Repaired in the same manor as the 1st 4 cracks, except no hammer peening	
1st BEWF	1294210	100 MPa	Base	E7018	Repaired in the same manor as the 1st 4 cracks, except no hammer peening	set5
2nd BEWW	343886	100 MPa	E7018	E7018		
2nd TCEF	204102	100 MPa	E7018	E7018	remove backing bar and repaired the same as set 3	set 6
2nd TEWF	234389	100 MPa	E7018	E7018	repair the same as set 6	set 7
3rd BEWW	86556	100 MPa	E7018	E7018	Repaired in the same manor as the 1st 4 cracks, except no hammer peening	set 8
2nd BCWW	348316	100 MPa	E7018	E7018	Repaired in the same manor as the 1st 4 cracks, except no hammer peening	set 9
3rd BEEW	262818	100 MPa	E7018	E7018	Repaired in the same manor as the 1st 4 cracks, except no hammer peening	set10
2nd TEEW	448302	100 MPa	E7018	E7018	Repaired in the same manor as set 6	set 11
2nd TCWF	427730	100 MPa	E7018	E7018	Repaired in the same manor as set 6	set 12
3rd TEEW	80380	100 MPa	E7018	E7018	Repaired in the same manor as set 6	set 13
2nd TCEW	351982	100 MPa	E7018	E7018		
2nd TEEF	528682	100 MPa	E7018	E7018		
4th TEEW	68692	100 MPa	E7018	E7018	No repairs done on these cracks. * means that failure was not reached.	set 14
3rd TEEF*	68692	100 MPa	E7018	E7018		
3rd TCEF*	344653	100 MPa	E7018	E7018		
3rd TCEW*	68692	100 MPa	E7018	E7018		
2nd TCWW*	597374	100 MPa	E7018	E7018		
3rd TCWF*	121025	100 MPa	E7018	E7018		
3rd TEWF*	314473	100 MPa	E7018	E7018		
2ndTEWW*	420674	100 MPa	E7018	E7018		
4th BEEW	157856	100 MPa	E7018	E7018		
2nd BEEF*	698587	100 MPa	E7018	E7018		
2nd BCEF*	698587	100 MPa	E7018	E7018		
2nd BCEW*	420674	100 MPa	E7018	E7018		
3rd BCWW*	249058	100 MPa	E7018	E7018		
2nd BCWF*	698587	100 MPa	E7018	E7018		
2nd BEWF*	354701	100 MPa	E7018	E7018		
4th BEWW*	268145	100 MPa	E7018	E7018		

Table 3.3: Repair information table for simple-attachment specimen 2.

Legend
1st letter= Top or Bottom
2nd letter= Edge or Center
3rd letter= East or West
4th letter= Web or Flange

Specimen 2

Crack	Number of Cycles	Stress Range	Metal that Cracked	Repair Metal	Notes
1st TEEW	2666079	100 MPa	Base	N/A	Hammer peened before loading. No cracks formed
1st TEEF	2666079	100 MPa	Base	N/A	
1st TCEF	2666079	100 MPa	Base	N/A	
1st TCEW	2666079	100 MPa	Base	N/A	
1st TCWW	2666079	100 MPa	Base	N/A	
1st TCWF	2666079	100 MPa	Base	N/A	
1st TEWF	2666079	100 MPa	Base	N/A	
1st TEWW	2666079	100 MPa	Base	N/A	
1st BEEW	2666079	100 MPa	Base	N/A	
1st BEEF	2666079	100 MPa	Base	N/A	
1st BCEF	2666079	100 MPa	Base	N/A	
1st BCEW	2666079	100 MPa	Base	N/A	
1st BCWW	2666079	100 MPa	Base	N/A	
1st BCWF	2666079	100 MPa	Base	N/A	
1st BEWF	2666079	100 MPa	Base	N/A	
1st BEWW	2666079	100 MPa	Base	N/A	

set 1

Table 3.4: Repair information table for simple-attachment specimen 3.

Legend
1st letter= Top or Bottom
2nd letter= Edge or Center
3rd letter= East or West
4th letter= Web or Flange

Specimen 3

Crack	Number of Cycles	Stress Range	Metal that Cracked	Repair Metal	Notes		
1st TCEW	782049	100 MPa	Base	E7018	access hole gouged out, 2-sided weld repair used on the flange	1st repair	
1st TCWF	782049	100 MPa	Base	E7018	TEWF fractured 3/4 of beam depth: repaired with crack tip drilled out, 2-sided weld repair and 2, 152x203x6 mm doubler plates welded onto web	1st repair	
1st TEWF	782049	100 MPa	Base	E7018			
1st TEEF	945595	100 MPa	Base	E7018	all done with 2-sided weld repairs	2nd repair	
1st BEEF	945595	100 MPa	Base	E7018			
1st BCEW	945595	100 MPa	Base	E7018			
1st BCWW	945595	100 MPa	Base	E7018	2-sided weld repairs w/ HP, crack in web at TCEF fixed with a 2-sided weld repair after crack tip drilled out with a 17mm hole	3rd repair	
1st TCEF	1060068	100 MPa	Base	E7018			
1st BCWF	1060068	100 MPa	Base	E7018	2-sided weld repair	4th repair	
1st BCEF	1102045	100 MPa	Base	E7018	2-sided weld repair, with the crack in the web at BEEF drilled out w/ a 17mm hole	5th repair	
2nd BEEF	287161	100 MPa	E7018	E7018	2-sided weld repair, with the crack in the web at BCEW drilled out w/ a 17mm hole	6th repair	
2nd TCEW	450707	100 MPa	E7018	E7018			
2nd BCEW	287163	100 MPa	E7018	E7018	2-sided weld repair	7th repair	
2nd BCWW	287163	100 MPa	E7018	E7018			
1st TCWW	1311976	100 MPa	Base	E7018	2-sided weld repair w/ web repaired with a 2-sided weld repair	8th repair	
2nd TCWF	465155	100 MPa	E7018	E7018	2-sided weld repair w/ web repaired with a 2-sided weld repair	9th repair	
3rd TCEW	683709	100 MPa	E7018	E7018			
2nd TCWF	1134416	100 MPa	E7018	E7018	2-sided weld repair	10th repair	
2nd TEEF	1368142	100 MPa	E7018	E7018			
3rd BCWW	1040006	100 MPa	E7018	E7018	2-sided weld repair	11th repair	
3rd TCWW	544566	100 MPa	E7018	E7018			
4th TCEW	621259	100 MPa	E7018	E7018	2-sided weld repair	12th repair	
3rd BEEF	13979744	100 MPa	E7018	E7018	final crack	runouts	
3rd TEEF*	316993	100 MPa	E7018	E7018	Runouts of repair welds		
2nd TCEF*	1570662	100 MPa	E7018	E7018			
5th TCEW*	93006	100 MPa	E7018	E7018			
4th TCWW*	308649	100 MPa	E7018	E7018			
3rd TCWF*	714265	100 MPa	E7018	E7018			
2nd TEWF*	1848681	100 MPa	E7018	E7018			
2nd BCEF*	1528685	100 MPa	E7018	E7018			
3rd BCEW*	1356999	100 MPa	E7018	E7018			
4th BCWW*	316993	100 MPa	E7018	E7018			
2nd BCWF*	1570662	100 MPa	E7018	E7018			
1st BEWF*	2630730	100 MPa	E7018	E7018			Doubler plate on web from repair #1 stiffened this so it would not crack Preemptively hammer peened
1st TEEW*	2630730	100 MPa	E7018	E7018			
1st TEWW	2630730	100 MPa	E7018	E7018			
1st BEEW	2630730	100 MPa	E7018	E7018			
1st BEWW	2630730	100 MPa	E7018	E7018			

Table 3.5: Repair information table for simple-attachment specimen 4.

Legend	
1st letter=	Top or Bottom
2nd letter=	Edge or Center
3rd letter=	East or West
4th letter=	Web or Flange

Specimen 4

Crack	Number of Cycles	Stress Range	Metal that Cracked	Repair Metal	Notes	
1st TCEF	884607	100 MPa	Base	E7018	17mm holes drilled to start access holes, remainder of holes gouged	repair 1
1st TEWF	884607	100 MPa	Base	E7018	All flanges repaired with a 2-sided weld repair and then hammer peened	
1st BCEF	884607	100 MPa	Base	E7018	TEWF web repair - 17mm hole drilled at crack tip, 2 sided weld repair,	
1st BCWW	884607	100 MPa	Base	E7018	24mm* hole used to remove weld termination	
1st BEWF	884607	100 MPa	Base	E7018		repair 2
1st TEEF	1041225	100 MPa	Base	E7018	14mm holes drilled to start access holes, remainder of holes gouged out	
1st TCEW	1041225	100 MPa	Base	E7018	Flanges repaired with 2-sided weld repairs	
1st TCWF	1041225	100 MPa	Base	E7018		
1st BEEF	1041225	100 MPa	Base	E7018		
1st BCEW	1041225	100 MPa	Base	E7018		
1st BCWF	1041225	100 MPa	Base	E7018		
1st TCWW	1163191	100 MPa	Base	E7018	gouge out access hole, 2 sided weld repair for flange	repair 3
2nd TEEF	215768	100 MPa	E7018	E7018	2-sided weld repair for flange and web	repair 4
2nd TCEW	242734	100 MPa	E7018	E7018	2-sided weld repair for flange	repair 5
2nd BCWF	682526	100 MPa	E7018	E7018	2-sided weld repair for flange , 24mm hole drill at crack tip in web	repair 6
2nd BEEF	758276	100 MPa	E7018	E7018	2-sided weld repair for flange	repair 7
3rd TCEW	732416	100 MPa	E7018	E7018	2-sided weld repair for flange and web	repair 8
2nd BCEW	1077352	100 MPa	E7018	E7018	2-sided weld repair for flange	repair 9
3rd TEEF	913346	100 MPa	E7018	E7018	2-sided weld repair for flange and web	repair 10
2nd TCWW	1111081	100 MPa	E7018	E7018	2-sided weld repair for flange , 24mm hole drill at crack tip in web	repair 11
2nd TCWF	1277605	100 MPa	E7018	E7018	2-sided weld repair for flange , 24mm hole drill at crack tip in web	repair 12
3rd TCWF	381744	100 MPa	E7018	E7018	2-sided weld repair for flange	repair 13
3rd BCEW	581997	100 MPa	E7018	E7018	BCEW had a 24mm hole drilled at the crack tip	
1st TEEW*	2823612	100 MPa	Base	N/A	preemptive hammer peening	final failure and runouts
1st TEWW*	2823612	100 MPa	Base	N/A		
1st BEEW*	2823612	100 MPa	Base	N/A		
1st BEWW*	2823612	100 MPa	Base	N/A		
2nd TCEF*	1939005	100 MPa	E7018	N/A	hammer peened in repair number 1	
2nd TEWF*	1939005	100 MPa	E7018	N/A		
2nd BCEF*	1939005	100 MPa	E7018	N/A		
2nd BCWW	1939005	100 MPa	E7018	N/A		
2nd BEWF*	1939005	100 MPa	E7018	N/A		
4th TEEF*	653273	100 MPa	E7018	N/A	weld repair runouts	
4th TCEW*	807237	100 MPa	E7018	N/A		
3rd TCWW*	549340	100 MPa	E7018	N/A		
4th TCWF*	122911	100 MPa	E7018	N/A		
3rd BEEF*	1024111	100 MPa	E7018	N/A		
4th BCEW*	122911	100 MPa	E7018	N/A		
3rd BCWF*	1099861	100 MPa	E7018	N/A		

Table 3.6: Repair information table for simple-attachment specimen 5.

Legend	
1st letter=	Top or Bottom
2nd letter=	Edge or Center
3rd letter=	East or West
4th letter=	Web or Flange

Specimen 5

Crack	Number of Cycles	Stress Range	Metal that Cracked	Repair Metal	Notes	
1st TEEW*	2000000	100 MPa	Base	N/A	All attachments were preemptively hammer peened. No cracks found.	repair set 1
1st TEEF*	2000000	100 MPa	Base	N/A		
1st TCEF*	2000000	100 MPa	Base	N/A		
1st TCEW*	2000000	100 MPa	Base	N/A		
1st TCWW*	2000000	100 MPa	Base	N/A		
1st TCWF*	2000000	100 MPa	Base	N/A		
1st TEWF*	2000000	100 MPa	Base	N/A		
1st TEWW*	2000000	100 MPa	Base	N/A		
1st BEEW*	2000000	100 MPa	Base	N/A		
1st BEEF*	2000000	100 MPa	Base	N/A		
1st BCEF*	2000000	100 MPa	Base	N/A		
1st BCEW*	2000000	100 MPa	Base	N/A		
1st BCWW*	2000000	100 MPa	Base	N/A		
1st BCWF*	2000000	100 MPa	Base	N/A		
1st BEWF*	2000000	100 MPa	Base	N/A		
1st BEWW*	2000000	100 MPa	Base	N/A		

Table 3.7: Repair information table for complex-attachment specimens.

Full-scale repair table

Crack	Number of Stress		Metal that Repair		Notes
	Cycles	Range	Cracked	Metal	
SW#1	508810	78.4 MPa	Base	E71-T1	No holes drilled at the end of the crack, no shielding gas used on one side of weld.
SW#2	46420	78.4 MPa	E71-T1	E7018	19 mm holes drilled at ends of weld repair to remove defects
SW#3	197190	78.4 MPa	E7018	E7018	Holes at ends of crack not filled, but ground out with Dremmel tool
SW#4	88760	78.4 MPa	E7018	E7018	Same as SE #2, except 13 mm backing bar was used and a 254mmx76mmx19mm doubler plate was welded over the repair on the outside flange
SW#5	198380	71.4 MPa	E7018	NA	Same as SW#4, except that a 102mmx241mmx19mm doubler was added to the web
SW#6	263160*	71.4 MPa	E7018	NA	Had an 3 mm crack that was not growing after this number of cycles
SE #1	732750	78.4 MPa	Base	E7018	19 mm holes drilled at ends of weld repair to remove defects
SE #2	59560	78.4 MPa	E7018	E7018	25 mm holes drilled at weld termination, after previous holes were plug welded. A 6 mm thick backing bar was used
SE #3	128090	78.4 MPa	E7018	E7018	Same as SE #2
SE #4	82880	78.4 MPa	E7018	E7018	Same as SW#4, except for a 76mmx229mmx19mm and a 95mmx254mmx19mm doubler plates were added to the flange and web respectively.
SE #5	359420*	71.4 MPa	E7018	NA	Had an 6 mm crack that was not growing after this number of cycles
NE #1	943300	78.4 MPa	Base	E7018	No stop holes drilled after weld repair at end of crack. Cracks not through thickness when repaired.
NE #2	107480	78.4 MPa	E7018	E7018	13 mm stop holes where drilled at the ends of the repair weld.
NE #3	85220	78.4 MPa	E7018	E7018	13 mm stop holes where drilled at the ends of the repair weld. 6 mm backing bars were used for plug welding previous stop hole. Top toe of weld was hammer peened
NE #4	71330	78.4 MPa	E7018	E7018	Same as NE # 1, except for the bottom toe of the weld was hammer peened.
NE #5	97130	78.4 MPa	E7018	NA	Final failure of a 267 mm crack that was not repaired
NW#1	943300	78.4 MPa	Base	E7018	Same as NE # 1
NW#2	121000	78.4 MPa	E7018	E7018	Same as NE #2
NW#3	142610	78.4 MPa	E7018	E7018	Same as NE #3, but bottom toe was also hammer peened.
NW#4	97130*	78.4 MPa	E7018	NA	Still uncracked after this number of cycles

Table 3.8: Typical chemistry composition for steel used in web frame specimens

	C	Mn	P	S	Si	Ni	Cr	Mo	Cu	Al	Ti	V
Grade 50	0.06	1.20	0.010	0.003	0.18	0.19	0.08	0.044	0.43	0.029	0.001	0.001
A36	0.17	0.31	0.006	0.002	0.24	0.17	0.06	0.039	0.30	0.008	0.001	0.001

Table 3.9: Typical strain gage results for simplified web frame specimens

Gage	Strain ($\mu\epsilon$)	Stress (MPa)
1	-730	-146
2	800	160
3	690	138
4	-1070	-214
5	1020	204
6	-750	-150
7	468	93.6
8	840	168
9	110	22
10	16.6	3.32
11	-121.5	-24.3
12	930	186

Table 3.10: Summary of cracks and repairs on simplified web frame specimen 1

Location	Description	Stress Range (MPa)	Additional Cycles to Failure	Cumulative Cycles to Failure
Webframe-longitudinal connection at cutout C	12 mm thru-thickness	138	27,900	27,900
Repair #1	14 mm stop hole		281,000	309,000
Stiffener weld at cutout C	57 mm thru-thickness	280	300,000	300,000
Repair #1	25 mm stop hole		100	300,100
Repair #2	Vee-and-weld plus 2 - 6 mm thick welded doubler plates		N/A	654,500**
Longitudinal-web frame connection at D	140 mm surface	117	300,000	300,000
Repair #1	Hammer peened		N/A	3,100,000**
Bottom hull at cutout C	32 mm surface crack	165	1,400,000	1,400,000
Repair #1	Hammer peened		1,700,000	3,100,000

Mean Stress = half of stress range shown

**-indicates runout

Table 3.11: Summary of cracks and repairs on simplified web frame specimen 2

Location	Description	Stress Range (MPa)	Additional Cycles to Failure	Cumulative Cycles to Failure
Radius at cutout A	25 mm thru-thickness	100	71,900	71,900*
Repair #1	57 mm stop hole		N/A	2,000,000**
Radius at cutout B	50 mm thru-thickness	-165	318,900	318,900*
Repair #1	57 mm stop hole		N/A	2,000,000**
Radius at cutout C	40 mm thru-thickness	-110	584,200	584,200*
Repair #1	38 mm stop hole		N/A	2,000,000**
Radius at cutout D	25 mm thru-thickness	155	71,900	71,900*
Repair #1	57 mm stop hole		1,308,100	1,380,000
Repair #2	38 mm stop hole		691,900	2,000,000
Lug plate at D	80 mm thru-thickness	155	1,380,000	1,380,000
Repair #1	Vee-and-weld both sides		620,000	2,000,000
Bottom hull at cutout C	40 mm surface	165	584,000	584,000
Repair #1	Hammer Peened		262,000	846,000
Longitudinal-webframe connection at D	130 mm surface	180	586,000	586,000
Repair #1	Hammer Peened		1,279,000	1,865,000
Longitudinal-lug plate connection at D	25 mm surface	150	1,562,000	1,562,000
Repair #1	Hammer Peened		640,000	2,000,000

Mean Stress = half of stress range shown

*-indicates crack was initiated by saw cut

**-indicates runout

Table 3.12: Summary of cracks and repairs on simplified web frame specimen 3

Location	Description	Stress Range (MPa)	Additional Cycles to Failure	Cumulative Cycles to Failure
Radius at cutout A	22 mm thru-thickness	138	340,000	340,000*
Repair #1	38 mm stop hole		N/A	2,500,000**
Radius at cutout B	32 mm thru-thickness	-214	340,000	340,000*
Repair #1	38 mm stop hole		N/A	2,500,000**
Radius at cutout C	19 mm thru-thickness	-150	340,000	340,000*
Repair #1	14 mm stop hole		N/A	2,500,000**
Radius at cutout D	25 mm thru-thickness	205	114,000	114,000*
Repair #1	76 mm stop hole		1,886,000	2,000,000
Repair #2	Vee-and-weld plus bolted doubler plate		N/A	2,500,000**
Stiffener weld at cutout C	22 mm thru-thickness	160	663,000	663,000
Repair #1	38 mm stop hole		1,337,000	2,000,000
Repair #2	24 mm stop hole		500,000	2,500,000
Longitudinal-webframe connection at D	89 mm surface	180	680,000	680,000
Repair #1	Hammer Peened		616,000	1,296,000
Repair #2	Vee-and-weld		704,000	2,000,000
Repair #3	Vee-and-weld plus hammer peening		N/A	2,500,000**

Mean Stress = half of stress range shown

*-indicates crack was initiated by saw cut

**-indicates runout

Table 3.13: Summary of cracks and repairs on simplified web frame specimen 4

Location	Description	Stress Range (MPa)	Additional Cycles to Failure	Cumulative Cycles to Failure
Radius at cutout A	38 mm thru-thickness	111	835,000	835,000*
Repair #1	14 mm stop hole		N/A	3,580,000**
Radius at cutout B	32 mm thru-thickness	-184	583,000	583,000*
Repair #1	8 mm stop hole		N/A	3,580,000**
Radius at cutout C	32 mm thru-thickness	-105	835,000	835,000*
Repair #1	6 mm stop hole		N/A	3,580,000**
Radius at cutout D	44 mm thru-thickness	175	583,000	583,000*
Repair #1	24 mm stop hole + bolt		N/A	3,580,000**

Mean Stress = half of stress range shown

*-indicates crack was initiated by saw cut

**-indicates runout

Table 3.14: Summary of cracks and repairs on simplified web frame specimen 5

Location	Description	Stress Range (MPa)	Additional Cycles to Failure	Cummulative Cycles to Failure
Radius at cutout A	92 mm thru-thickness	116	1,467,800	1,467,800*
Repair #1	17 mm stop hole		1,595,500	3,063,300**
Radius at cutout B	70 mm thru-thickness	-188	1,709,000	1,709,000*
Repair #1	17 mm stop hole		1,354,300	3,063,300**
Radius at cutout C	70 mm thru-thickness	-122	1,709,000	1,709,000*
Repair #1	17 mm stop hole		1,354,300	3,063,300**
Radius at cutout D	48 mm thru-thickness	178	141,600	141,600*
Repair #1	24 mm stop hole		905,400	1,047,000
Repair #2	32 mm stop hole		420,800	1,467,800
Repair #3	35 mm stop hole		1,595,500	3,063,300
Longitudinal/web frame connection at D	203 mm thru-thickness	180	1,210,500	1,210,500
Repair #1	Weld crack without arc gouging		257,300	1,467,800
Repair #2	Vee-and-weld--change from fillet to groove weld		1,595,500	3,063,300**
Longitudinal/web frame connection at C	203 mm thru-thickness	130	1,734,500	1,734,500
Repair #1	Vee-and-weld--change from fillet to groove weld plus hammer peening		1,328,800	3,063,300**
Bottom hull at cutout C	32 mm thru-thickness	165	1,734,500	1,734,500
Repair #1	17 mm stop hole		1,328,800	3,063,300**

Mean stress = half of stress range shown

*-indicates crack was initiated by sawcut

**-indicates runout

Table 3.15: Measured stress ranges in complex web frame specimens

Gage	Specimen 1--with lug		Specimen 2--no lug	
	Strain ($\mu\epsilon$)	Stress (MPa)	Strain ($\mu\epsilon$)	Stress (MPa)
1	25.7	5.14	--	--
2	274	54.7	--	--
3	1220	244	1130	227
4	546	109	276	55.3
5	472	94.4	201	40.2
6	335	67.1	14.4	2.89
7	455	91	1220	245
8	0.144	0.029	222	44.5
9	0.0718	0.014	5.60	1.12
10	170	33.9	296	59.1
11	390	77.9	-6.80	-1.40
12	-117	-23.4	-24.2	-4.80
13	-49.1	-9.82	17.9	3.60

Note: Gages 1 and 2 not used on Specimen #2

Table 3.16: Summary of cracks and repairs on complex web frame specimen 1

Location	Description	Stress Range (MPa)	Additional Cycles to Failure	Cummulative Cycles to Failure
Webframe at bottom of longitudinal connection	50 mm thru-thickness	150	3,050,000	3,050,000
Repair #1	76 mm stop hole		N/A	6,000,000**
Back of Longitudinal at connection to webframe	145 mm thru-thickness	150	3,050,000	3,050,000
Repair #1	Vee-and-groove weld plus hammer peening		635,000	3,685,000
Repair #2	Weld on bracket		2,315,000	6,000,000
Flat bar stiffener at longitudinal connection	70 mm thru-thickness	150	3,432,000	3,432,000
Repair #1	Vee-and-weld		253,000	3,685,000
Repair #2	Vee-and-weld plus bracket added to other side		985,000	4,670,000

Mean Stress = zero

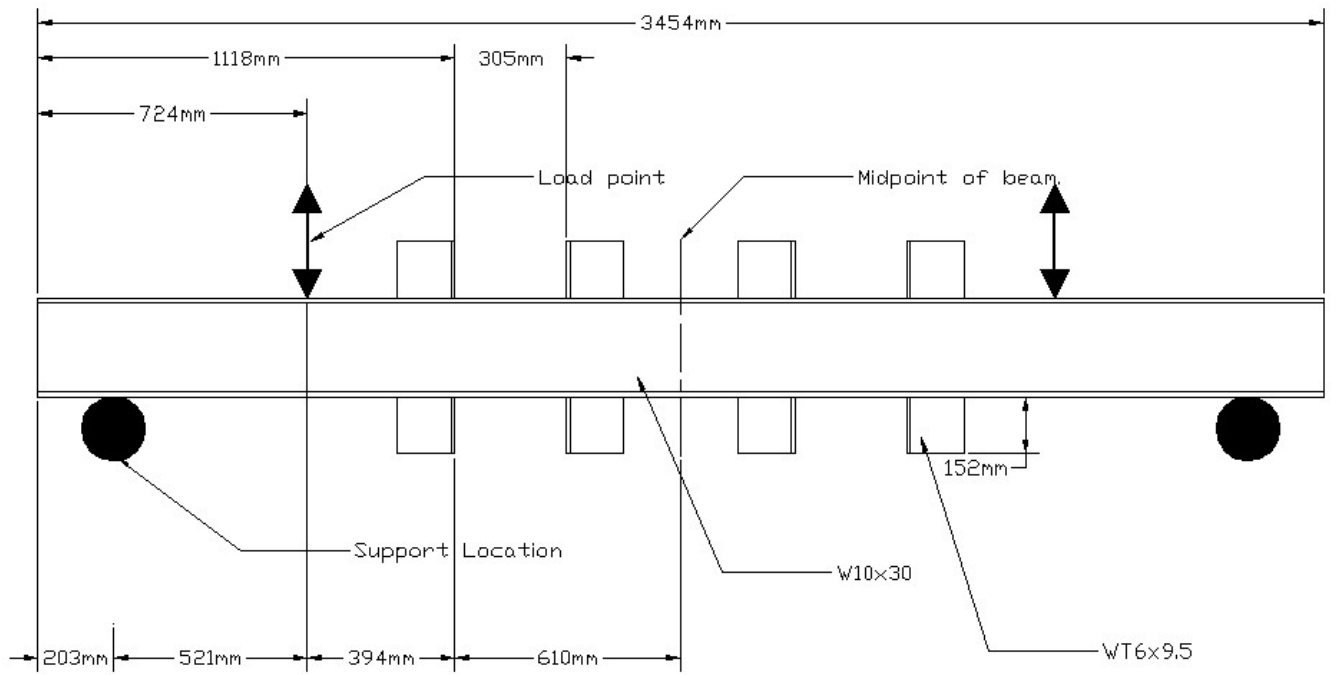
**-indicates runout

Table 3.17: Summary of cracks and repairs on complex web frame specimen 2

Location	Description	Stress Range (MPa)	Additional Cycles to Failure	Cummulative Cycles to Failure
Webframe-longitudinal connection	35 mm thru-thickness	200	1,266,000	1,266,000
Repair #1	38 mm stop hole		N/A	3,000,000**
Longitudinal-bar stiffener connection	32 mm thru-thickness	200	1,266,000	1,266,000
Repair #1	14 mm stop hole		71,000	1,337,000
Repair #2	14 mm stop hole		127,000	1,464,000
Repair #3	Vee & weld + doubler + bracket		N/A	3,000,000**

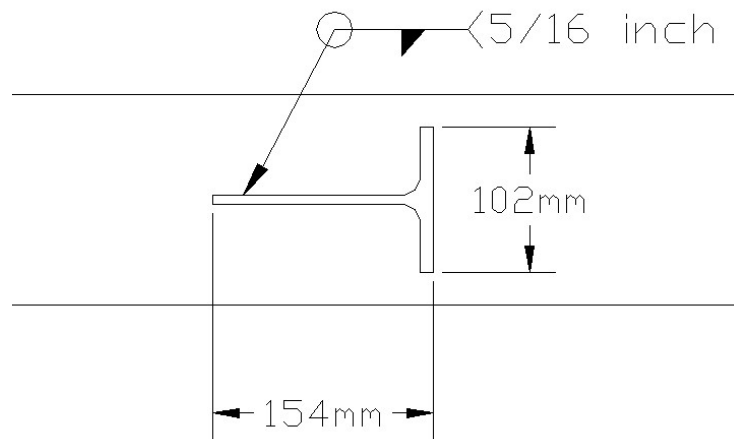
Mean stress = zero

**-indicates runout



NOTE: Symmetric about midpoint.

a) Elevation of specimen showing load and reaction points.



b) Weld details of tee-section attachments.

Figure 3.1: Drawing of simplified-attachment model



Figure 3.2: Simple-attachment specimen before testing.



Figure 3.3: Simple-attachment specimen in test setup.

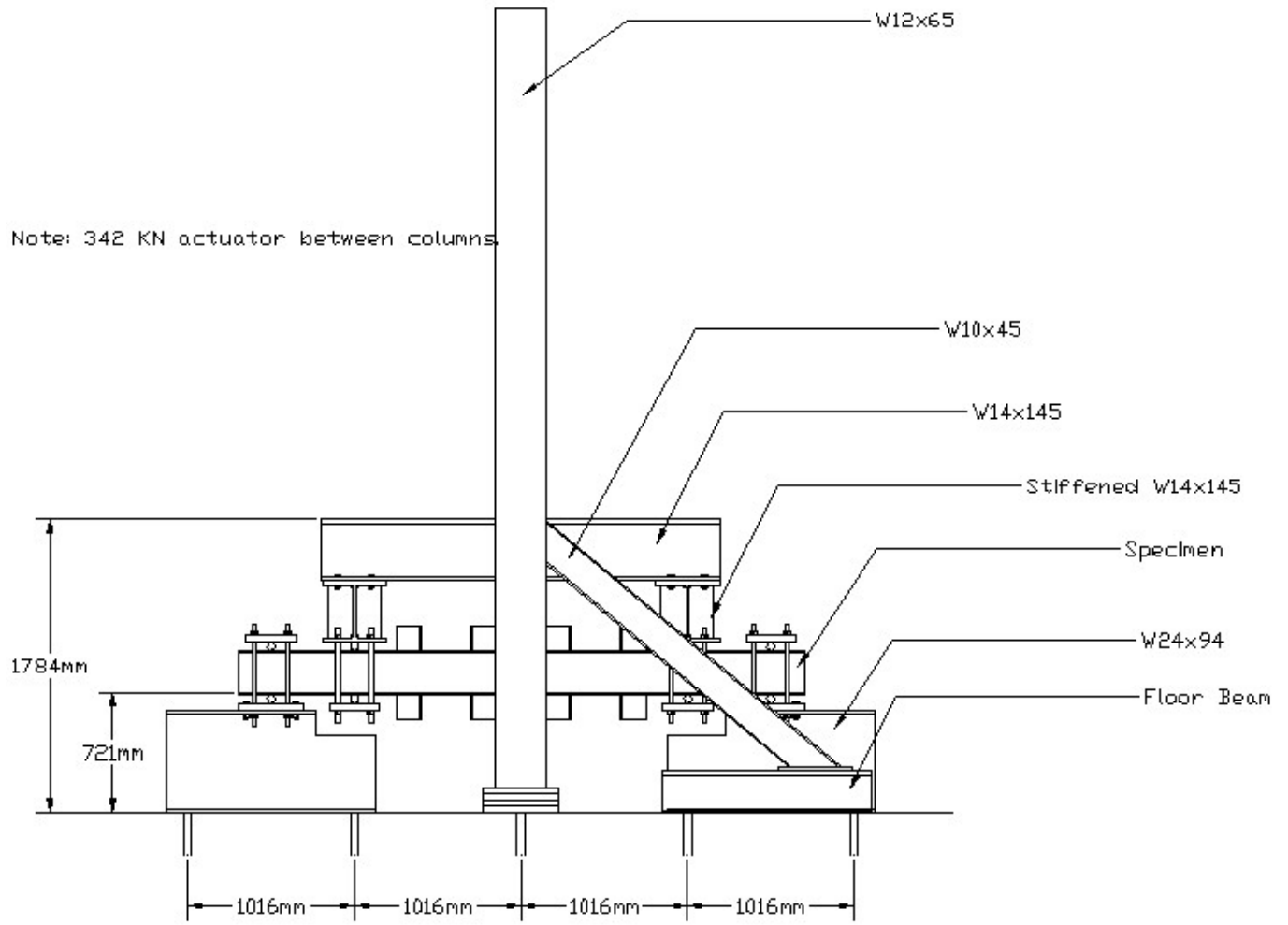


Figure 3.4: Simple-attachment specimen test setup.



Figure 3.5: Clamped-roller connection.

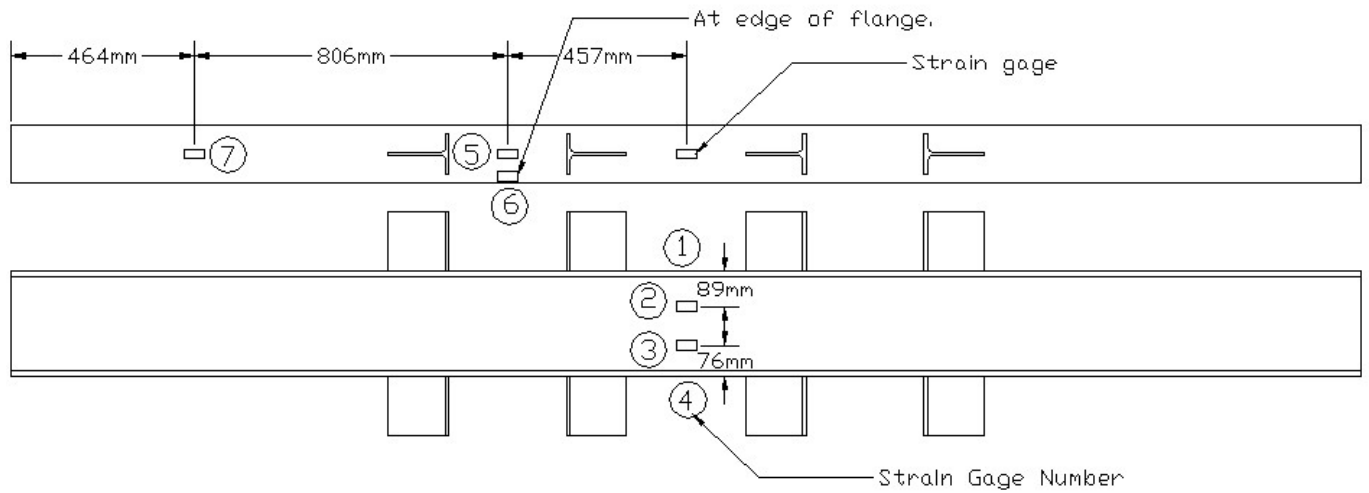
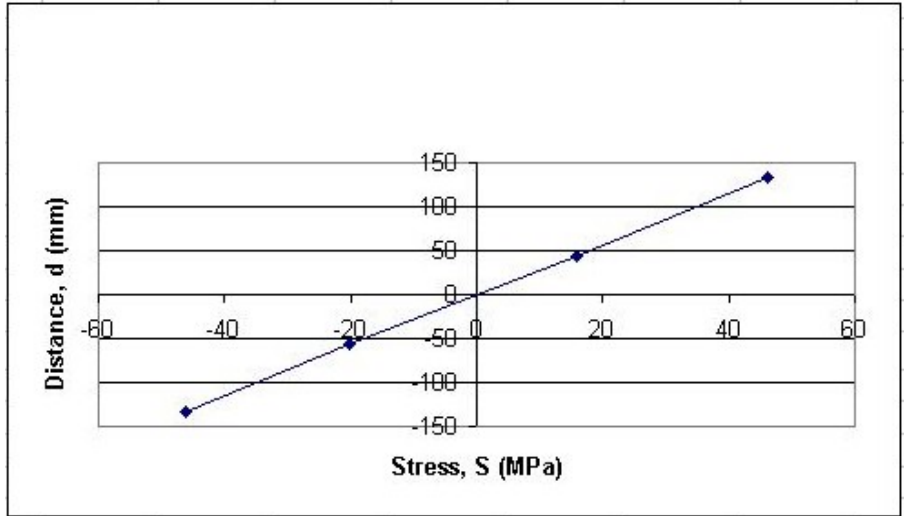
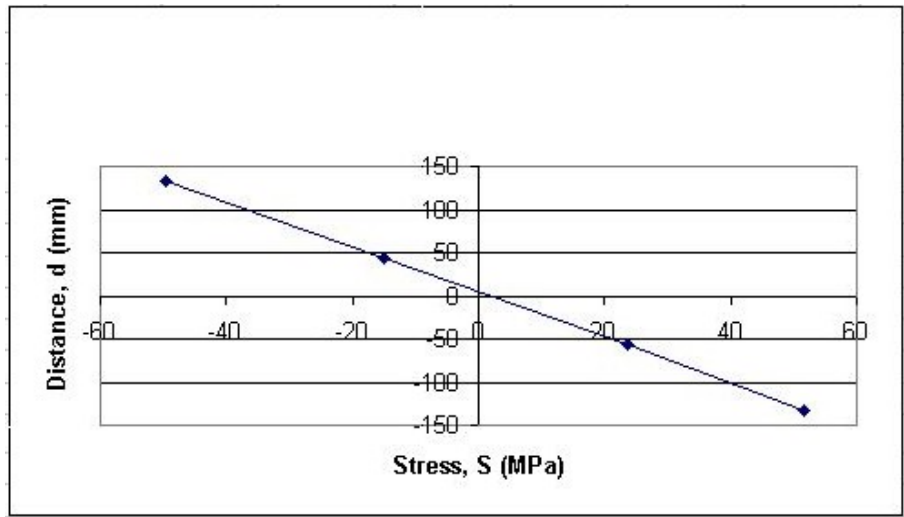


Figure 3.6: Strain-gage layout.

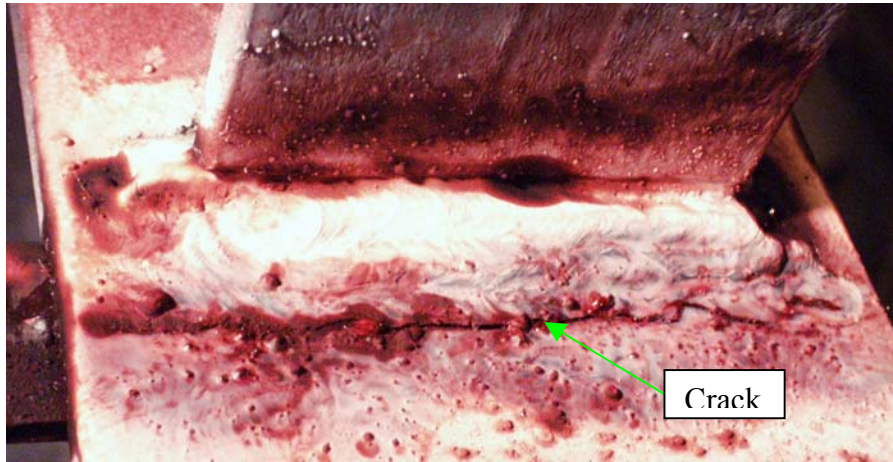


a) Actuator in compression.

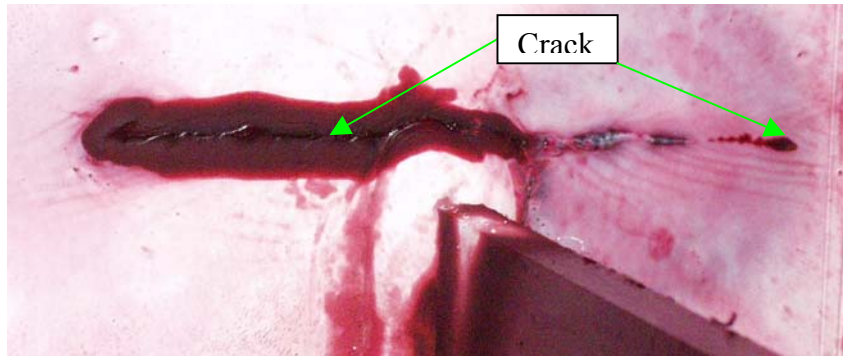


b) Actuator in tension.

Figure 3.7: Stress distribution through the depth of the beam with actuator in tension.



a) Typical crack at flange end of attachment.



b) Typical crack at web end of attachment.

Figure 3.8: Typical cracks in simple-attachment specimens (enhanced by dye penetrant) at the point defined as “failure”.

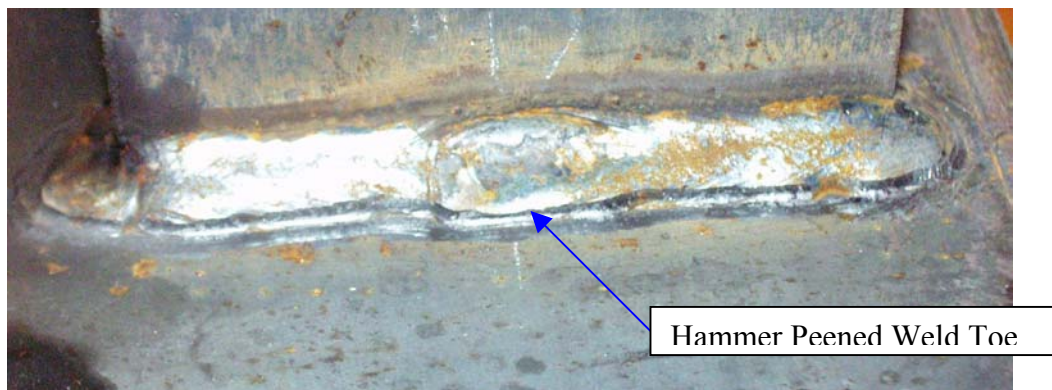


Figure 3.9: Preemptive hammer peening the weld toe.

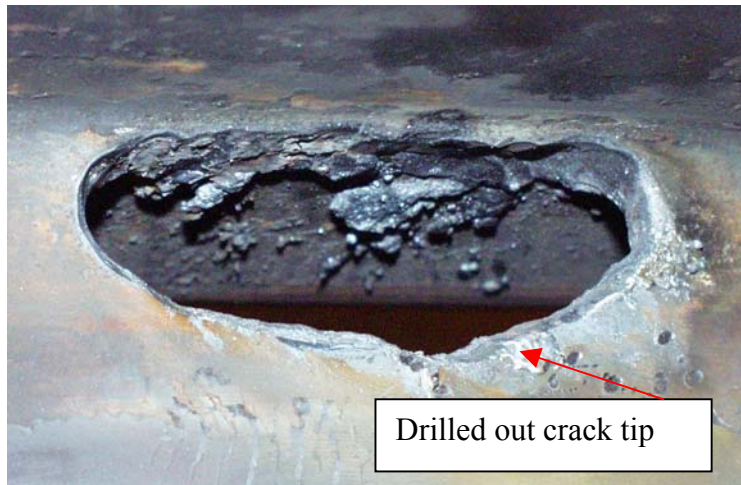


Figure 3.10: Access hole for backside of repairs.



Figure 3.11: Single sided weld repair with backing bar.



a) Attachment side



b) Web side.

Figure 3.12: Single sided weld repair with backing bar removed.

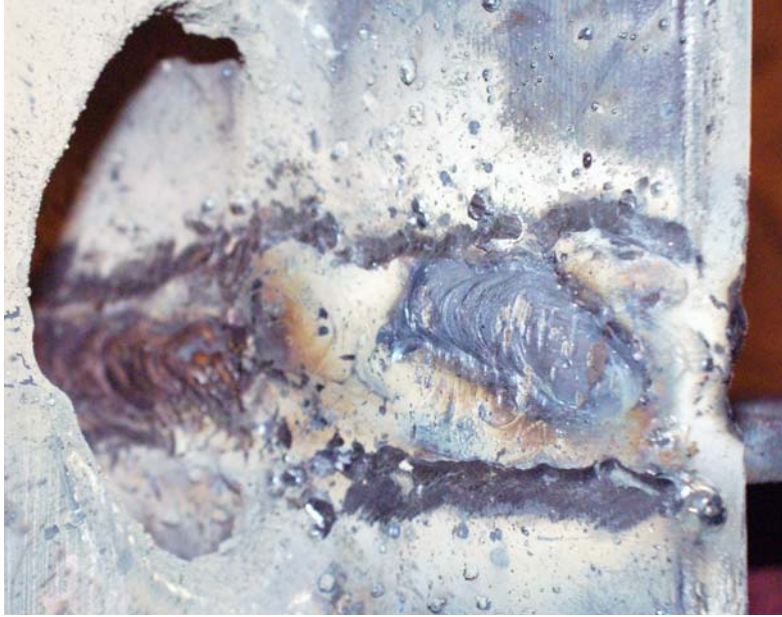


Figure 3.13: The web side of a two-sided weld repair.

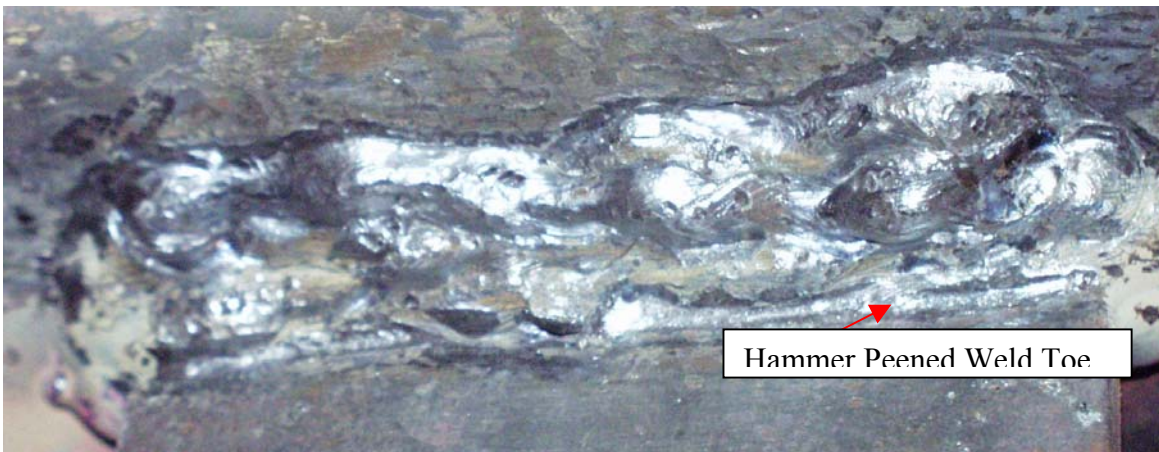


Figure 3.14: The attachment side of a two-sided weld repair with hammer peening.

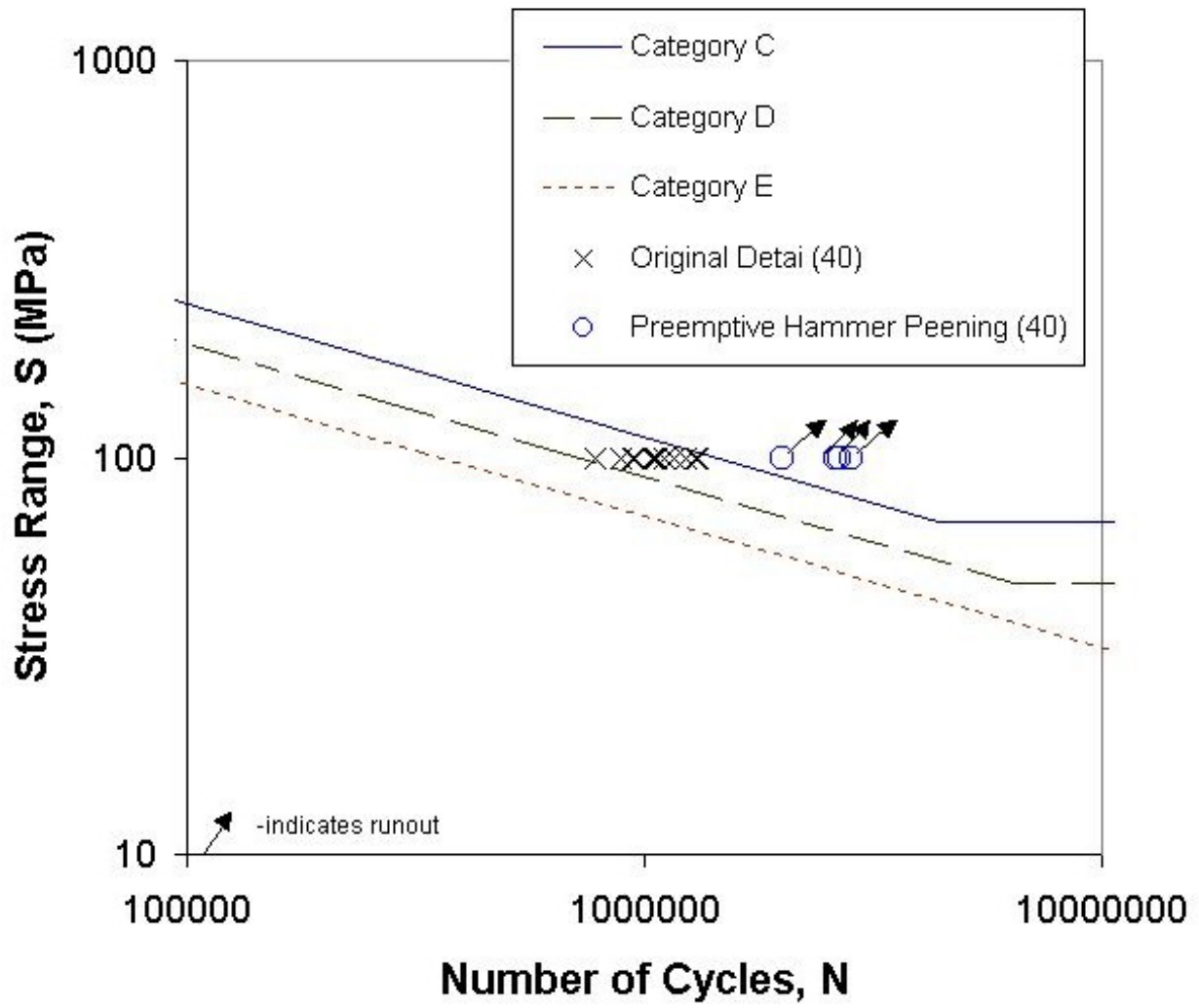


Figure 3.15: S-N curve for original detail and preemptive hammer peening.

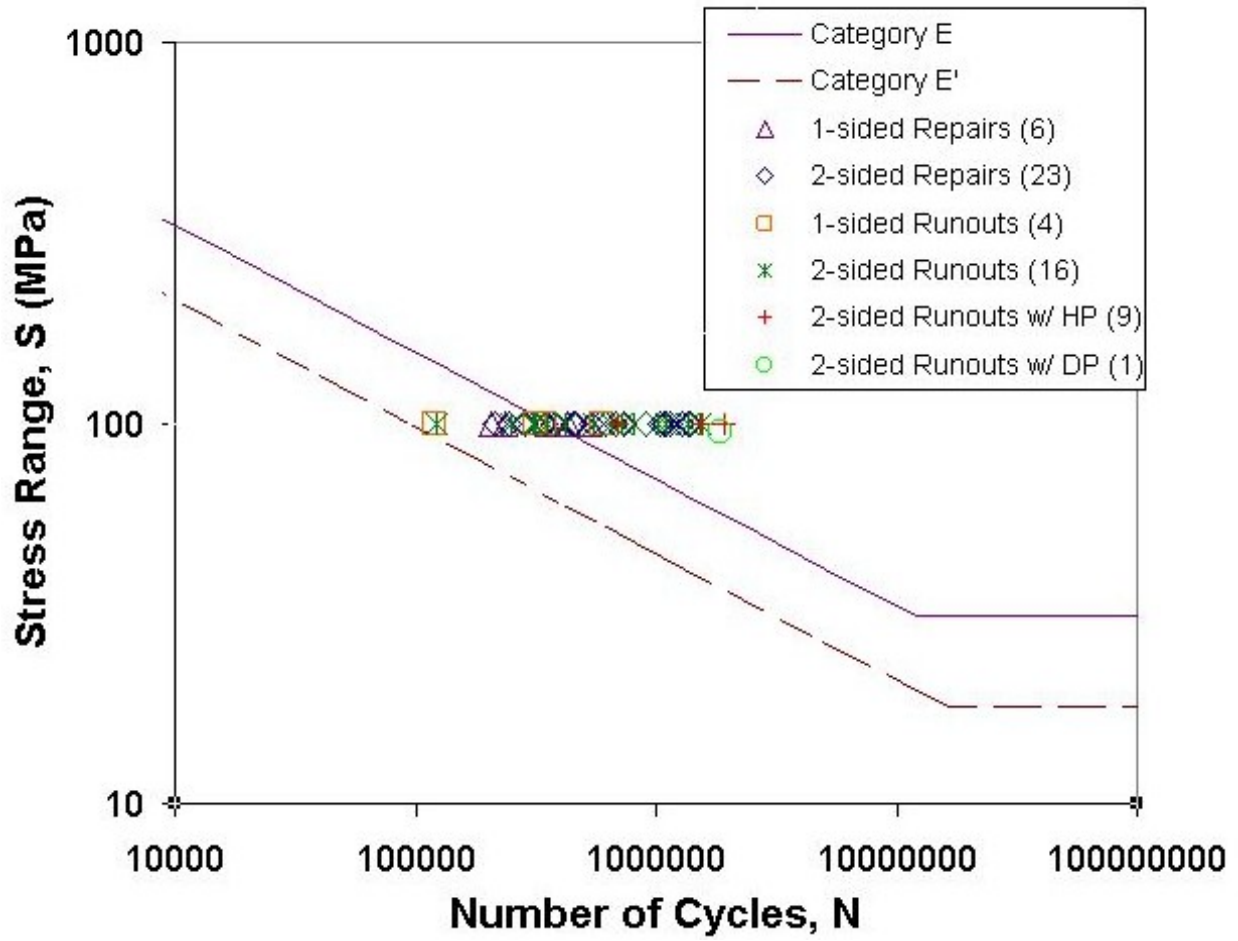


Figure 3.16: S-N curves for simple attachment specimen repairs.

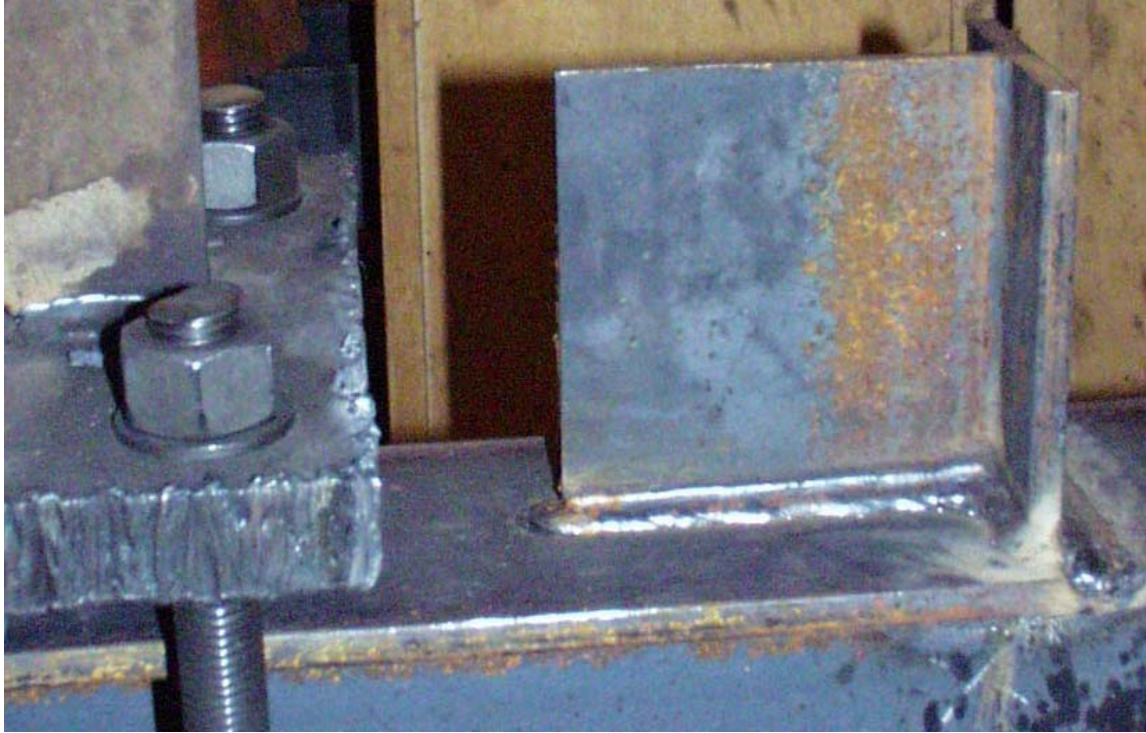


a) Large crack.



b) Repair of crack.

Figure 3.17: Simple attachment specimen doubler plate repair.



a) Top flange.



b) Bottom flange.

Figure 3.18: Area of specimen with inadequate access to attachment for weld repairs.

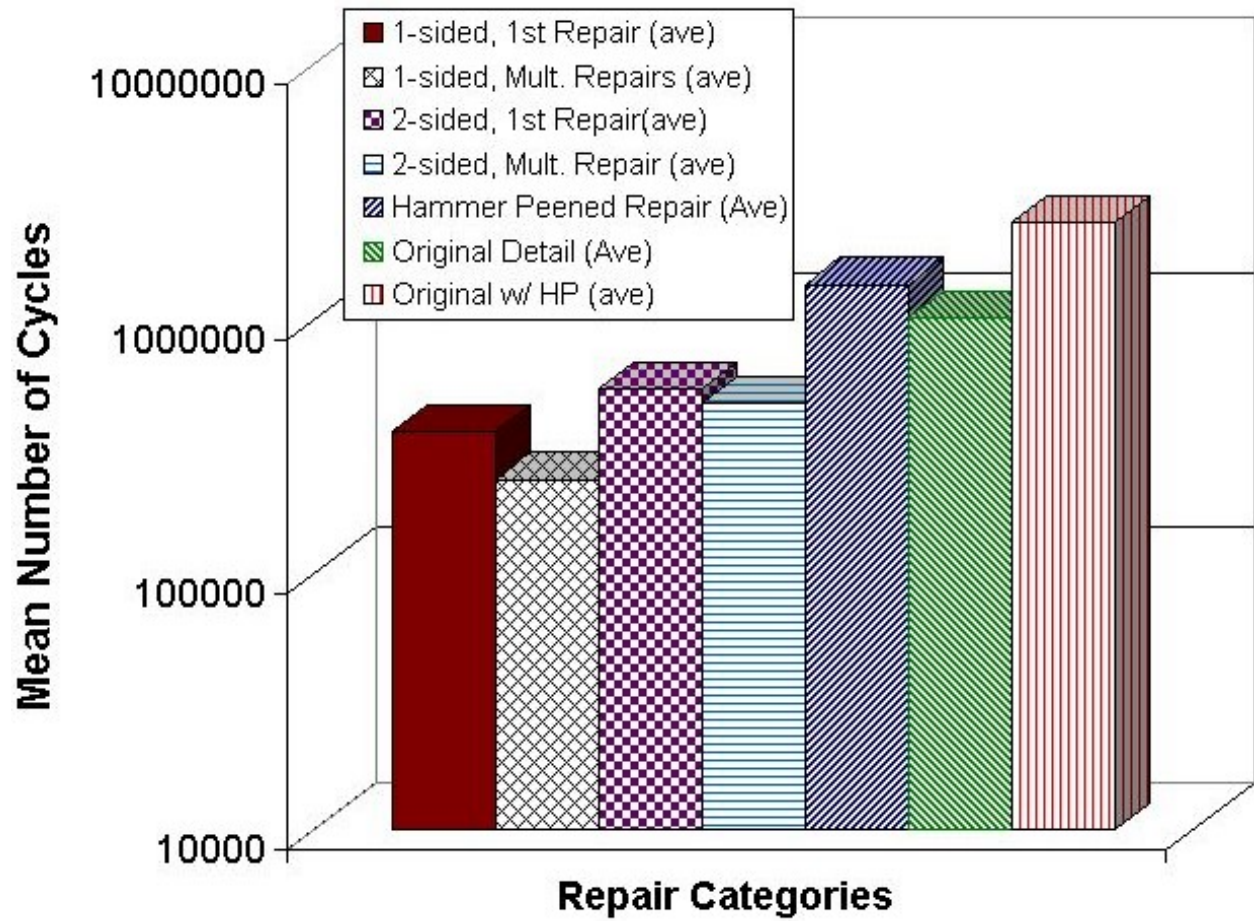
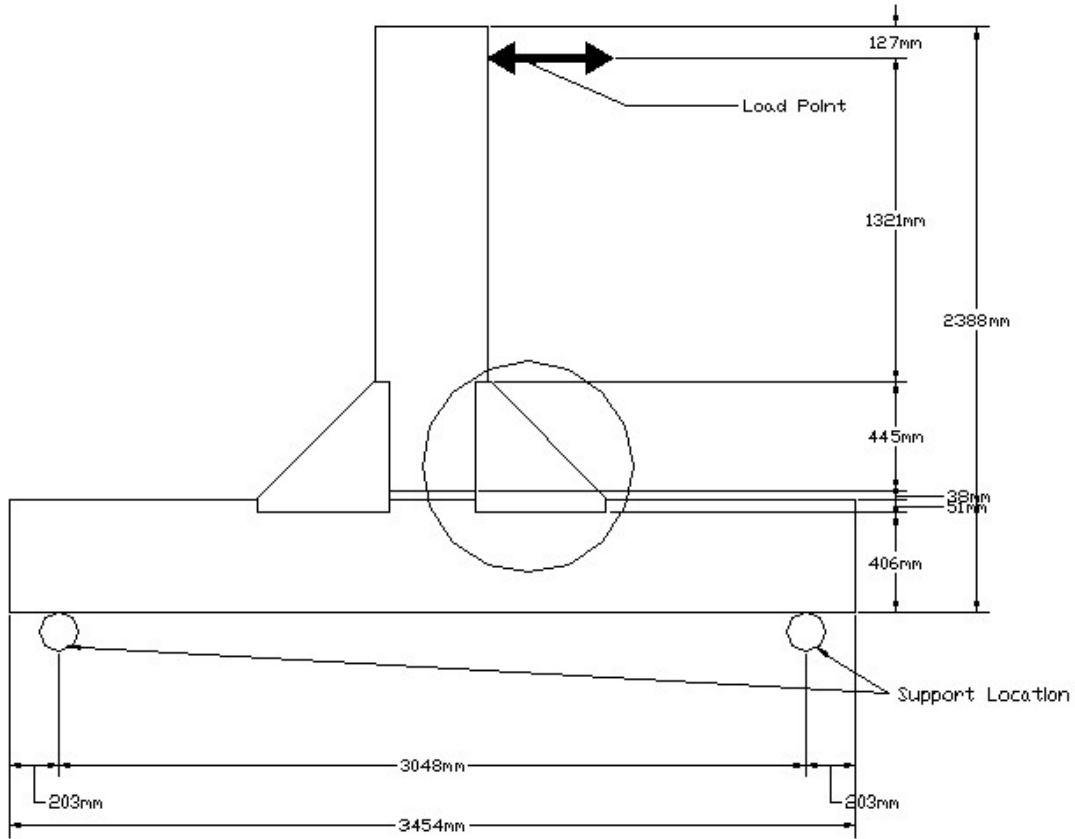
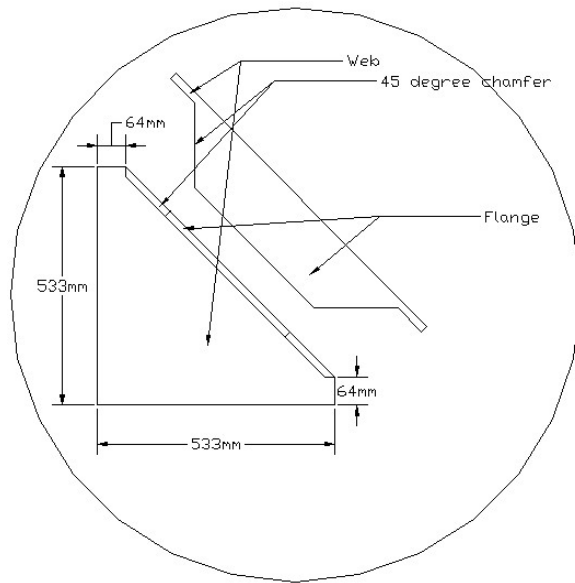


Figure 3.19: Mean life of the logarithmic life of different repair types and original detail at 100 MPa stress range.

Note: All sections come from an MC18x42.7



a) Dimensions and loading.



b) Detail of bracket.

Figure 3.20: Complex bracket attachment specimen.



Figure 3.21: A complex-attachment specimen.



Figure 3.22: Complex-attachment brackets.



Figure 3.23: Complex-attachment test setup.

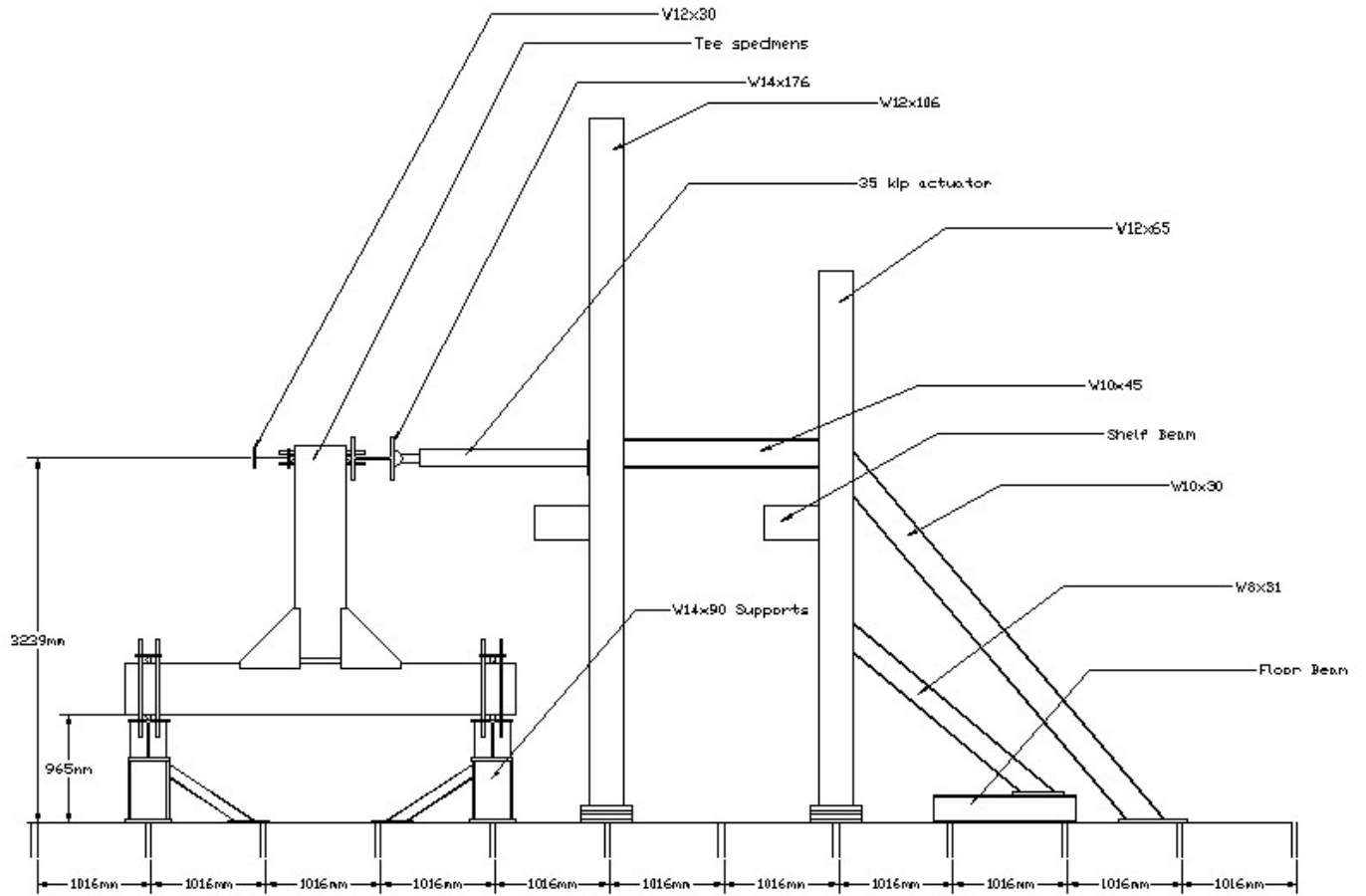


Figure 3.24: Drawing of test setup.



Figure 3.25: Clamped-roller support connection.

Strain Guage layout for
Torsion on both specimens

Strain Guage layout for
stem on North specimen

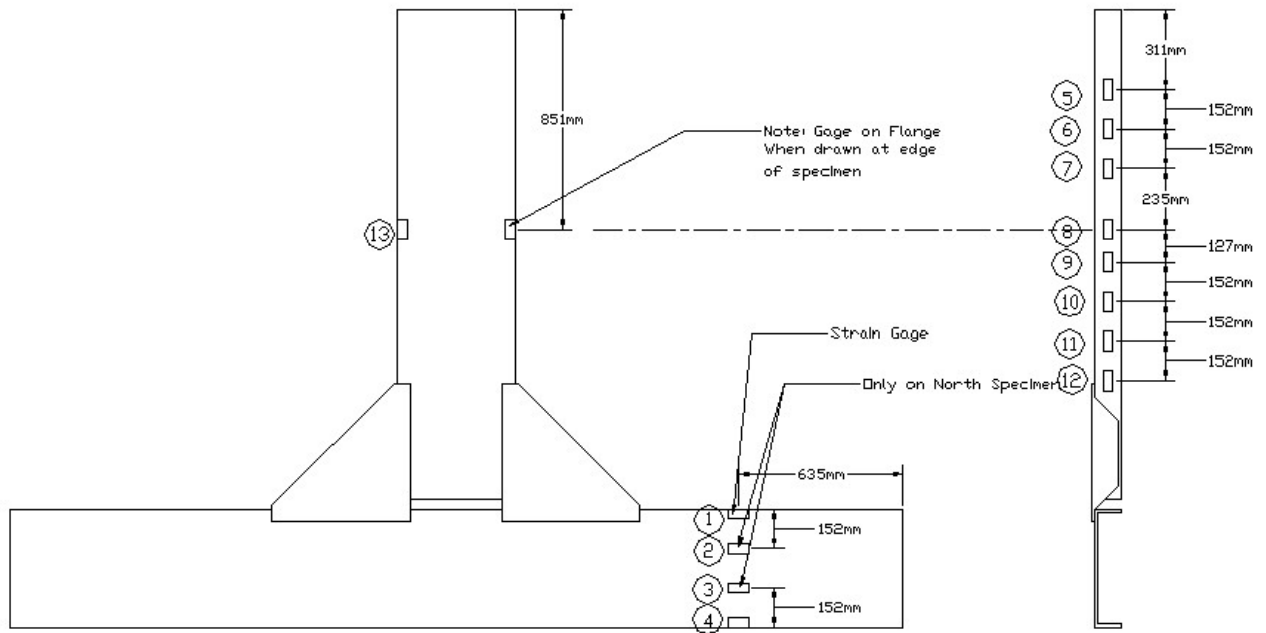
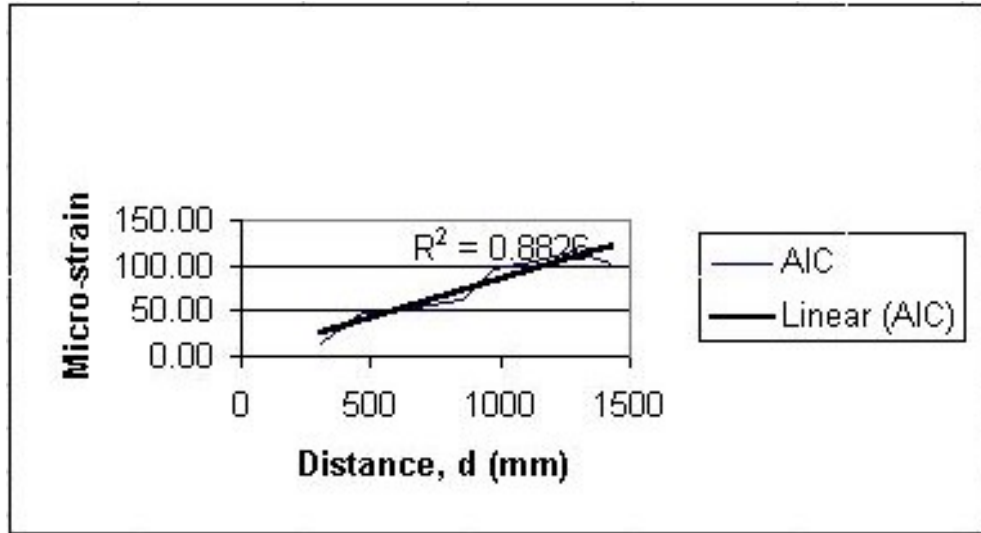
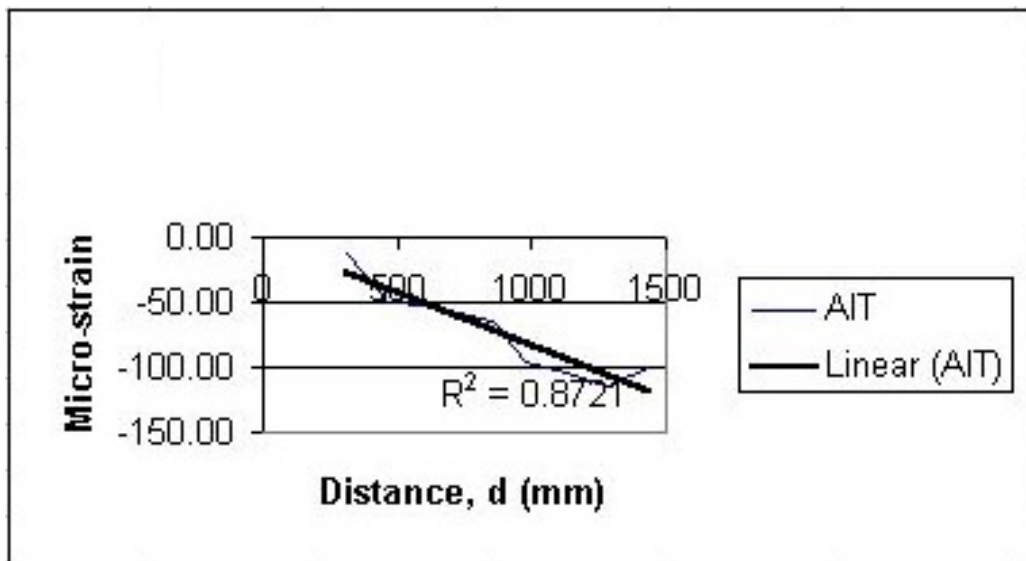


Figure 3.26: Drawing of strain gage layout.

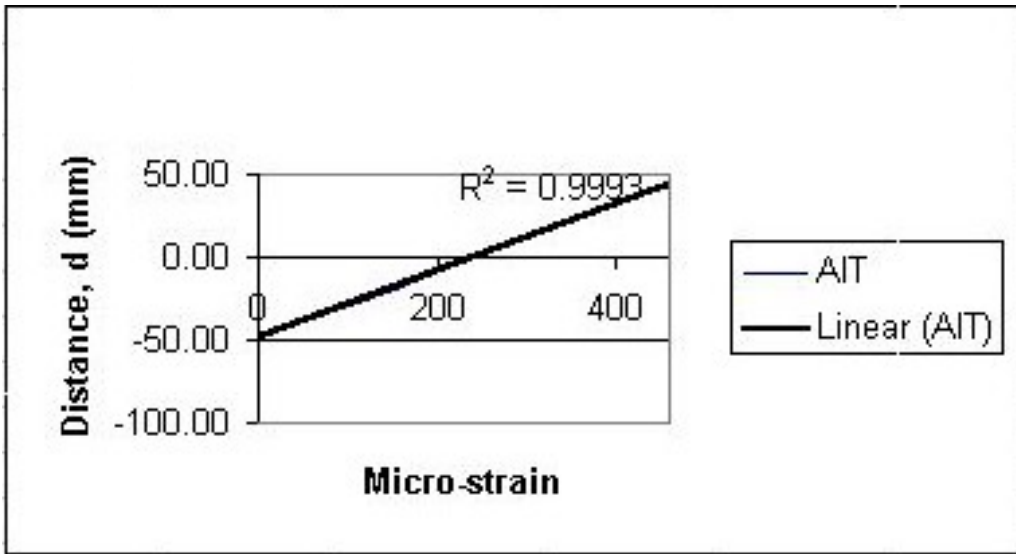


a): Actuator in compression (AIC)

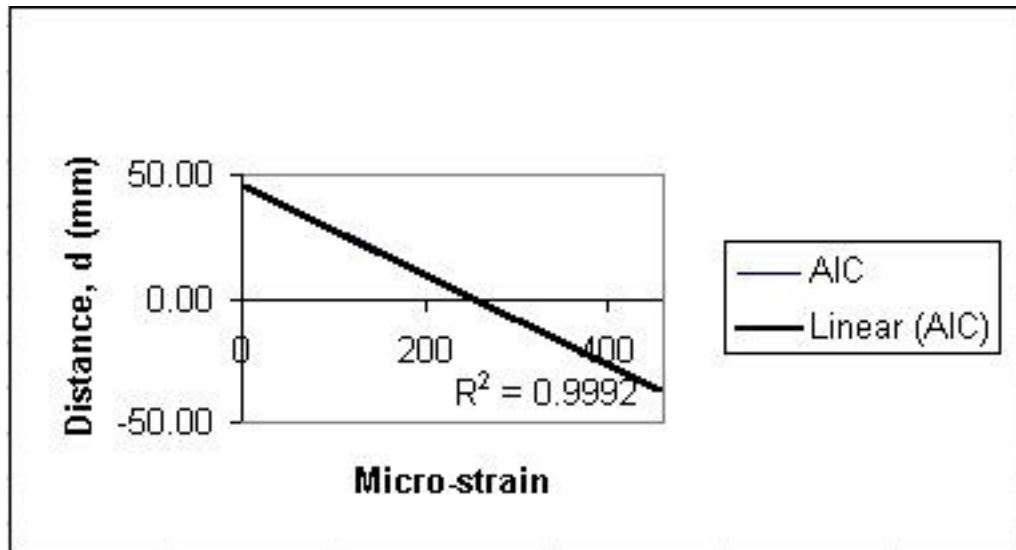


b) Actuator in tension (AIT)

Figure 3.27: Strain gradient along the vertical stem of the tee.



a) actuator in tension.



b) Actuator in compression

Figure 3.28: Linear strain distribution through the depth of the horizontal girder

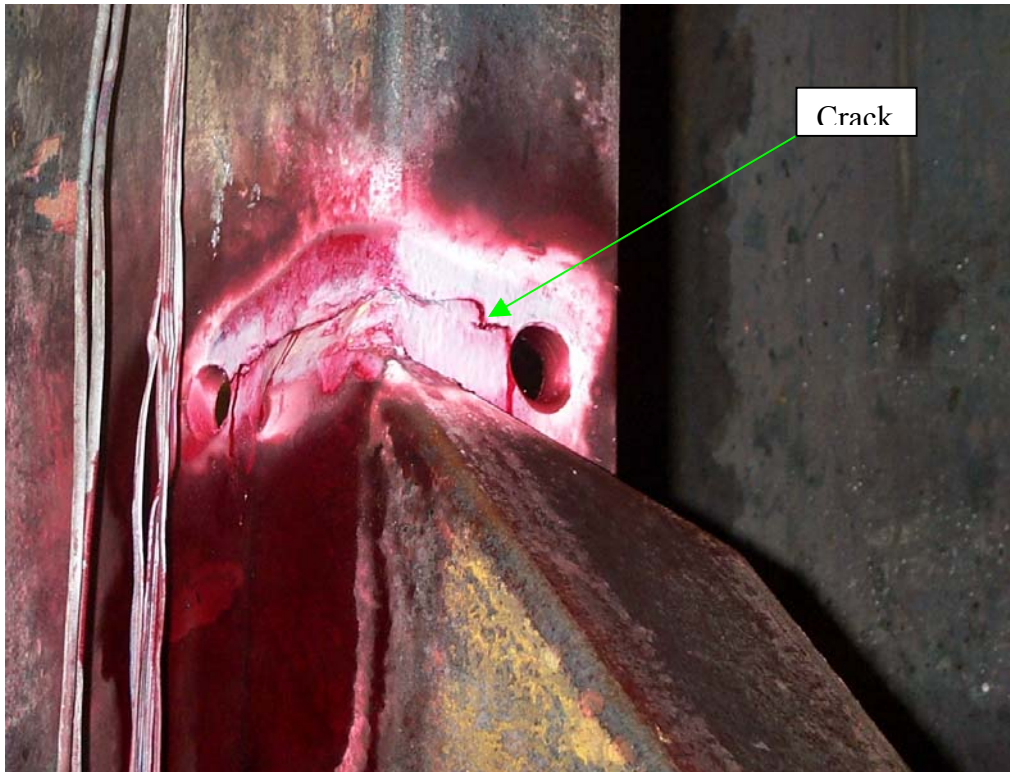


Figure 3.29: A typical crack at the top of the bracket in the complex-attachment specimen.



Figure 3.30: Weld repair of crack not yet through-thickness without termination holes.



Figure 3.31: Weld repair of typical through-thickness crack with termination holes drilled to larger diameter after the weld is complete.



Figure 3.32: Weld repair with ground termination holes.



Figure 3.33: Weld ground after repair.



Figure 3.34: Weld that has been hammer peened after repair.

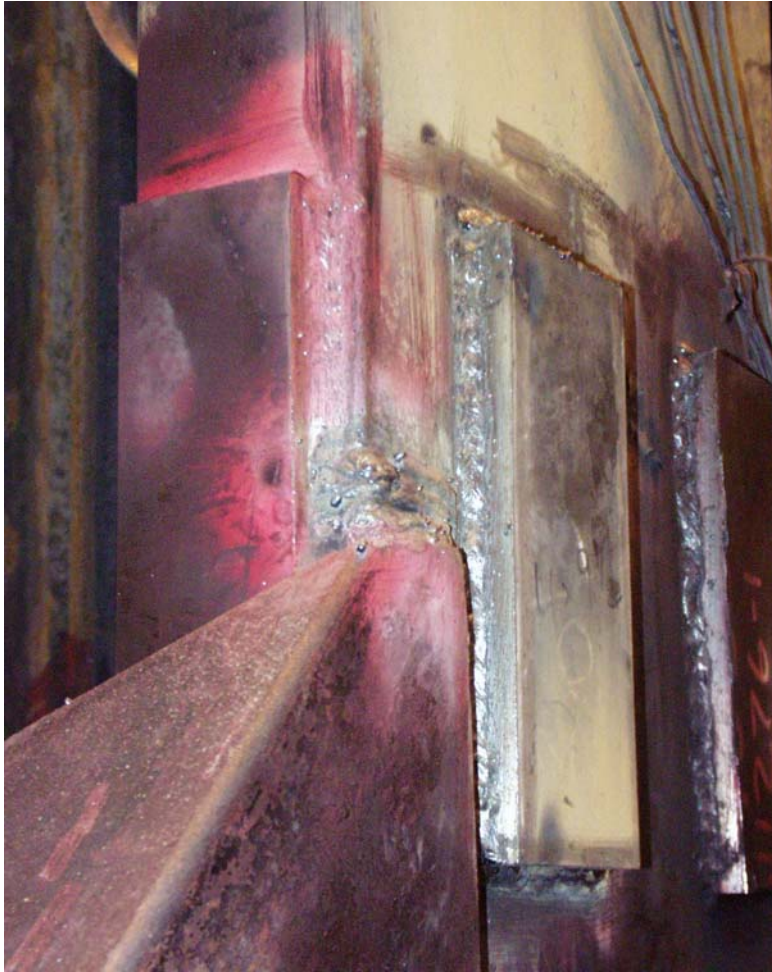


Figure 3.35: Doubler plates welded to reinforce detail.

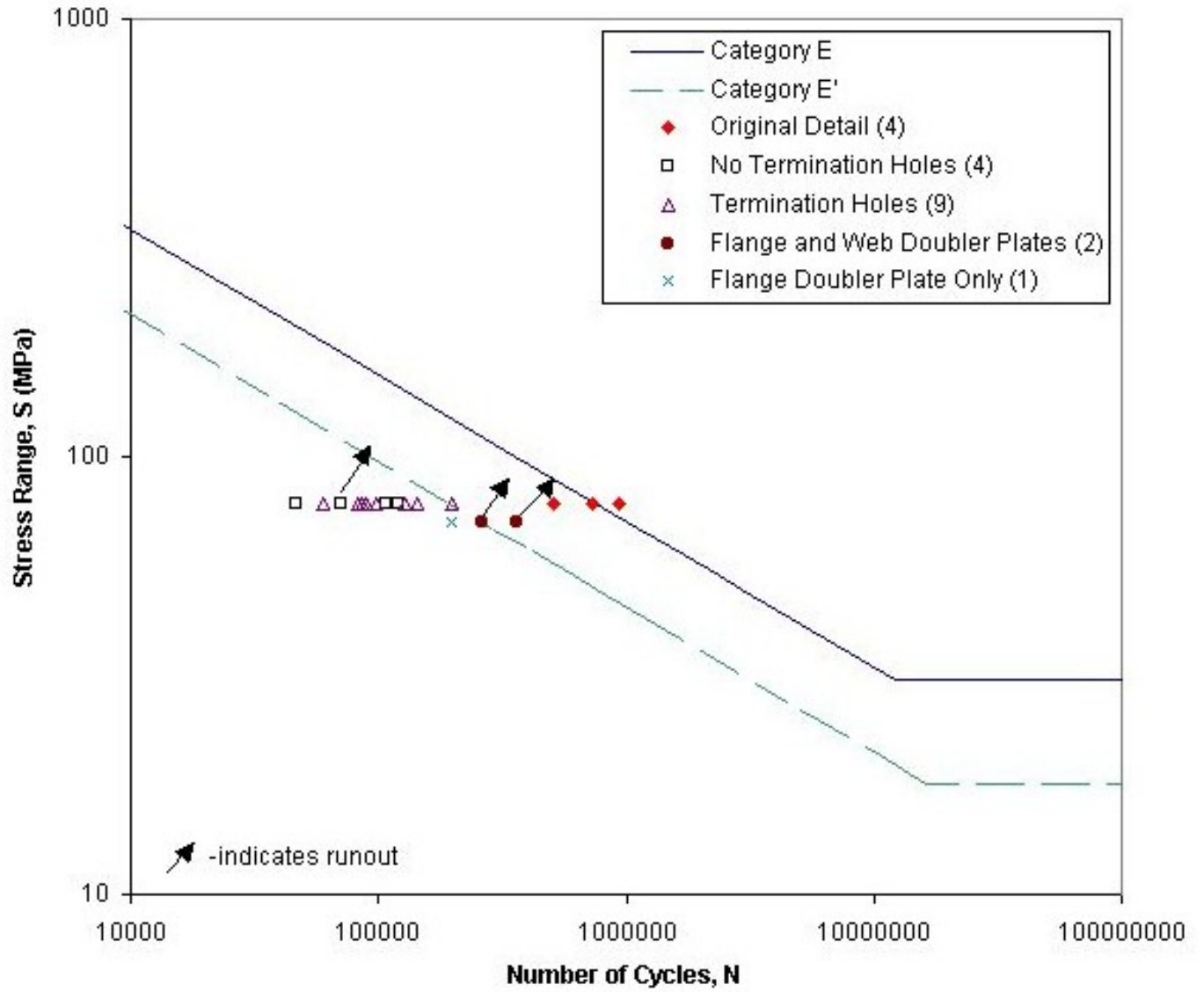


Figure 3.36: S-N curve for complex-attachment specimen.

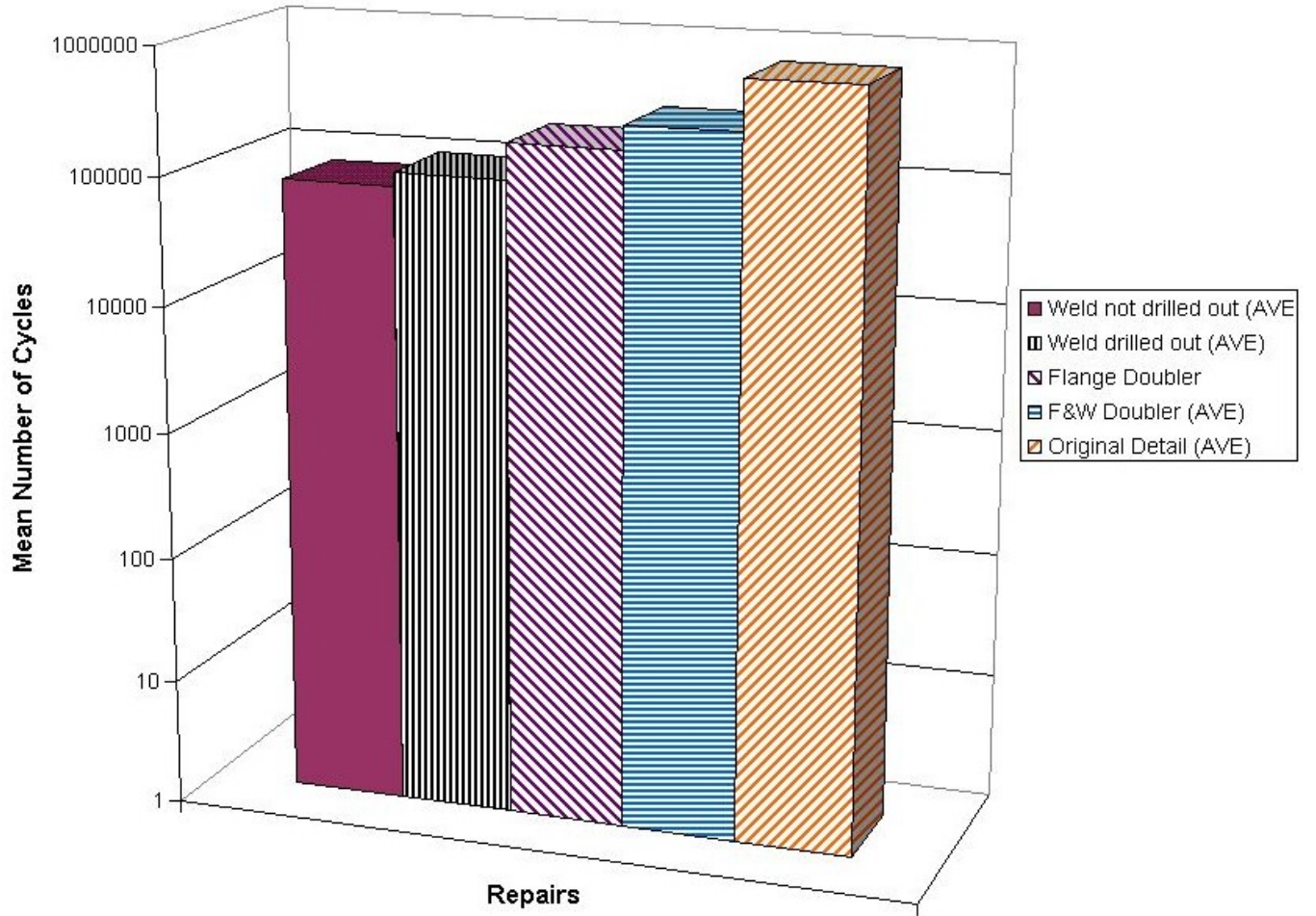


Figure 3.37: Repairs mean value of logarithmic life.

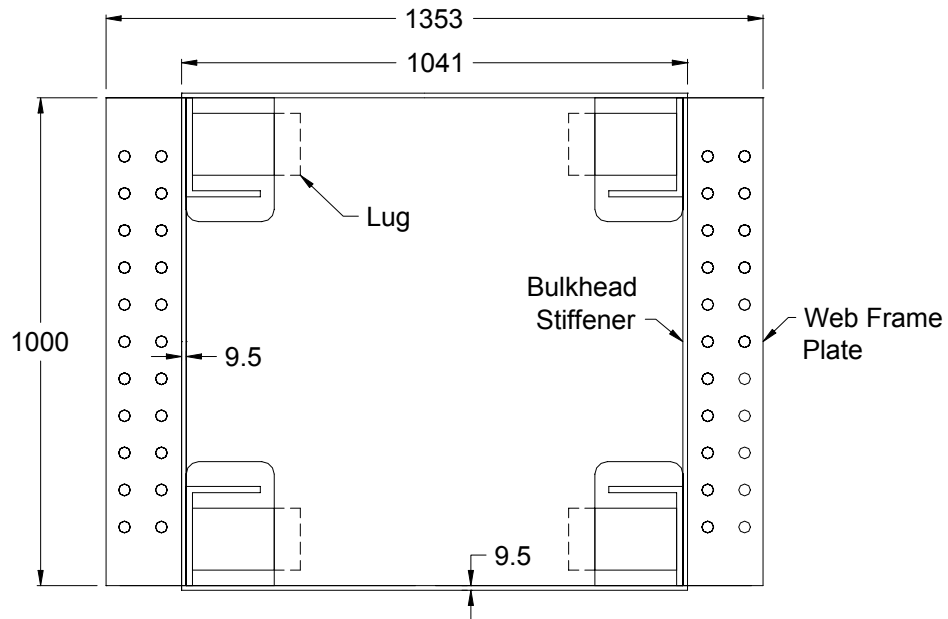


Figure 3.38 Simplified longitudinal/web frame connection specimen drawing
(dimensions in mm)

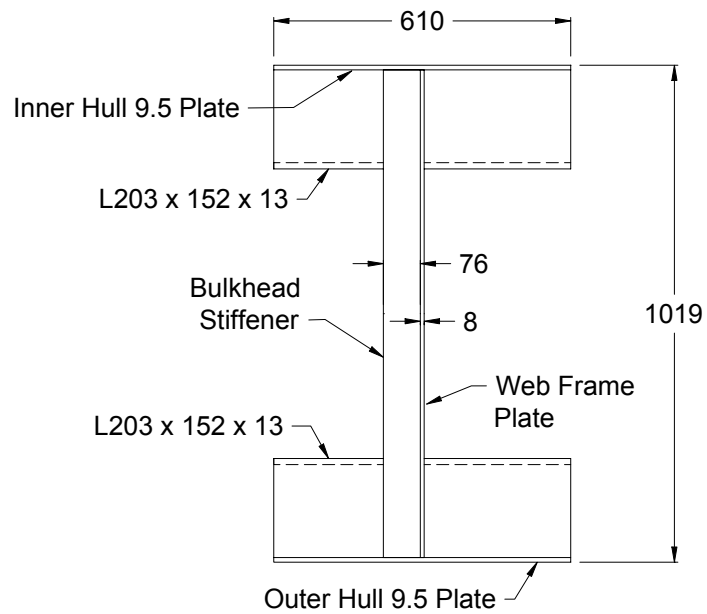


Figure 3.39 Simplified longitudinal/web frame connection specimen drawing (side view)

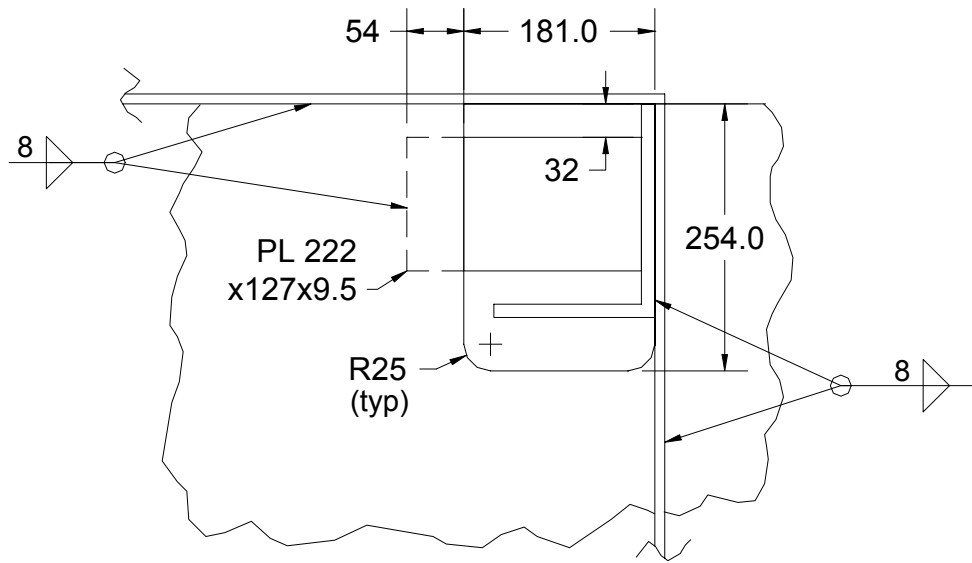


Figure 3.40 Typical connection detail (dimensions in mm)

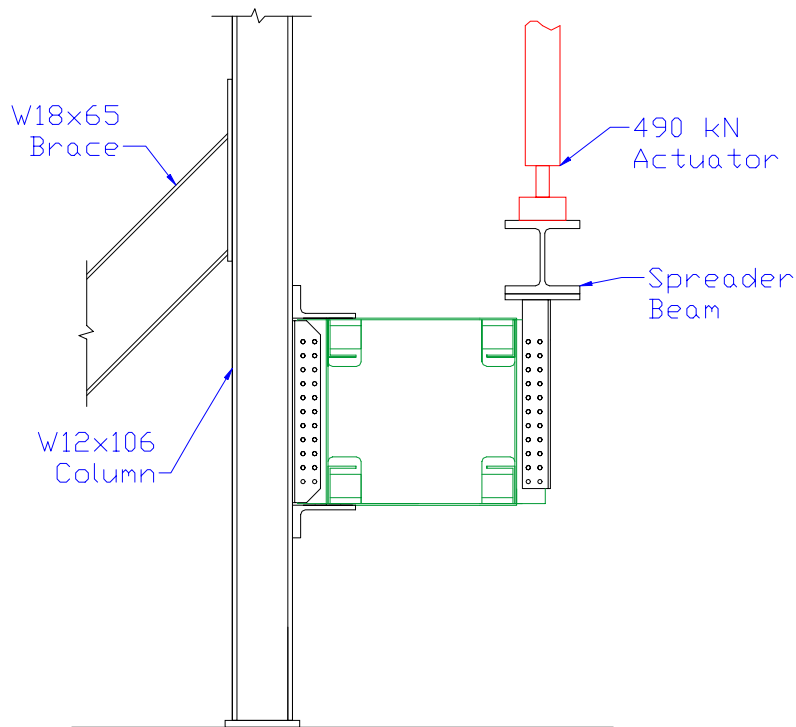


Figure 3.41 Simplified web frame specimen test setup



Figure 3.42 Photo of simplified web frame specimen in test fixture

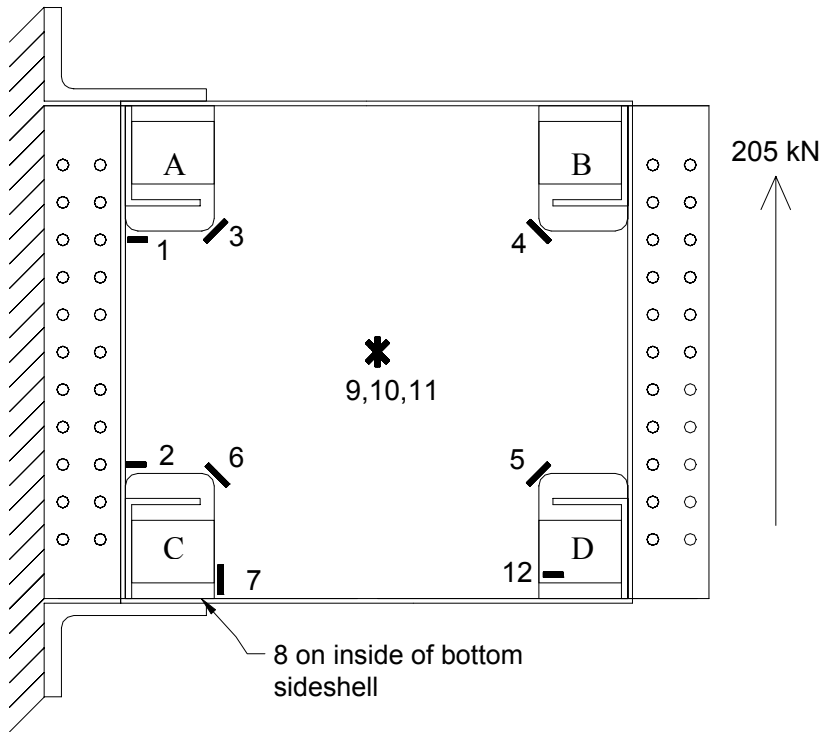


Figure 3.43 Strain gage layout for simplified web frame specimens

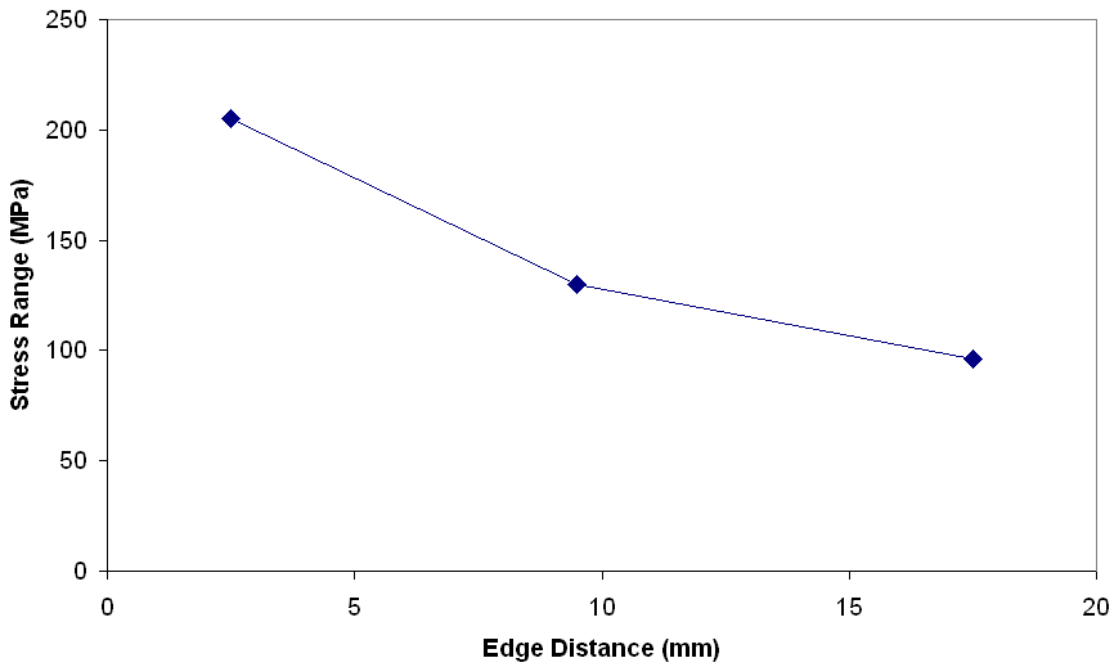


Figure 3.44 Stress gradient approaching cutout radius at detail D

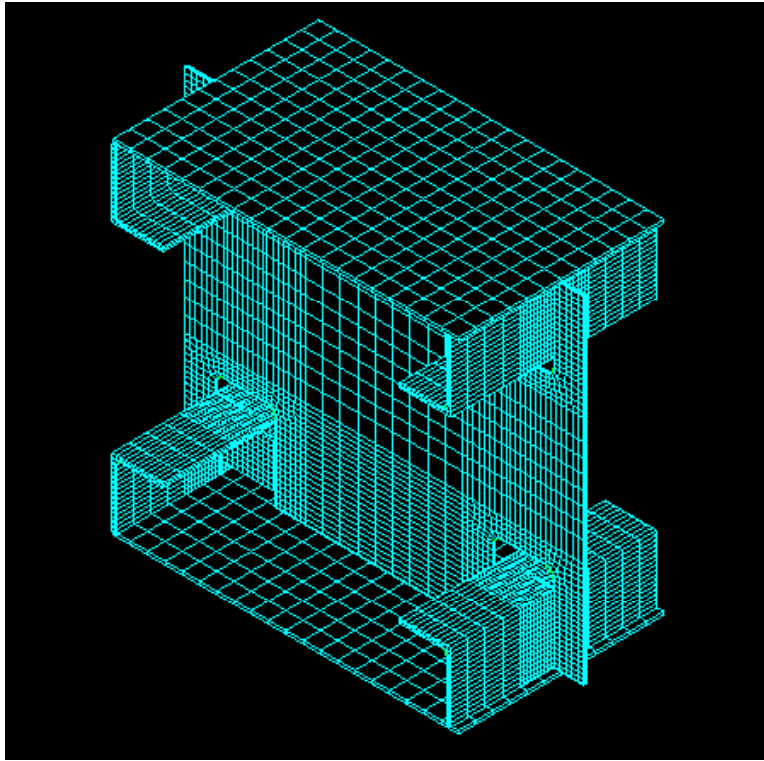


Figure 3.45 Finite element model of simplified web frame specimen

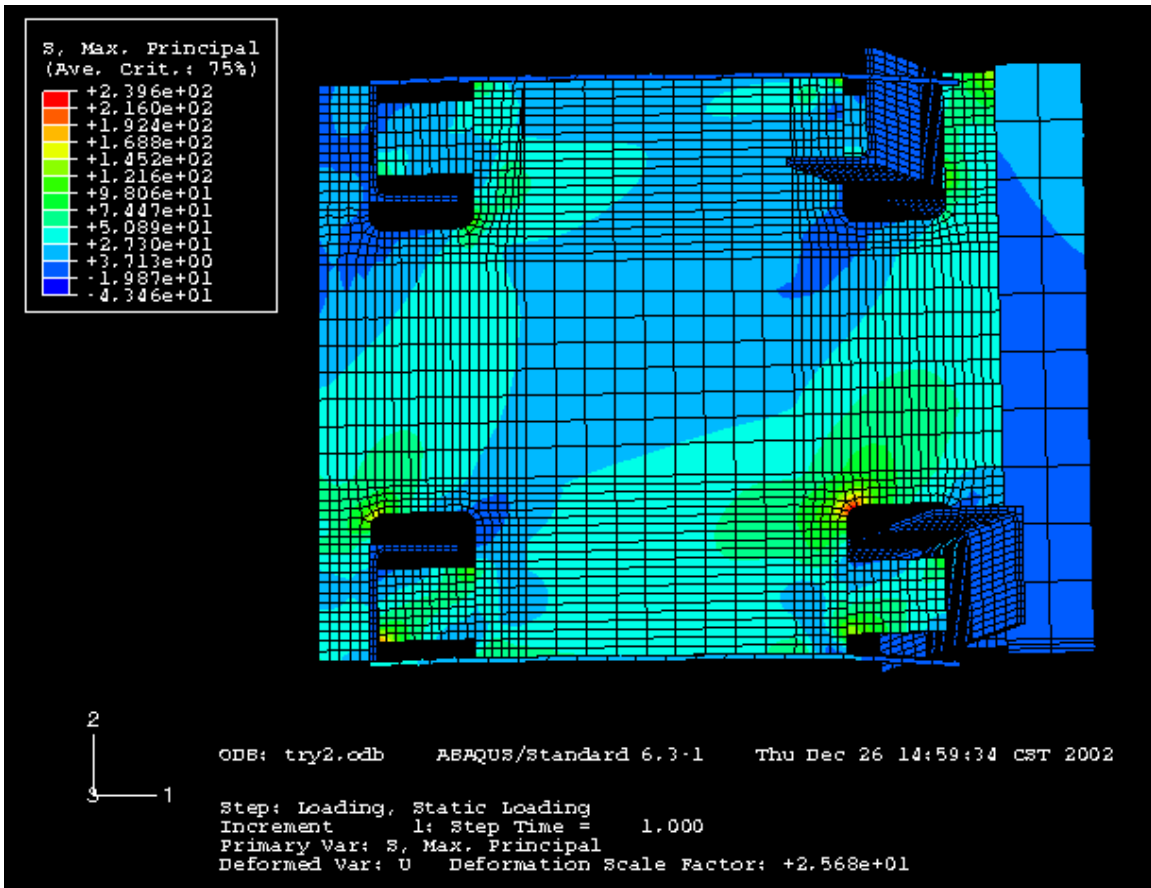


Figure 3.46 Finite element results for simplified web frame specimen (stress in MPa)



Figure 3.47 Typical saw cut and tack weld used to initiate cracks at cutouts



Figure 3.48 Typical crack in web frame growing out of a cutout



Figure 3.49 Typical stop hole repair in web frame

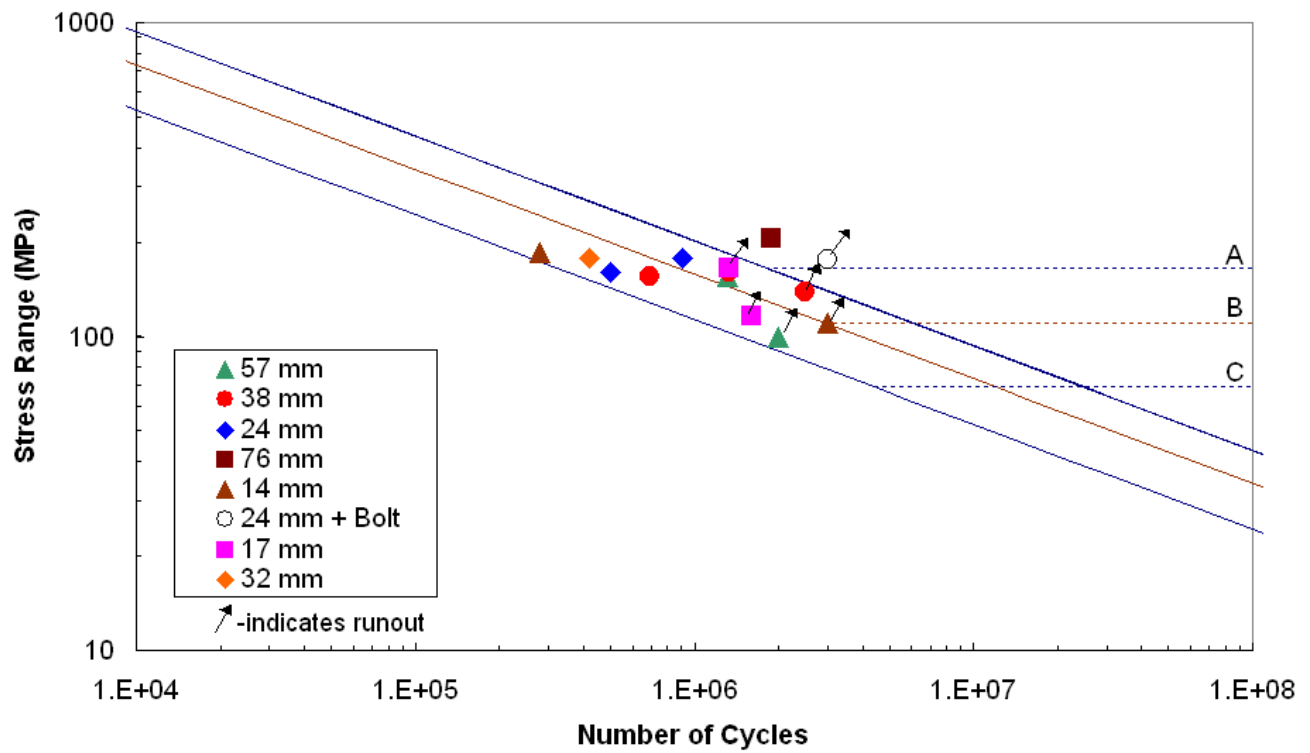


Figure 3.50 S-N curve showing the fatigue data for different sized stop hole repairs



Figure 3.51 Repair of a crack in the web frame using a 24 mm stop hole and fully tensioned high-strength bolt

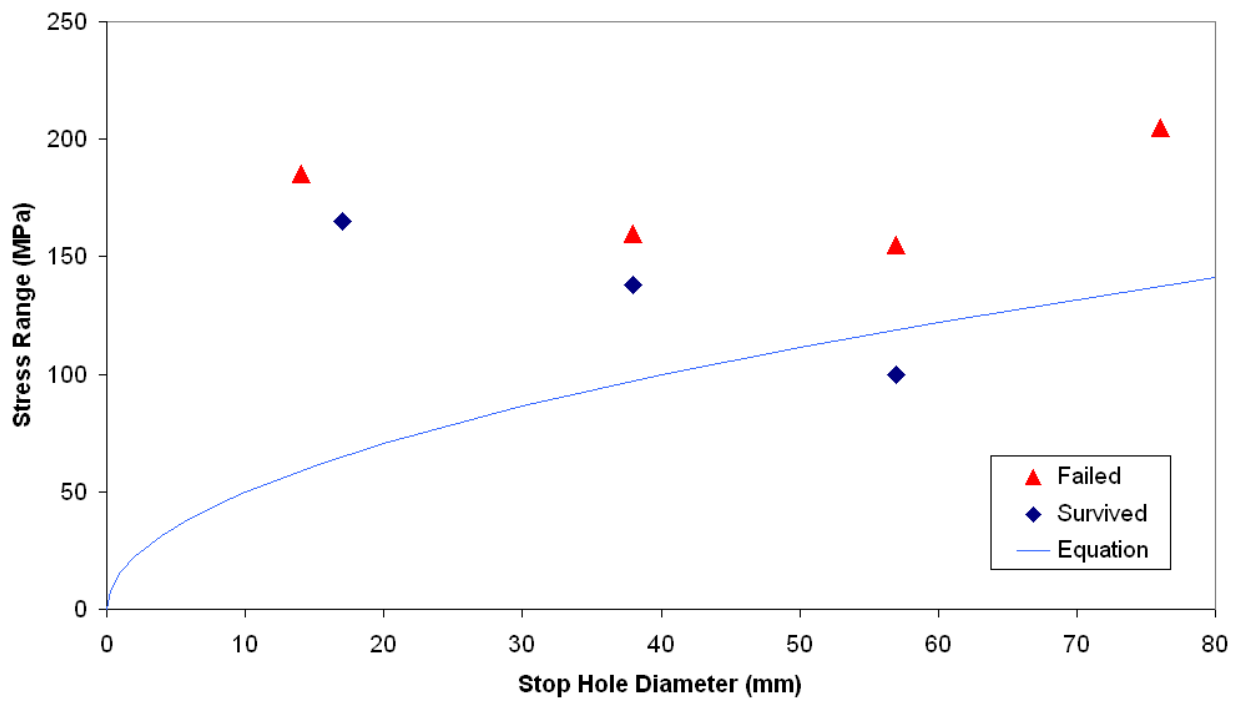


Figure 3.52 Stop hole performance for 25 mm cracks in 345 MPa steel

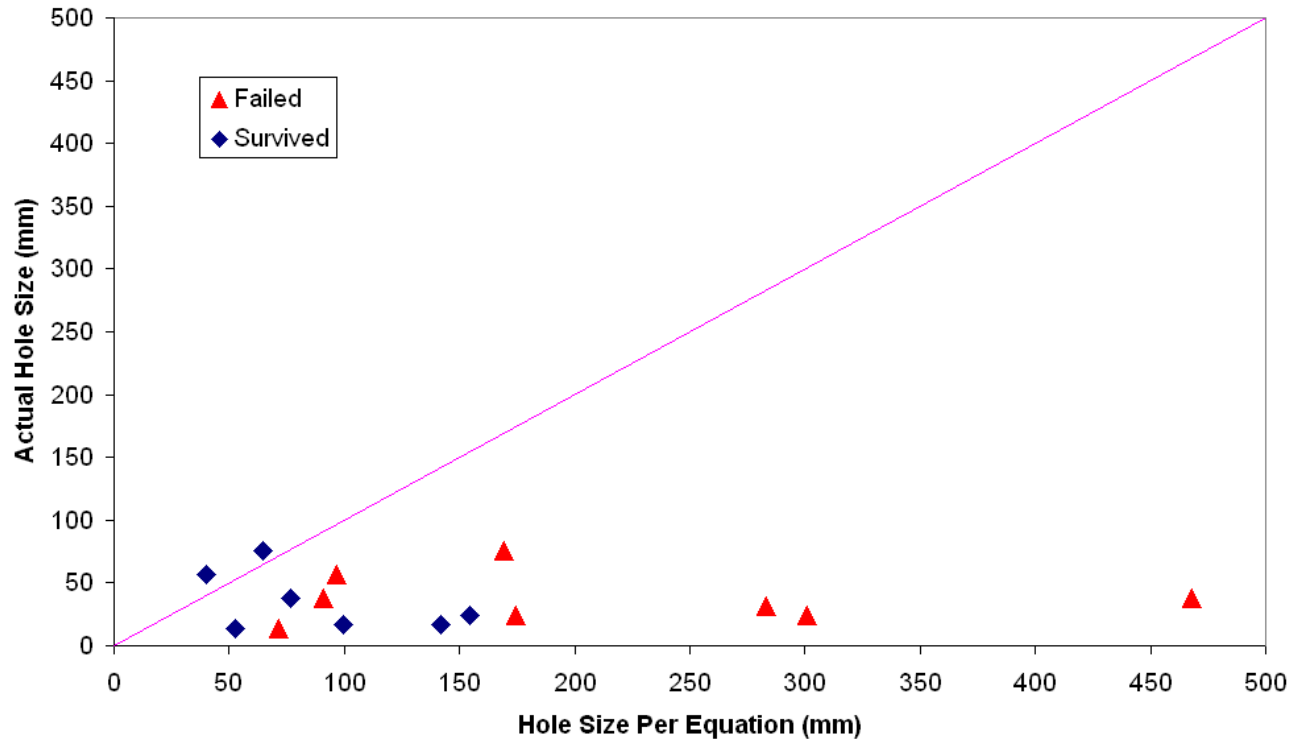


Figure 3.53 Performance of stop hole repairs relative to equation

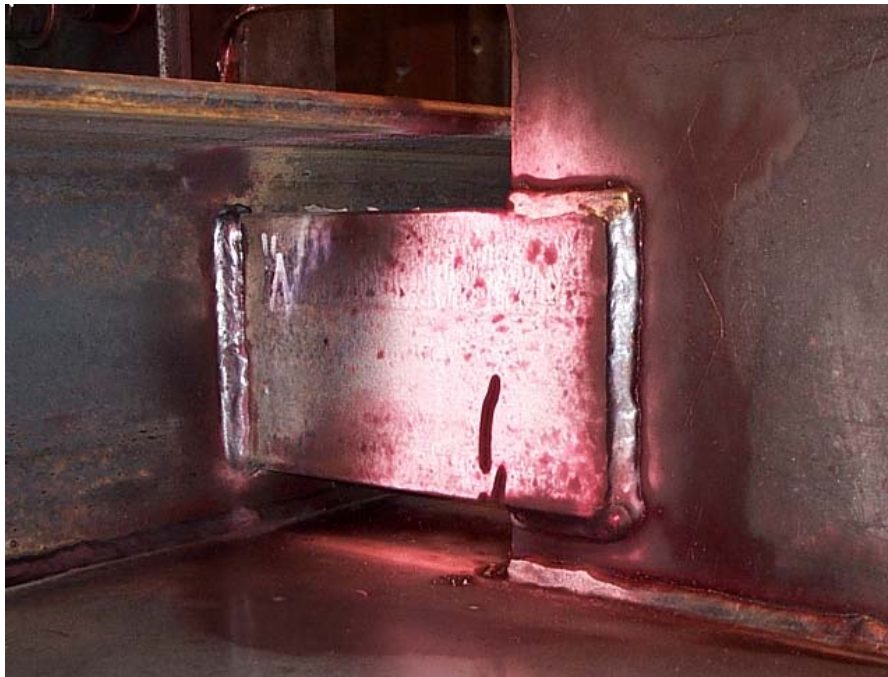


Figure 3.54 Crack forming in lug after stop hole repair



Figure 3.55 Repair failures at other radius at cutout C



Figure 3.56 130 mm long crack after failure of 76 mm stop hole



Figure 3.57 130 mm long crack after weld repairing

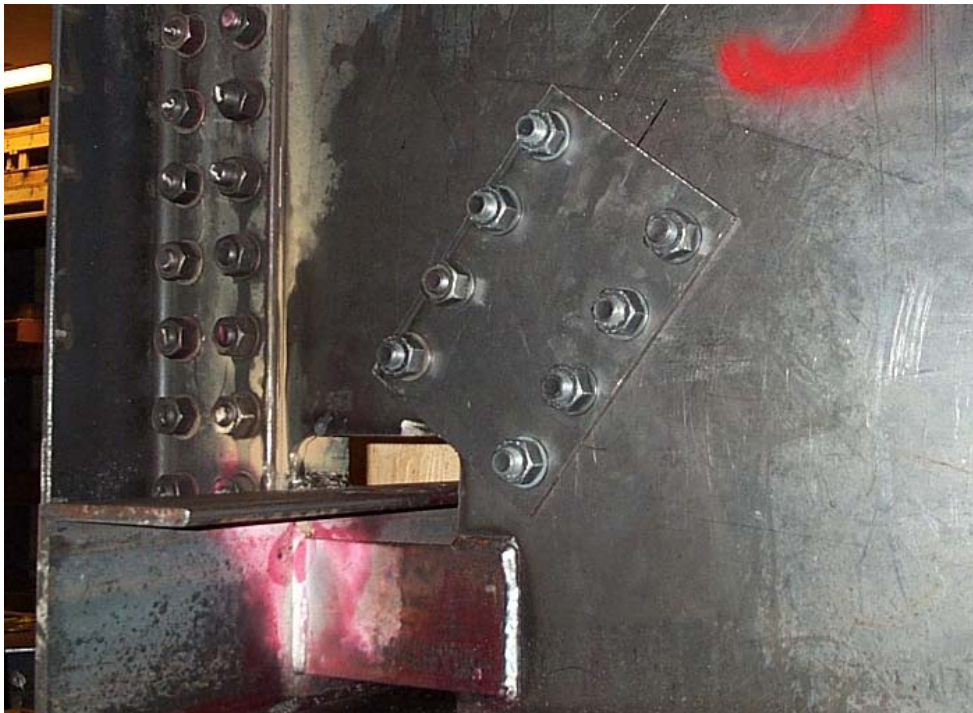


Figure 3.58 130 mm long crack repaired using bolted doubler plates after weld repairing



Figure 3.59 Weld repair in cracked lug plate (original crack shown in Fig. 3.54)

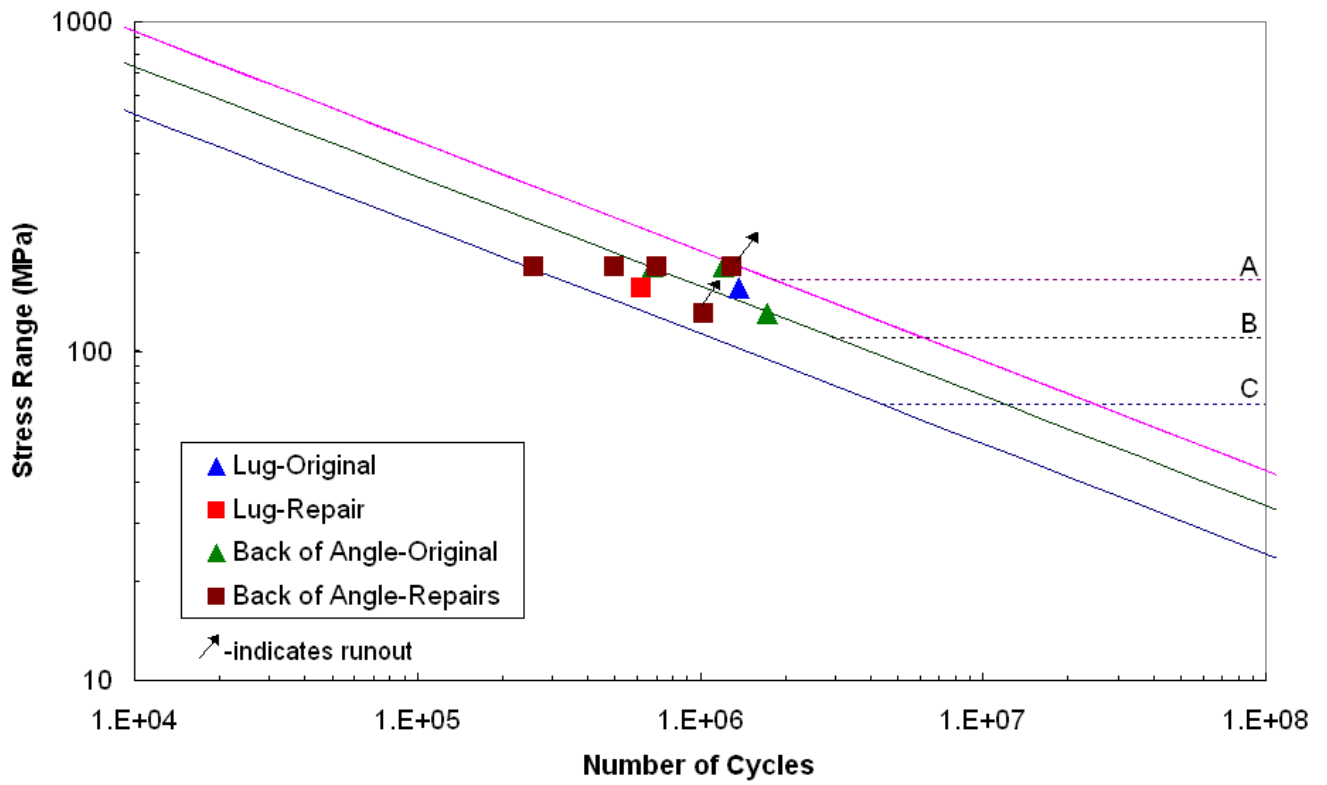


Figure 3.60 S-N curve showing performance of weld repairs



Figure 3.61 Crack forming at web frame-longitudinal connection

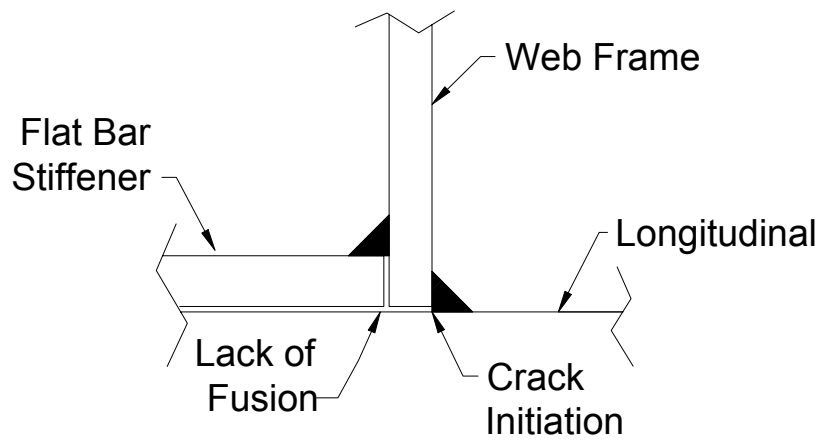


Figure 3.62 Drawing of section through web frame at connection to longitudinal



Figure 3.63 Weld repair at web frame-longitudinal connection



Figure 3.64 Crack forming in bottom hull at cutout

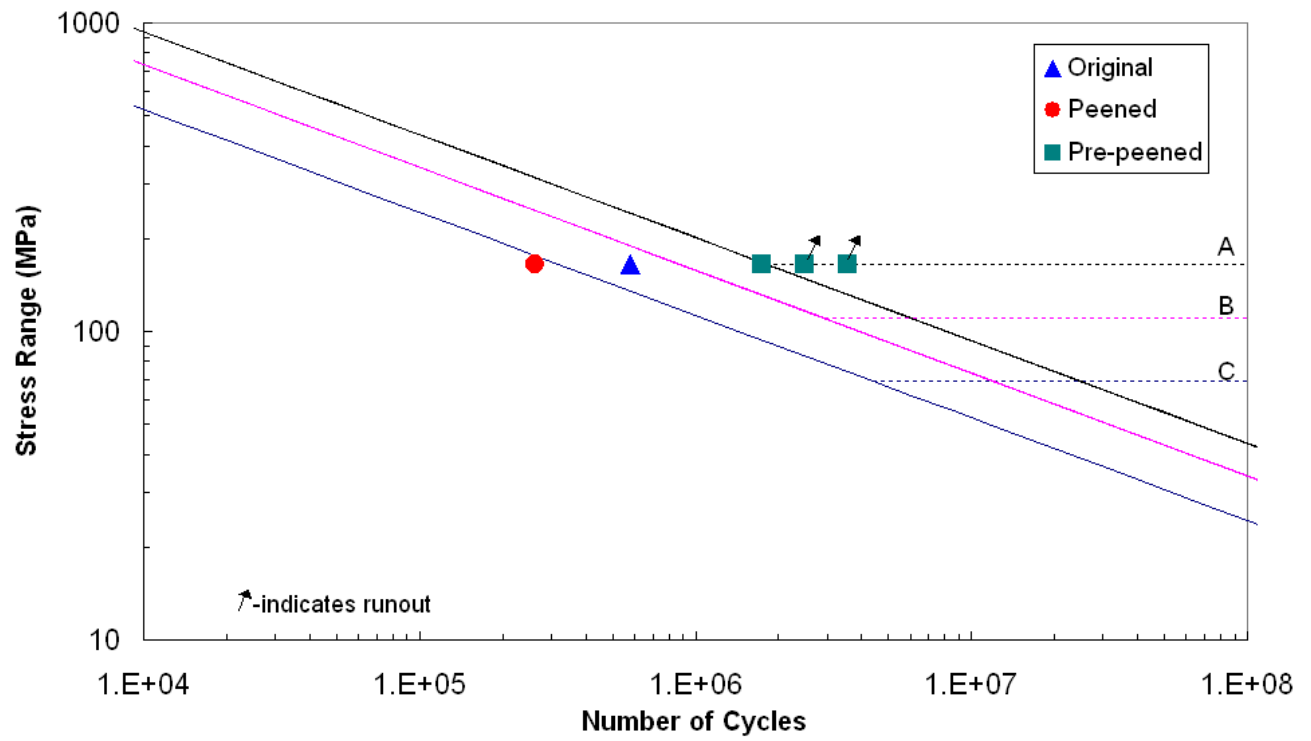


Figure 3.65 S-N curve showing life of original and repaired bottom hull detail at cutout

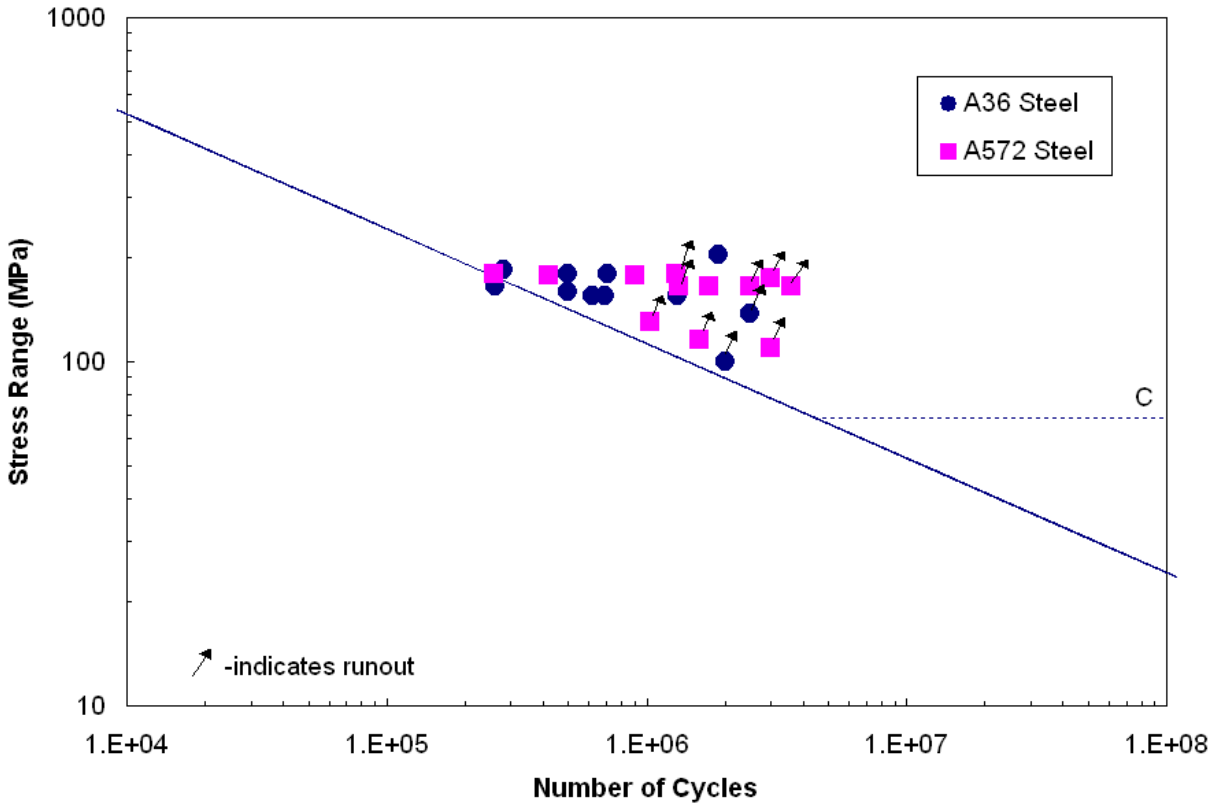


Figure 3.66 S-N curve comparing repairs made to different types of steel

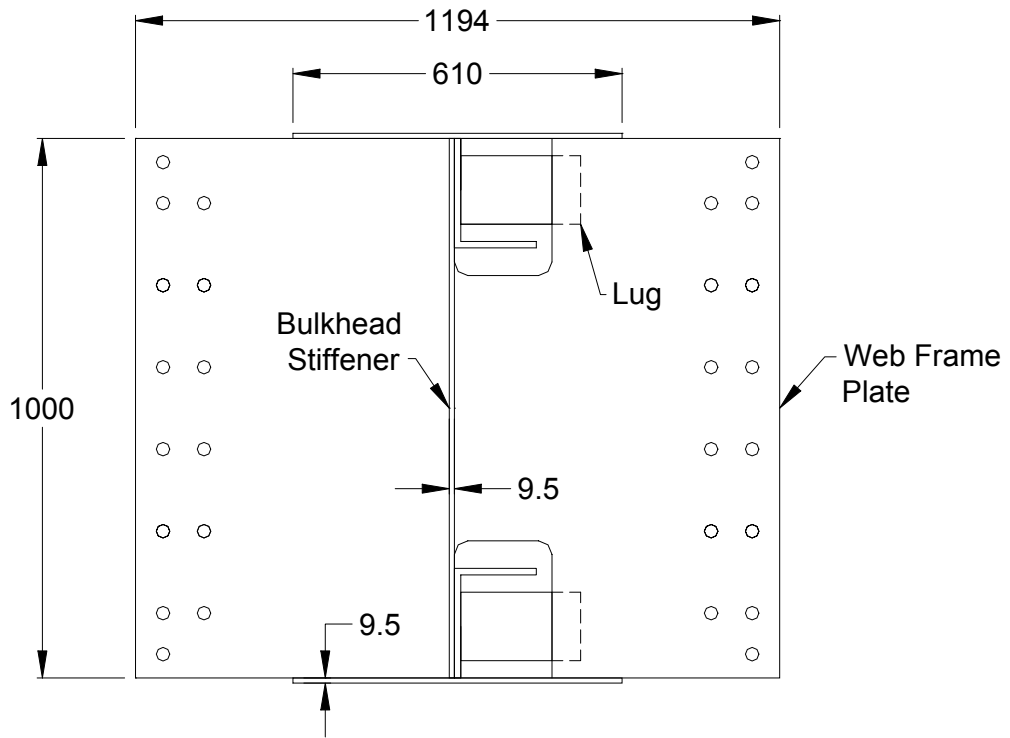


Figure 3.67 Full scale longitudinal/web frame connection specimen drawing (front view)

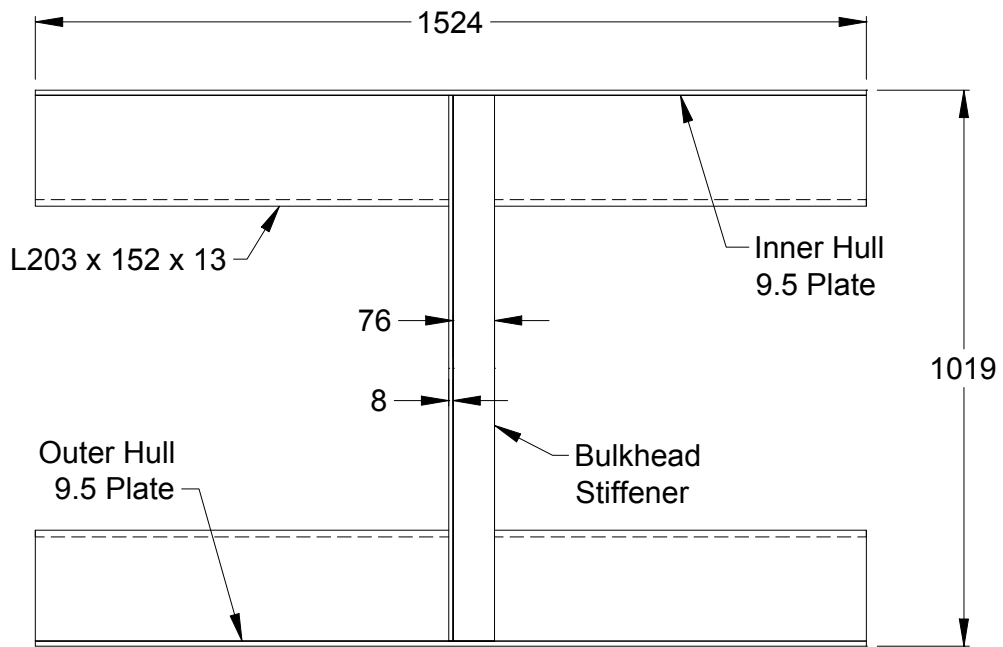


Figure 3.68 Full scale test specimen (side view)

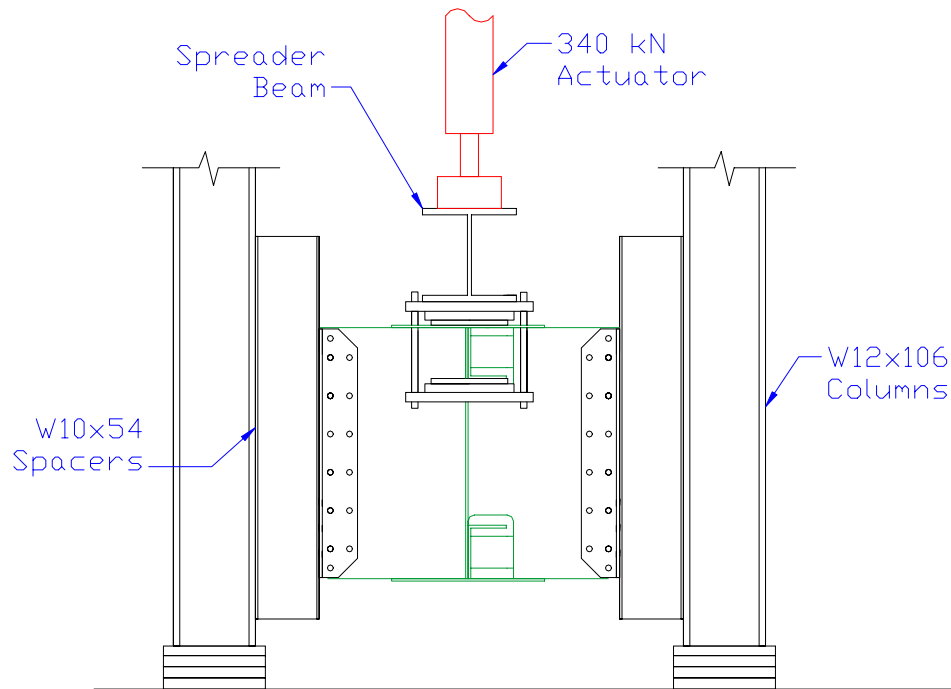


Figure 3.69 Full scale web frame specimen test setup (front view)

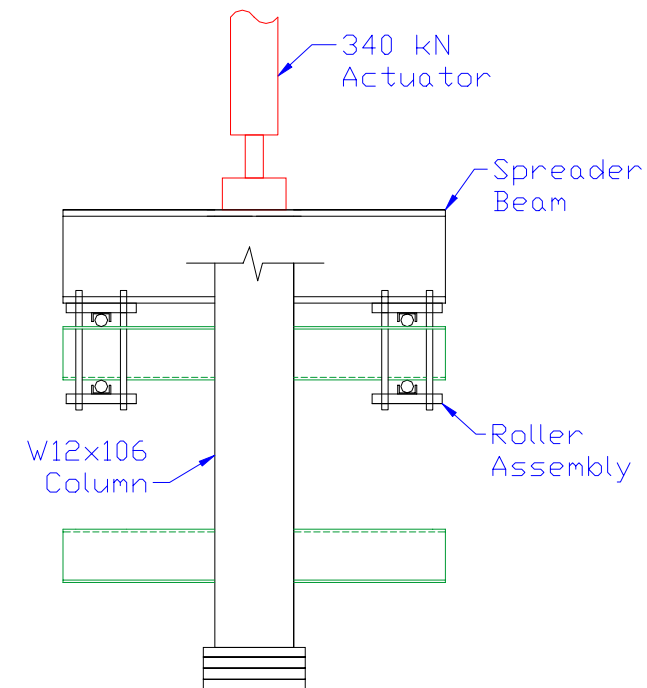


Figure 3.70 Full scale web frame specimen test setup (side view, column partially removed)



Figure 3.71 Photo of full scale web frame specimen in test fixture

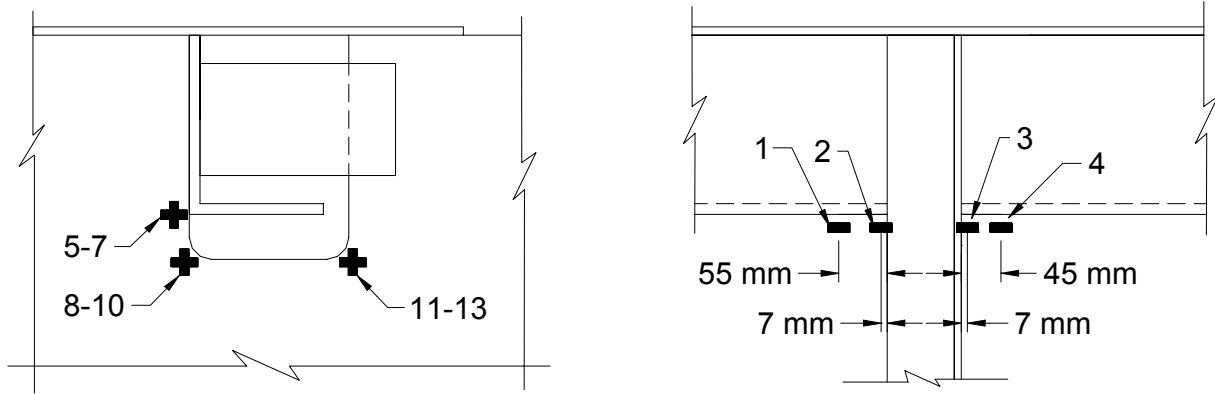


Figure 3.72 Strain gage layout for full scale web frame specimens

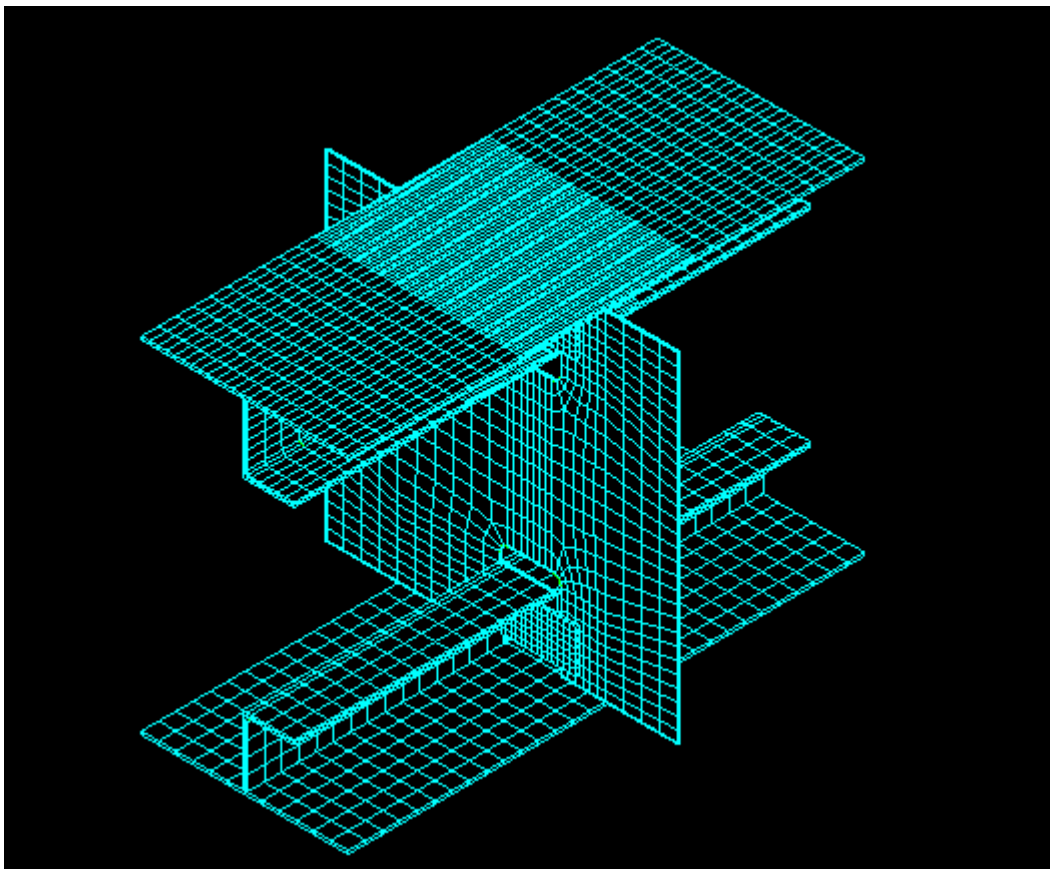


Figure 3.73 Finite element model of full scale web frame specimen

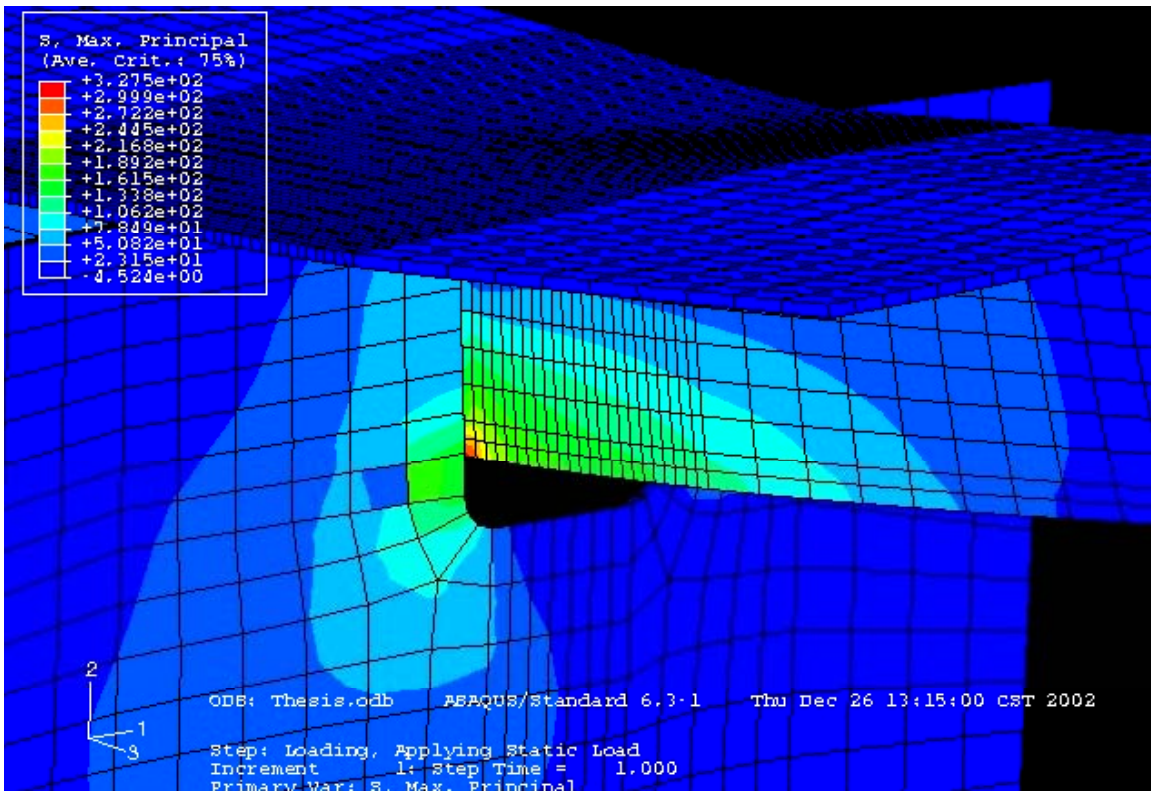


Figure 3.74 Finite element results for full scale web frame specimen showing hot-spot at longitudinal-web frame weld

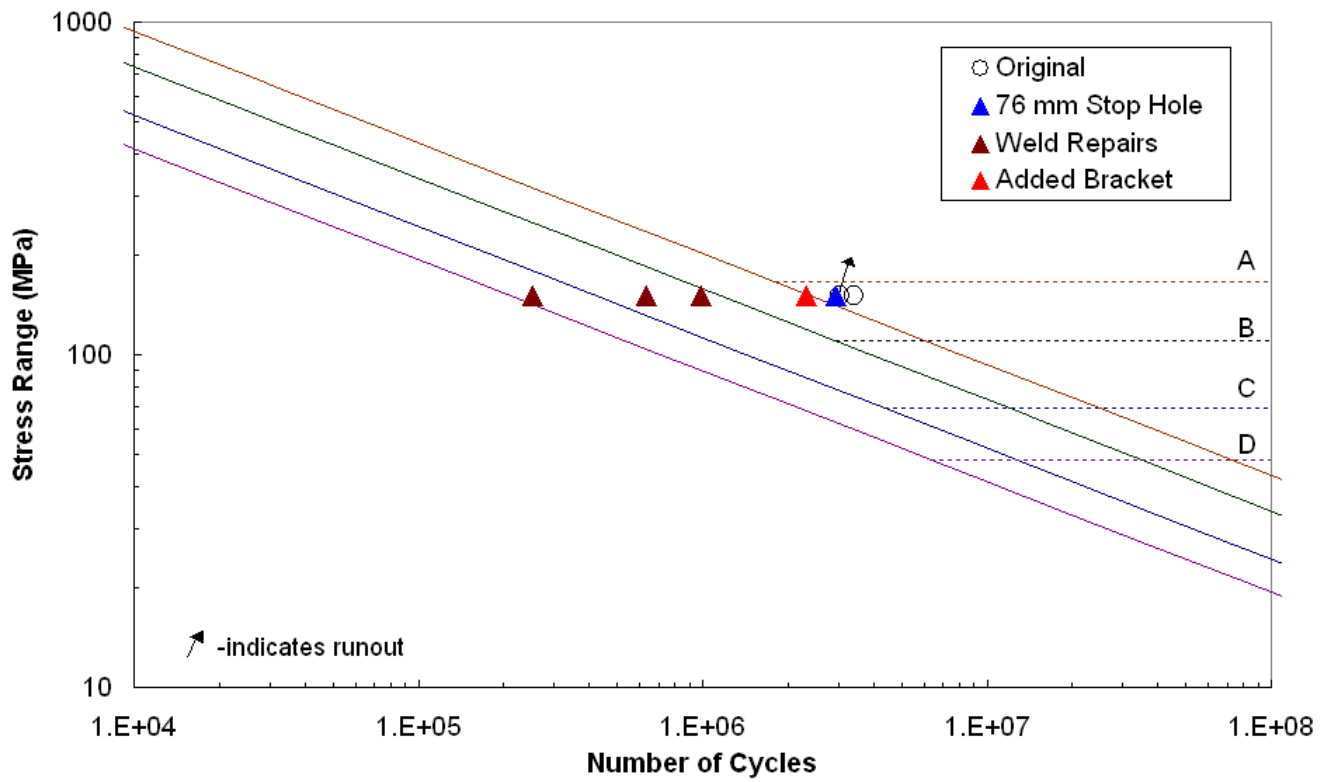


Figure 3.75: S-N curve showing life of original and repaired complex specimen 1

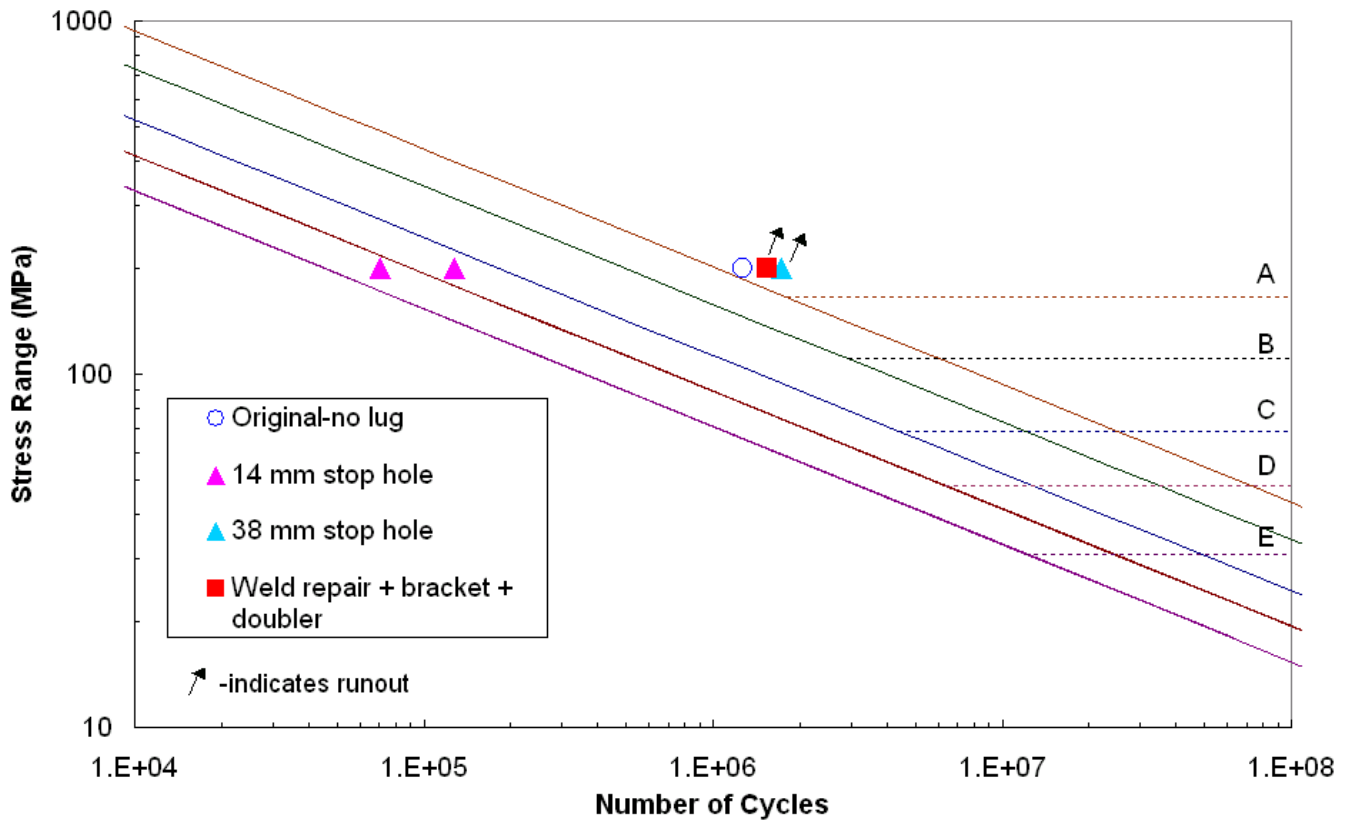


Figure 3.76: S-N curve showing life of original and repaired complex specimen 2



Figure 3.77: Typical crack in web frame at edge of longitudinal



Figure 3.78: 76 mm stop hole in web frame (specimen 1)



Figure 3.79: Stop hole repairs in specimen 2



Figure 3.80: Crack along back of longitudinal at connection to web frame (specimen 1)



Figure 3.81: Vee-and-weld repair along back of longitudinal (specimen 1)



Figure 3.82: Bracket added to stiffen connection (specimen 1)



Figure 3.83: Crack propagating from stop hole into flat bar stiffener (specimen 1)



Figure 3.84: First weld repair of cracked flat bar stiffener (specimen 1)



Figure 3.85: Complete failure of flat bar stiffener (specimen 1)



Figure 3.86: Failure of added bracket (specimen 1)



Figure 3.87: Ineffective 14 mm stop holes in flat bar stiffener (specimen 2)



Figure 3.88: Doubler welded to flat bar stiffener (specimen 2)



Figure 3.89: Additional bracket (specimen 2)

4 SUMMARY

1. Four different specimen types of three different structural details were fatigue tested until cracking occurred, had their cracks repaired by different techniques, and were retested under fatigue loading until cracking occurred again. The process was either continued until the specimens could not be repaired any more due to multiple cracks, or discontinued when a repair technique resulted in a fatigue life significantly better than the original detail.
2. Using the nominal-stress-range approach or the hot-spot stress range approach, the lower-bound fatigue strength of the repaired details was related to the next lowest S-N curve from the set of S-N curves for fatigue categories A through E and E' used in the United States for bridges and other structures. These S-N curves can be translated to equivalent British Standard S-N curves, if desired.

4.1 ATTACHMENTS AND BRACKET DETAILS

1. Strain gage measurements show that the nominal stresses in the beams with attachments and the bracket detail can be accurately determined from simple bending equations. Therefore, the fatigue test results for these types of details can be analyzed in terms of the nominal stress range.
2. Non-load-bearing attachments greater than 100 mm in length are expected to be Category E details and the test data indicated the attachments were slightly better than this.
3. Hammer peening the weld toes can increase the fatigue resistance of uncracked attachment details by at least one full category to Category D.

4. Hammer peening can be an effective repair for shallow surface cracks at attachments less than 3 mm deep.
5. Weld repairs of through thickness cracks at attachments were made by arc-gouging a groove at the crack, arc-gouging an access hole in the beam web below the flange, and welding against a backing bar. These weld repairs at the attachment details were a Category E' detail. The ratio of the fatigue strength of the repair to the original detail is 0.64. The ratio of the life of the repaired detail to the original life is the cube of the ratio of the fatigue strength, or 0.27. For example, if one of these details cracked in ten years, the repair would be expected to last at least 2.7 years.
6. If the toes of the repair weld at an attachment detail are hammer peened, the fatigue strength is at least Category D. Therefore, the ratio of the fatigue strength of the hammer-peened repair to the original detail is 1.25. The ratio of the life of the repaired detail to the original life is 2.0. For example, if one of these details cracked in ten years, the hammer-peened repair would be expected to last at least 20 years, probably enough to qualify as permanent.
7. The original lap-joint bracket detail was expected to be a Category E' detail and the test data were consistent with this expectation. All of the different weld repairs came out below Category E', so there is no equivalent nominal stress range category low enough to describe these repairs. The ratio of the fatigue life of the repair to the original detail is 0.42 if the ends of the weld are drilled out and 0.30 if the weld is terminated in a tapered groove without holes.
8. It was not possible to get access to both sides of the specimen to perform hammer peening. Hammer peening just one side of this lapped bracket detail improved the fatigue strength but not as much as one full Category, so it is considered ineffective.
9. The doubler plate repair proved to be by far the best repair. The two-doubler plate repair reached the category E' life and neither repair had any noticeable crack growth. The repair using just a single doubler plate on the flange of the specimen proved to be better than just a

weld repair, but it failed from distortional fatigue in the web. In addition to increasing the life at the repair location, the doubler plates moved the critical point farther up the stem of the tee to a lower stress location.

4.2 LONGITUDINAL/WEB-FRAME CONNECTION

1. Cracks at the longitudinal/web-frame connection typically occur at the cutout in the web frame, at the vertical weld between the longitudinal and the web frame, at the lug plate lap weld, and at the weld toe where the hull connects to web frame at a cutout. The stresses are very complex at these locations and therefore the hot-spot stress range approach is used to analyze fatigue life. In the hot-spot-stress-range approach, the lower-bound fatigue strength will be related to the Category C S-N curve, since this is the S-N curve for a short attachment or butt weld with little stress concentration other than that associated with the weld toe. This S-N curve is approximately equivalent to the “T” hot-spot stress range S-N curve used in the British Standards.
2. Finite-element analyses were performed and the predicted hot-spot stress ranges at key locations were verified by strain-gage measurements on the specimens.
3. Stop holes were found to be an effective retrofitting technique for cracks occurring in this connection. An equation relating the diameter of the hole required to arrest a crack to the initial crack length and the stress range was found to be conservative but not excessively conservative. Stop holes alone are much less expensive than weld repairs. All details repaired with stop holes survived more cycles without failure than the original detail or longer than Category C. The addition of a fully-tensioned high strength bolt in the stop hole increases the fatigue resistance even more.
4. Cracks that occur at the one-sided fillet weld between the longitudinal and web frame are caused by a lack of fusion defect inherent in the connection. These can best be repaired by arc gouging through the fillet weld into the web frame and replacing with a full-

penetration groove weld. This should be followed by hammer peening the weld toes. If this is done, the ratio of the fatigue strength of the repaired detail to the original detail can be expected to be about 0.95, and the ratio of the life of the repair to the original would be 0.86.

5. Surface cracks up to 3 mm deep at the hull where it meets a cutout can be repaired by hammer peening. Hammer peening this detail prior to cracking can improve it by approximately one fatigue category. Peening is not effective for cracks originating at the weld root.

5 CONCLUSIONS

1. When a detail is cracked and repaired by any of the techniques presented in this report, the residual life after repair is independent of the number of cycles before the repair. Thus the repairs essentially reset the fatigue life.
2. The fatigue strength of various repair techniques was characterized in terms of S-N curves and also in terms of the ratio of the residual fatigue life to the life of the original detail. If the future loading can be assumed to be the same as the past loading, the ratio of the repair life to the original life allows rapid assessment of the residual life of repaired details without explicit estimates of the future loading.
3. Vee-and-weld repairs made at locations of butt welds and access holes usually restore the fatigue life of these details to that of the original detail. However, vee-and-weld repairs made in base metal or in fillet-welded attachments typically reduce the fatigue strength of structural details by one fatigue strength category, so that repair welds will typically have an expected life after repair that is only about half of the time until the detail cracked originally.
4. Doubler plate repairs are a poor fatigue strength (Category E') detail, however many original details on ships are also Category E' details or worse. These poor details may be restored to their original fatigue strength by application of welded doubler plates.
5. Repair of cracks with stop holes, where the geometry of the detail permits, will make the fatigue strength of the repaired structural detail as good as, if not better than the original detail.
6. Use of fatigue life improvement techniques such as hammer peening will restore the fatigue life of a weld repair to the original fatigue strength of the structural detail, and may even increase the fatigue life.

6 RECOMMENDATIONS

1. The draft ASTM procedure Standard Practice for Repair of Fatigue Cracks in Steel Ship Structure given as Appendix A of this report should be published as an ASTM Guide for use in the repair of ship structures.
2. The ratios of the lives of repairs to the lives of the original details presented in this report can be easily used by non-specialists to assess the residual life of various repair options to choose the most efficient options with the required residual life.
3. Whenever practical, repair welds to cracked structural details in ship structure should be followed by a fatigue life improvement technique such as hammer peening.
4. A more systematic study of the effects of repair weld quality and use of fatigue life improvement techniques on repair welds should be made.
5. The studies made in this project should be expanded to include a wider range of structural details so that even better guidance will be available for repair of cracks in ship structures.

APPENDIX A

Standard Practice for Repair of Fatigue Cracks in Steel Ship Structure

1. Scope

- 1.1 This practice describes methods for evaluation of the most suitable repair technique for various types of cracks in steel ships resulting from fatigue and guidelines for the design and execution of the most effective repair techniques.
- 1.2 The values stated in SI units are to be regarded as the standard.
- 1.3 This standard does not purport to address all of the safety concerns, if any, associated with its use. It is the responsibility of the user of this standard to establish appropriate safety and health practices and determine the applicability of regulatory limitations prior to use.

2. Referenced Documents

2.1 ASTM Standards:

A131/A131M Standard Specification for Structural Steel for Ships

A320/A320M Specification for Alloy Steel Bolting Materials for Low-Temperature Service

F436 Standard Specification for Hardened Steel Washers

2.2 American Welding Society Standards:

D1.1 Structural Welding Code—Steel

D3.5 Guide for Steel Hull Welding

2.3 Other Standards:

ABS International, Rules for Building and Classing Steel Vessels

American Institute of Steel Construction (AISC), Manual for Steel Construction

3. Application

- 3.1 This standard is intended to be a guide for repairing typical fatigue cracks that occur at four types of ship structural details. These details are 1) butt welds, 2) fillet-welded attachments, 3) bracket connections, and 4) intersections of longitudinal stiffeners with transverse web frames.
- 3.2 The primary methods used to repair fatigue cracks include: 1) air arc-gouging and welding, 2) hole drilling at the crack tip, 3) hammer peening of the crack, 4) modifying the detail design by adding a doubler plate, stiffener, or rounded corner bracket to reduce the local stress, or 5) some combination of the above techniques.
- 3.3 The fatigue “Categories” discussed below refer to the fatigue design S-N curves in the AISC Manual of Steel Construction (Figure 1). The S-N curves are of the form:

$$N = C \cdot S^{-3} \quad (A-1)$$

$$\text{or } \log N = \log C - 3 \log S$$

where: N = number of cycles to failure,

C = constant dependent on detail category (Table 1)

and S = applied constant amplitude stress range

or effective stress range for variable-amplitude loading..

The S-N curves or Categories can be converted to equivalent Categories for other specifications using the cross reference data in Table 2.

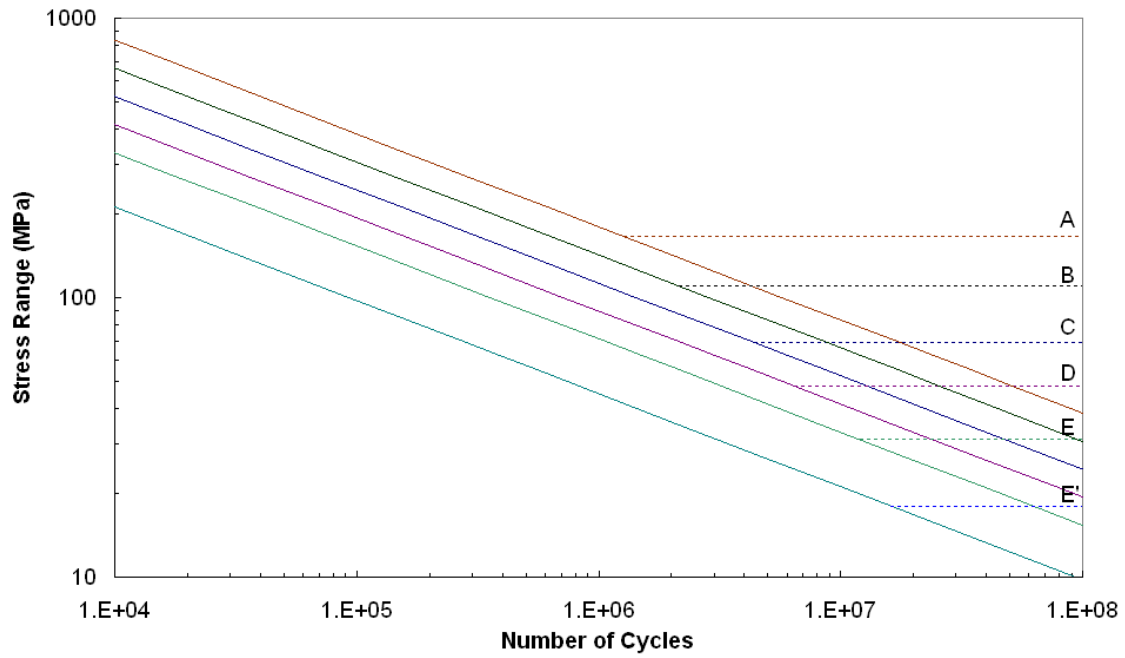


Figure 1: Nominal stress S-N curves used in AISC specifications

Table 1: Parameters for AISC S-N curves

AISC	Coefficient C times 10^{11} (MPa ³)	Threshold or Fatigue Limit (MPa)
A	82	165
B	39	110
B'	20	83
C	14	69
D	7.2	48
E	3.6	31
E'	1.3	18

Table 2: Cross-reference for S-N curves (nearest curve at 2×10^6 cycles)

AISC	Eurocode 3	BS 7608
A	160	B
B	125	C
B'	100	D
C	90	D
D	71	F
E	56	G
E'	40	W

- 3.4 When calculating the residual life of repaired details, it is not necessary to take into account the prior fatigue loading experienced by the metal immediately adjacent to the repair, i.e. the repair may be considered a new detail as far as estimating the residual life. However, if there are other details in the connection that were not treated or repaired (e.g. a weld access hole adjacent to a repaired butt weld), the fatigue lives of these other details are not affected by the repair and shall be considered as partially used up.
- 3.5 When the residual life of a repaired detail is compared to the life of the original detail in this section, it will be assumed that the loading will remain approximately the same in the future as it was in the past. If this is not the case, then the effective stress range must be calculated for the future loading and the life determined from the S-N curve.

3.6 **Butt welds in hull plate or stiffeners (including insert plates), access holes and drain holes** - (Figure 2). Butt welds are Category D details when new, regardless of the type of complete-joint-penetration weld detail. Access holes and drain holes are also Category D details, with the cracks likely to form at the weld terminations (usually a wrap-around weld or boxing weld) or sometimes at the apex of the holes, particularly when the flame cutting of the hole is very poor.

Shallow cracks, less than 3 mm deep, at the toes of the butt weld or at the toes of the wrap-around weld at the weld access hole or drain hole, may be repaired by hammer peening. Surface cracks at butt weld toes with a total length less than 30 mm will typically be less than 3 mm deep, while surface cracks at the weld terminations at access holes or drain holes may be 3 mm deep when they have a total length greater than 12 mm. The crack length should be verified using dye-penetrant testing (PT) or magnetic particle testing (MT) and it should be verified that there are no cracks on the other side of the plate. If there is sufficient concern about the depth of the crack, the depth can often be determined using the shear-wave ultrasonic-testing (UT) technique. Hammer peening should be applied to both weld toes of a butt weld and to both wrap-around welds at access holes or drain holes and will create a Category C detail at these locations. The life of the hammer peened welds will typically be at least twice the life of the original detail

If a hole may be drilled, cracks can either be completely removed with a hole saw or the tips of the crack may be drilled. For example, small cracks around the perimeter of the weld access hole or drain hole can be removed simply by enlarging the hole. Holes up to 200 mm in diameter may be practically cut with a hole saw. In large redundant structures there should not be any concern for the loss of section due to the hole. The stop hole repair will create a Category C detail and the life will typically be at least twice the life of the original detail.

Deeper surface cracks and through-thickness cracks may also be repaired effectively using air arc-gouging and welding. Usually, the repair butt weld is made at one of the toes of the original butt weld, leaving the other toe of the original weld untreated. Test data have shown that the other weld toe is effectively renewed as well, and that the entire original weld and the repair may be considered as a new Category D

detail, regardless of the detail, i.e. either two-sided or one-sided complete joint penetration welds, with and without backing, and with and without the edges ground flush. This same Category D applies to insert plates that are complete-joint-penetration groove welded to surrounding structure.

Cracks at access holes or drain holes that are too large to stop by drilling holes may be repaired as follows. A 25 mm hole is used to temporarily stop the crack. The crack is then arc-gouged between the weld-access hole and the stop-hole and welded (Figure 3). The best repair is a U-preparation with the weld made from one side and then backgouged and rewelded from the other side. After welding, the edge of the weld at the access hole should be ground flush and a slightly larger stop hole, 38 mm in diameter, should be drilled to remove the edge condition of the weld. This repair will restore the access hole to a Category D detail.

In the case of repairs at butt welds and access holes or drain holes, the fatigue strength of the repair weld is approximately the same as the original detail, so the residual life should be approximately the same as the life until the cracking occurred under similar loading. In the case of insert plates, the original fatigue strength in an open part of the hull plate is Category A, so the installation of an insert plate (Category D) will shorten the life considerably. However, it is likely that there are other Category D or worse details nearby, so the practical consequences of introducing another D detail are not significant.

If this estimated residual life of these weld repair details is not satisfactory, hammer peening of the original weld toes and the repair weld toes may be performed and this will increase fatigue strength to Category C. In this case, the residual life would be expected to be about twice the original life of the detail.

Doubler plates may be added to reinforce the structure near a cracked butt weld and reduce the stress ranges locally. Usually the butt welds are weld repaired first and then must be ground flush to accept the flat doubler plate. A bolted doubler plate (Figure 4) will be a Category D detail while a welded doubler plate will be a Category E detail if both the doubler and the underlying plate are less than 20 mm thick and a Category E' detail if either of the plates is 20 mm or thicker. The critical stress range for the doubler plate will be the nominal stress range in the underlying plate at the perimeter of the

doubler. Since these doubler plates will be the same or worse fatigue resistance than the original detail, the only way adding a doubler plate will be an improvement is if the doubler plate perimeters can be extended to areas of the panel with lower stress ranges.

Regardless of the approach to repair, the remaining parts of the butt weld and any neighboring butt welds or access holes will remain Category D details. If one of these butt weld details or access holes cracked, then similar details in neighboring areas are also likely in the verge of cracking. If it is necessary to have a residual life of these remaining parts of the weld or weld access holes, then they should be retrofit by hammer peening both weld toes. Access holes may be improved by grinding the perimeter of the access hole and hammer peening the part of the fillet weld that wraps around the end of the access hole. These operations should improve the details to Category C, and the residual life should be twice the life at which one of the details cracked.

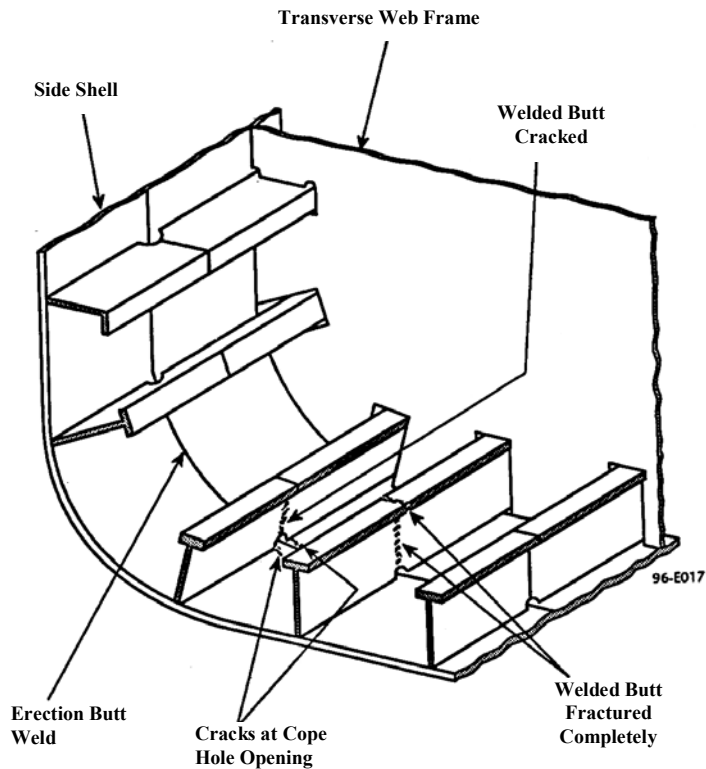
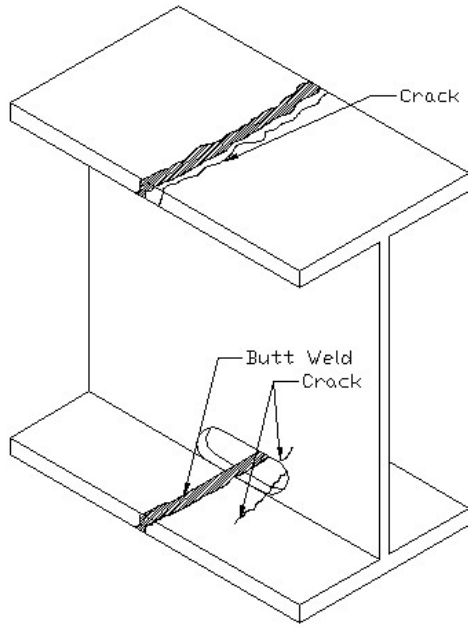
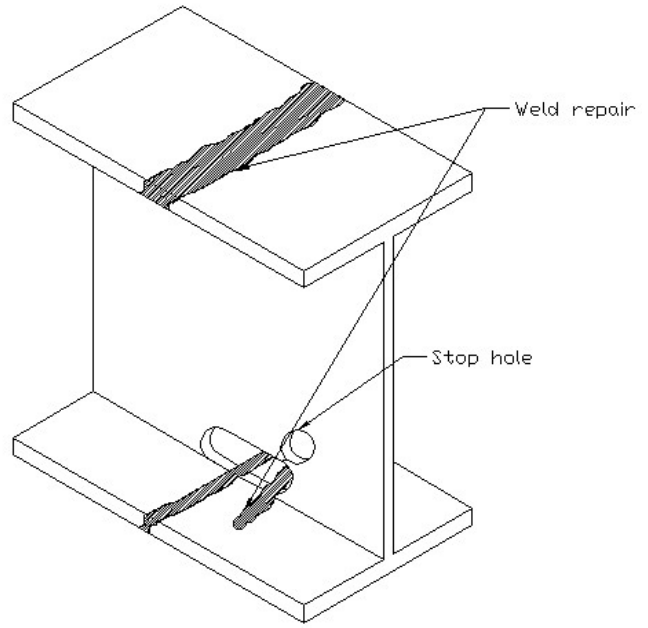


Figure 2: Crack locations at various butt weld details



Sketch of Damage



Sketch of Repair

Figure 3: Cracks and repairs at butt welds and access holes.



Figure 4: Bolted cover plate repair at a butt weld

3.7 **Fillet welded attachments** – The original details are typically Category E when they are new. Shallow cracks, less than 3 mm deep, may be repaired by hammer peening (Figure 5). Surface cracks along weld toes with a total length less than 30 mm will typically be less than 3 mm deep, while surface cracks at wrap-around welds on the nose of stiffeners may exceed 3 mm in depth when they have a total length greater than 12 mm. Hammer peening should be applied to all weld toes where the weld axis is perpendicular to the principal stress range, usually the weld toes parallel to the crack that formed. The hammer peening will create a Category D detail. The life of the hammer peened welds will typically be at least twice the life of the original detail

Deeper cracks may be repaired effectively using air arc-gouging and welding (Figure 6). If a crack is nearly all the way across the flange of a stiffener or other element, it is preferred to gouge a groove across the whole element so the weld may be terminated at the edges by cascading the weld beads. If a weld is in a continuous plate or is much less than the width of the plate, it is preferred that the weld repairs be made between drilled holes at least 25 mm diameter at the crack tips, and that after welding the holes are enlarged to 38 mm to clean up the weld ends. It is recognized that this is not always possible, and the test data show it is acceptable to terminate the weld in a gradually tapered groove.

Weld repairs at attachments may be considered as a new Category E' detail, regardless of the weld type, i.e. either two-sided or one-sided complete joint penetration welds, with and without backing, and with and without holes at the edges or with the edges ground flush. The ratio of the life of the repaired detail to the original life is 0.27. .

If this estimated residual life is not satisfactory, hammer peening of the original weld toes and the repair weld toes may be performed and this will increase fatigue strength to Category D. In this case, the residual life would be expected to be about twice the original life of the detail.

In addition to the weld repair, small stiffeners may be added to reinforce the structure and reduce the stress ranges locally. The terminations of these stiffeners will usually be a Category E detail, so this should give a residual life equal to the life of the original detail. This reinforcement may be useful when a detail has been repaired multiple times and the weld quality is very questionable. The reinforcement will effectively move

the critical location to a new location, the termination of the stiffener, so future cracking will not take place at the previous repair locations.

Regardless of the approach to repair, if one detail has cracked the remaining parts of the attachment and any neighboring similar attachments will remain on the verge of cracking. It is recommended that any nearby similar attachment details be hammer peened at the weld toes to restore the fatigue strength to Category D, and the residual life should be twice the life at which the detail cracked.



Figure 5: Peened weld that had a surface crack at fillet welded attachment

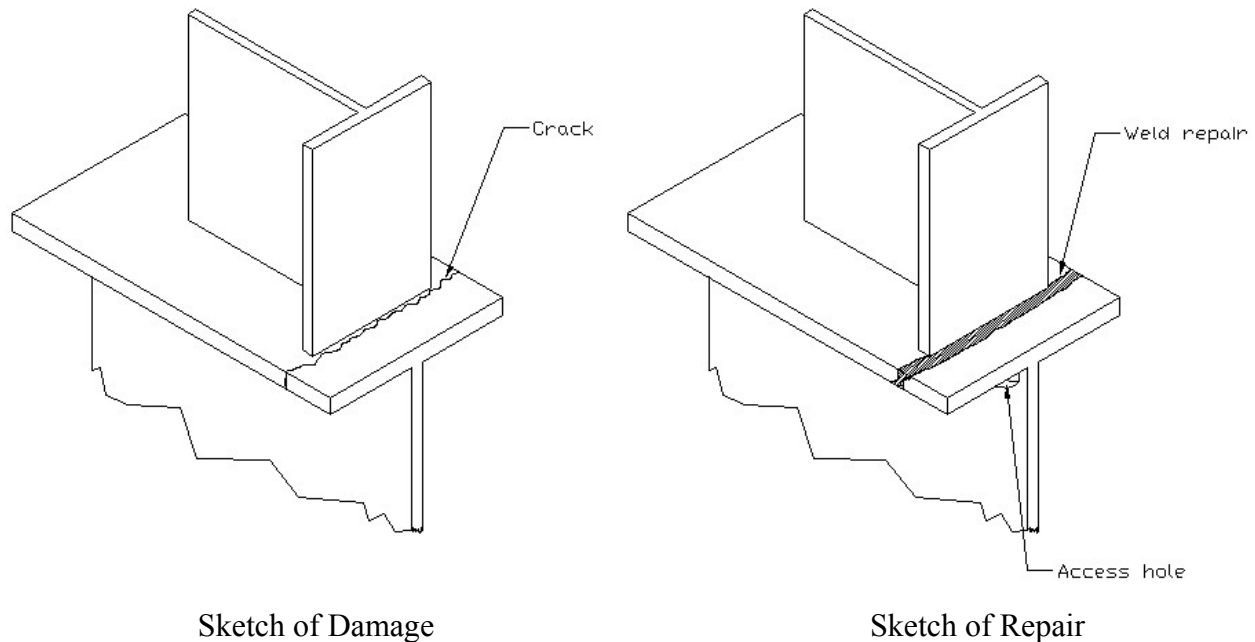


Figure 6: Crack and repair at attachment detail

3.8 **Bracket connections** – Bracket connections with lap welded connections are typically Category E' when they are new. Brackets that are attached to a flange or other transverse elements are usually Category E details.

Shallow cracks, less than 3 mm deep, at the welds of such brackets may be repaired by hammer peening (Figure 5). Surface cracks along weld toes with a total length less than 30 mm will typically be less than 3 mm deep, while surface cracks at the wraparound welds on the nose of stiffeners may be 3 mm deep when they have a total length greater than 12 mm. Hammer peening should be applied to all weld toes where the weld axis is perpendicular to the principal stress range, usually the weld toes parallel to the crack that formed. The hammer peening will create a Category E detail at lap welds and a Category D detail at the termination of brackets normal to a flange or other surface. The life of the hammer peened welds will typically be at least twice the life of the original detail

Deeper cracks may be repaired effectively using air arc-gouging and welding (Figure 7). The weld repair may be considered as a new Category E' detail, regardless of the weld type, i.e. either two-sided or one-sided complete joint penetration welds, with and without

backing, and with and without the edges ground flush. The ratio of the life of the repaired detail to the original life is 0.27. .

If this estimated residual life is not satisfactory, hammer peening of the original weld toes and the repair weld toes may be performed and this will increase fatigue strength to Category D. In this case, the residual life would be expected to be about twice the original life of the detail.

In addition to the weld repair, small doubler plates may be welded on to reinforce the structure and reduce the stress ranges locally (Figure 8). The terminations of these doublers will usually be a Category E detail, so this should give a residual life equal to the life of the original detail. This reinforcement may be useful when a detail has been repaired multiple times and the weld quality is very questionable. It will effectively move the critical location to a new location, the termination of the doubler, so future cracking will not take place at the old repair locations.

Regardless of the approach to repair, the remaining parts of the attachment and any neighboring similar attachments will remain on the verge of cracking. It is recommended that any nearby similar attachment details be hammer peened at the weld toes to restore the fatigue strength to Category D, and the residual life should be twice the life at which one of the details cracked.

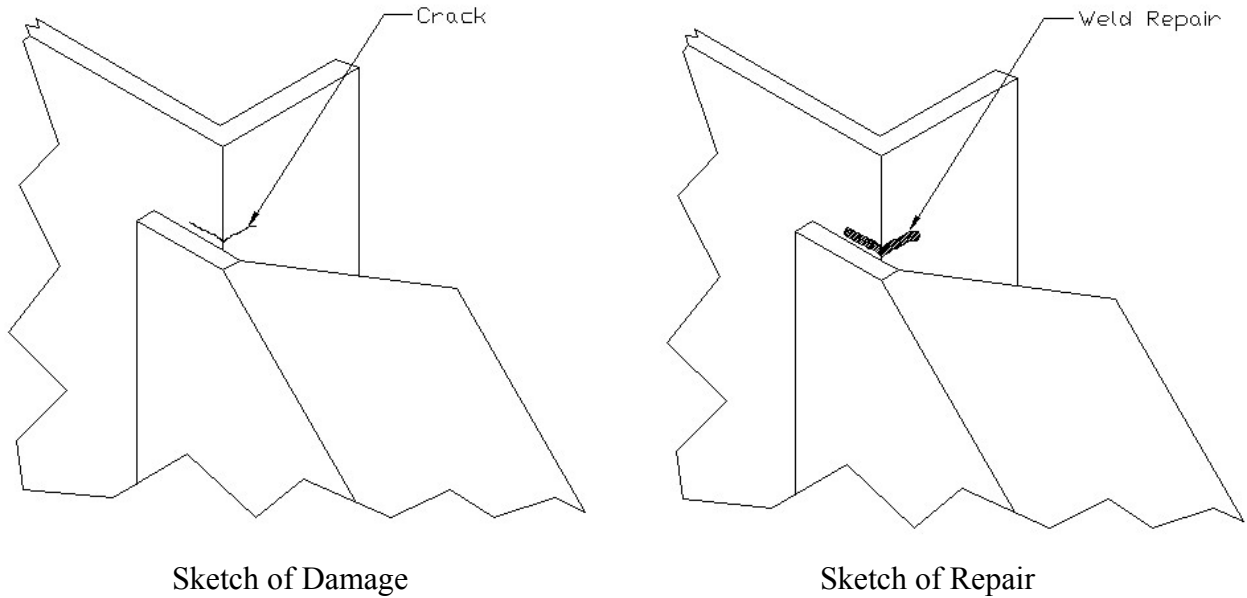


Figure 7: Crack and repair at bracket detail.

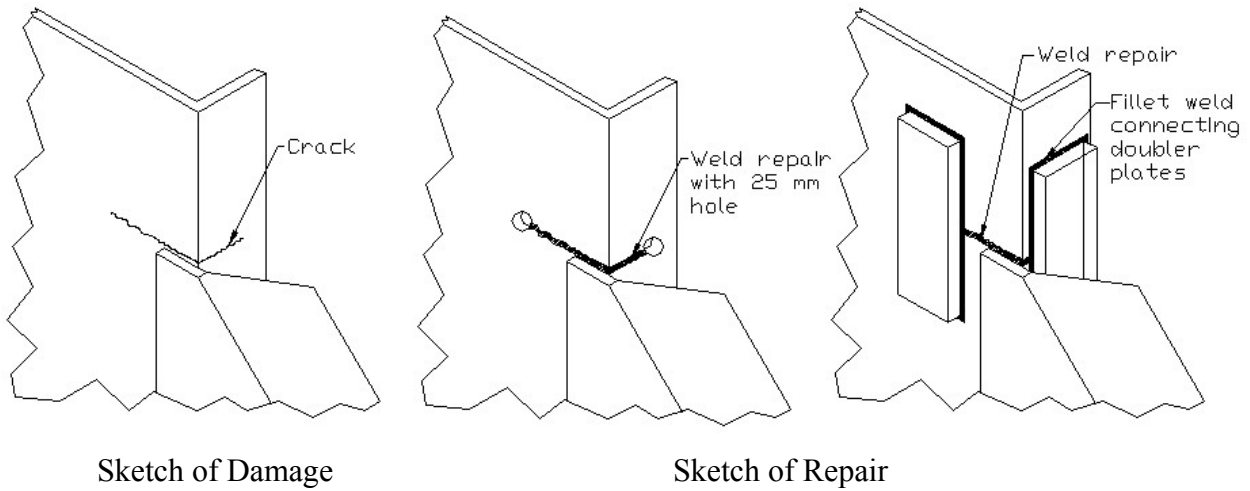


Figure 8: Crack and doubler plate repair at bracket detail

3.9 **Intersection of longitudinal stiffeners and transverse web frames** – This original detail is typically Category E when it is new. Cracking can occur in several ways at this detail, as shown in Figures 9-12.

Most often, cracks occur in the web frame at the cutout where the longitudinal passes through (Figure 9). These cracks commonly initiate at the curved radii of the

cutout and propagate into the web frame. Cracks such as these can best be repaired using hole drilling. The properly executed stop hole repair will create a Category C detail and the life will typically be at least four times the life of the original detail. Again, in large redundant ship structures there is no concern for loss of section due to the hole(s). If cracks at this location are large (greater than 300 mm), then they should be weld repaired and can be considered Category D. Doubler plates may be added after grinding the repair weld smooth to reinforce the structure and reduce the stress range locally, however the repair will still be Category D with the critical location moving to the outer edges of the doubler plate. As described above, the only way the doubler plate will be beneficial is if it is large enough to extend to areas of lower stress range.

Cracks may also occur at the root of the weld connecting the long leg of the longitudinal stiffener to the webframe (Figure 10). These cracks are best repaired by arc-gouging and replacing the fillet weld with a groove weld. An additional fillet weld should be added on top of the groove weld for reinforcement. Once this is complete, the toes of the repair weld should be hammer peened. This repair will increase the fatigue strength to Category C, approximately four times the original life of the detail.

Cracks occurring at the toe of the wrap-around weld at the web frame cutout (Figure 11) may be repaired by hammer peening if their depth is 3 mm or less. Surface cracks at this location will typically be less than 3 mm deep if they have a total length less than 12 mm. The crack length should be verified using dye penetrant testing (PT) or magnetic particle testing (MT). If there is sufficient concern about the depth of the crack, the depth can often be determined using the shear-wave ultrasonic-testing (UT) technique. Hammer peening should be applied all the way around the toe of this wrap-around weld and will create a Category C detail, making the repair life four times the life of the original detail. This repair should be reinspected regularly, however, to make sure that the initial crack was removed by the peening operation.

Cracks occurring in the lug plate that connects the longitudinal to the web frame (Figure 12) can be repaired using either air arc-gouging and welding, for short cracks, or replacing the lug plate, for longer cracks and fractures. If the crack does not extend the entire width of the lug (i.e. the lug is not completely fractured), it is preferred to first drill a 13 mm hole, then gouge a groove along the length of the crack and weld. After

welding, the hole should be enlarged to 19 mm to clean up the weld ends and the weld toes should be hammer peened. If the lug is completely fractured, then hole drilling is not necessary and the gouging and welding can be performed over the width of the lug plate, terminating at the edges by cascading the weld beads. Weld repairing this crack and hammer peening may be considered a new Category E' detail regardless of the weld type. The ratio of the repaired detail to the original life is then 0.5.

If this estimated residual life is not satisfactory, an additional lug plate of the same dimensions can be added to the opposite side of the web frame in addition to the weld repairs described above. This will improve the repair to Category E, the same as the original detail, but will cut the stress range in half, thus improving the life by a factor of eight.

Regardless of the approach to repair and regardless of which type of crack is repaired, if one detail or one part of a detail has cracked, the remaining parts and neighboring details will still be Category E and will remain on the verge of cracking.

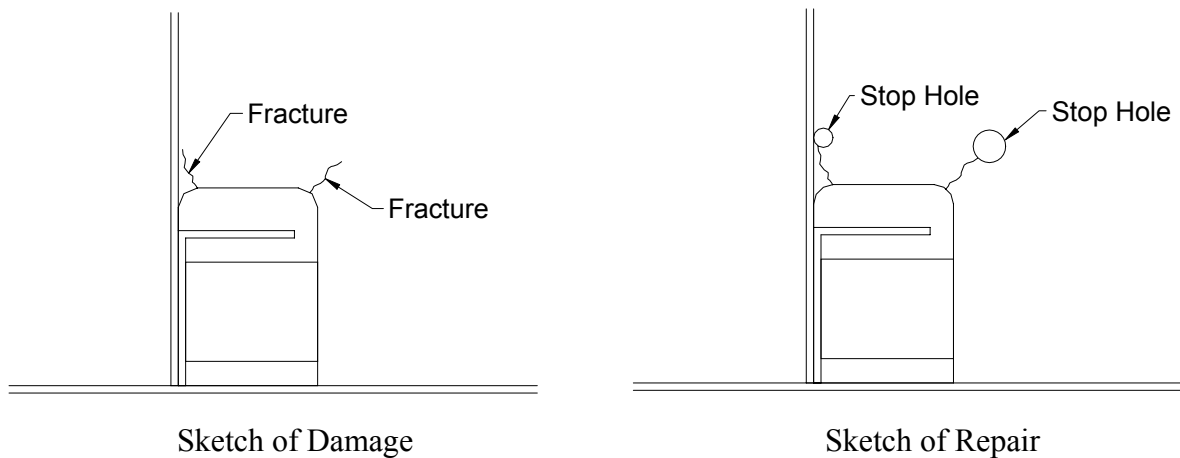
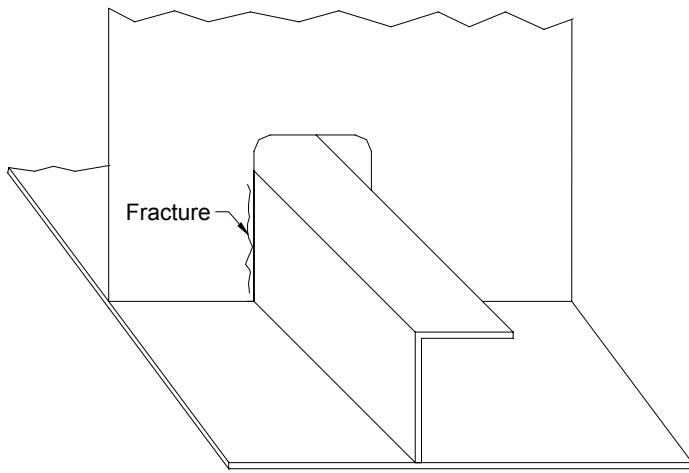
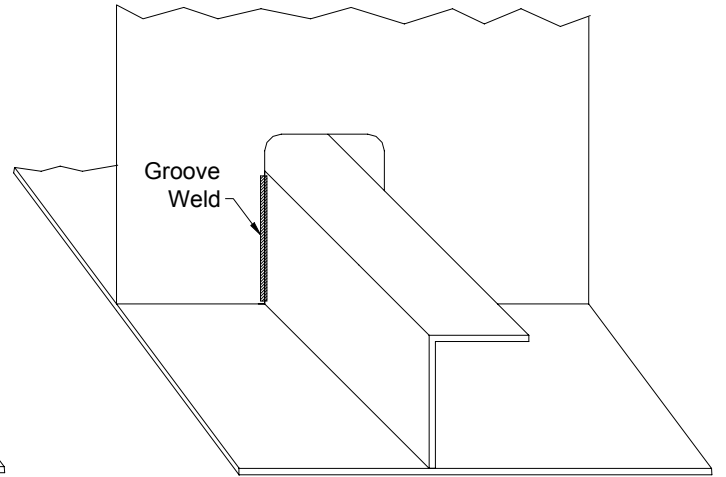


Figure 9: Cracks and repairs in the web frame occurring at the cutout

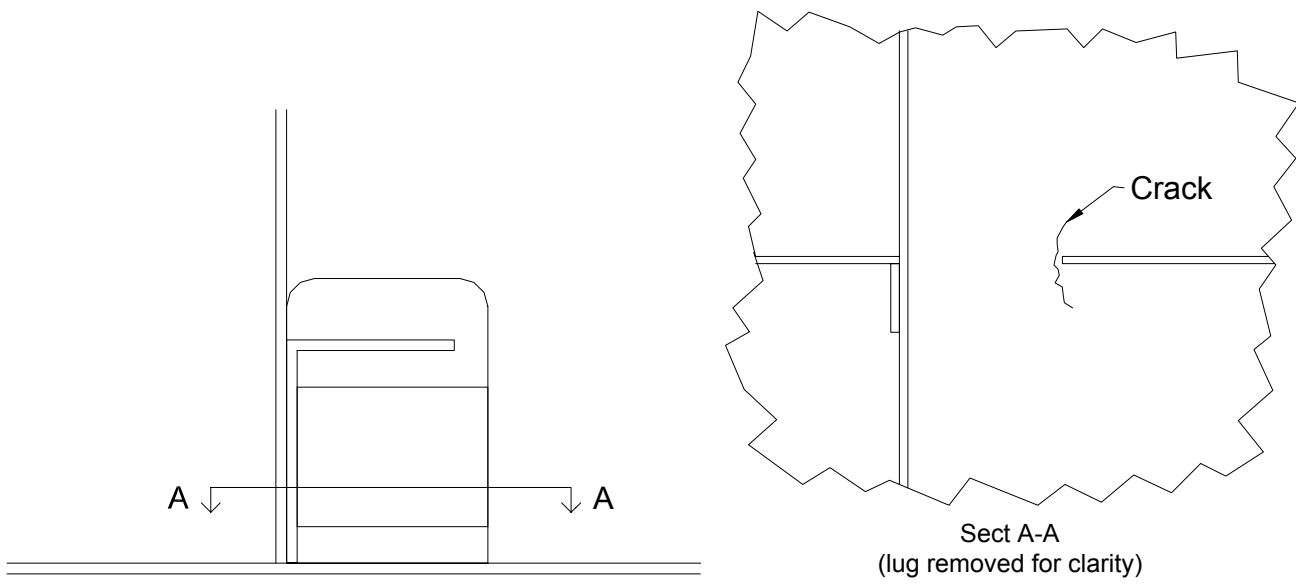


Sketch of Damage

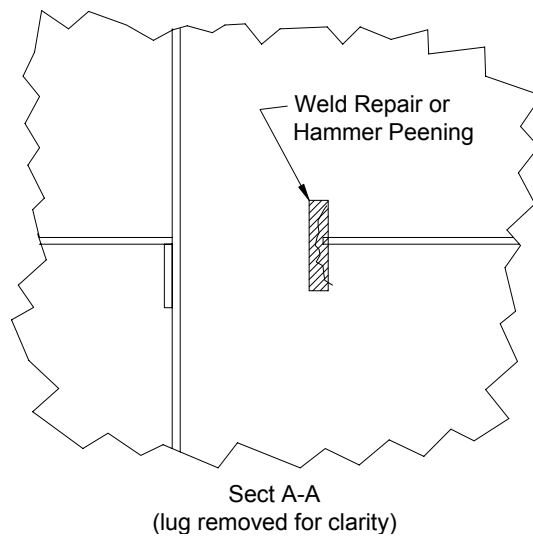


Sketch of Repair

Figure 10: Crack and repair for failed weld connecting longitudinal to web frame

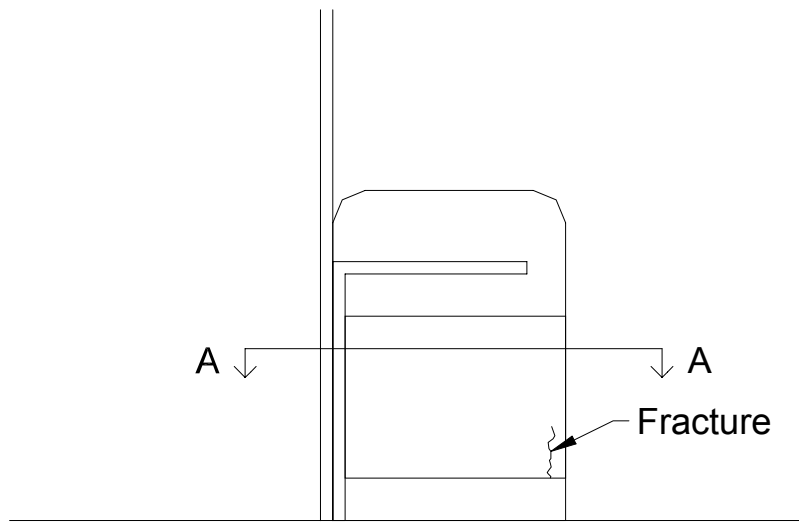


Sketch of Damage

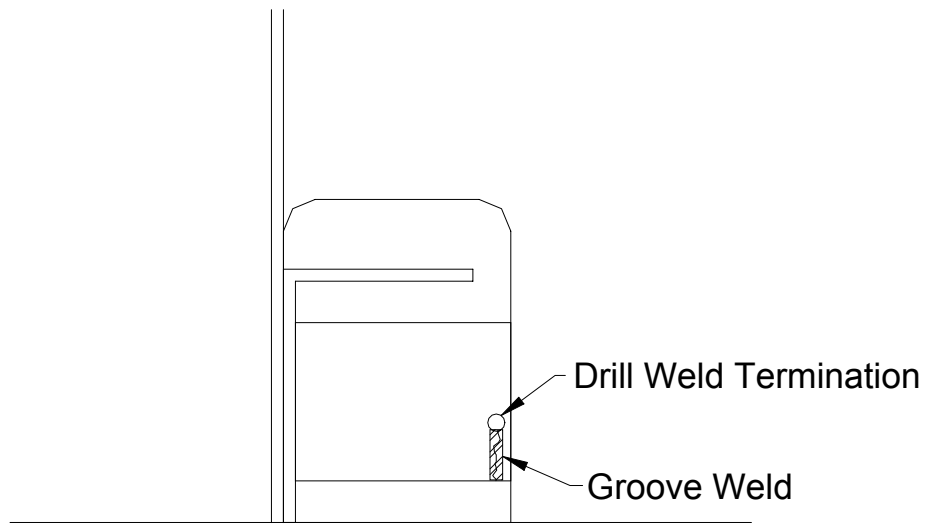


Sketch of Repair

Figure 11: Crack and repair in sideshell at wrap-around weld at web frame cutout



Sketch of Damage



Sketch of Repair

Figure 12: Crack and repair in lug plate

4. Materials and Equipment

4.1 Weld Repairs

Arc gouging: Air arc gouging can be done using standard equipment. Consumables ranging from 4.8 to 6.4 mm in diameter can be used depending on the thickness of base metal.

Weld process: Repairs can be made using the shielded metal arc welding (SMAW) process or the flux-cored arc welding (FCAW) process.

Consumables: All-position consumables should be chosen so that repairs can be made at any angle. Since the deformation of the repair weld will be constrained by surrounding structure, the strength of the finished repair weld is not an important issue. The lower the consumable strength the better to reduce welding residual stress, which can be a major concern in these highly restrained repair welds. The certified nominal minimum ultimate tensile strength shall not exceed 490 MPa (E70XX). Undermatched welding consumables with ultimate tensile strength less than 420 MPa (E60XX and less) are available and should be used if possible. A low-hydrogen SMAW electrode such as E6018 or E7018 is recommended to help prevent hydrogen cracking. If using the FCAW process, gas shielding is preferred to keep the diffusible hydrogen to a minimum, although suitable self-shielded consumables may also be used. The consumable should have a minimum Charpy V-notch value of at least 34 Joules at -29 degrees C.

High-strength steel: There is a high risk of hydrogen cracking when repair welding high-strength steel (yield strength 480 MPa or greater). Weld repairs should only be used for high-strength steel if other types of repairs such as bolted doubler plates are not possible. Undermatched consumables shall be used when welding high-strength steel in order to reduce the residual stresses caused by welding. Also minimum preheat requirements per AWS D3.5 (at least 120 degrees C) must be met for welding high strength steel to reduce the possibility of hydrogen cracking.

4.2 Hole Drilling

4.2.1 Drill bits: A titanium-coated high speed steel drill bit is recommended for drilling holes 15 mm and smaller.

4.2.2 Hole saws: Holes larger than 15 mm should be cut using a cobalt-alloy hole saw.

4.2.3 Drill: A portable drill with an electromagnetic base is recommended. Refer to manufacturer's recommendations to determine optimum type of drill, motor, etc.

Note: Flame-cut holes are not permitted

4.3 Hammer Peening

4.3.1 Tool: A pneumatic or hydraulic impact hammer can be used with a chisel bit. See manufacturer's recommendations for further information.

4.4 Detail Modifications

4.4.1 Material: Any type of steel that meets ASTM A131 standards may be used for detail modifications. Weld metal should be the same as described in 4.1. If bolts are used, then all bolting materials should conform to ASTM 320 standards. Washers should conform to ASTM F436.

4.4.2 Workmanship: Brackets, plates, and stiffeners may be flame cut, however, if a radiused corner is used, it must be ground smooth or saw cut.

5. Procedures

5.1 Weld Repairs

- 5.1.1 Weld consumables and welding procedure should be prequalified or qualified in accordance with the applicable codes and specifications. In general, weld procedures that are acceptable for new construction should be acceptable for repair welds with the following additional requirements.
- 5.1.2 To ensure reasonable fatigue life, repair welds should meet the workmanship and weld quality standards in the applicable codes and specifications, including as a minimum the standards for repair welds given in AWS D3.5.
- 5.1.3 Visually locate the crack tip (or tips for two-ended or multi-ended cracks). It is recommended but not required that dye-penetrant testing (PT) or magnetic particle testing (MT) be used to enhance the visual location of the crack tips. The crack tip should be located on both sides of a member if the crack is through-thickness and if access is possible. Mark a point about 6mm past the visually identified crack tips in the direction of the crack propagation.
- 5.1.4 Determine if crack tip can be drilled out, depending on potential leakage or lack of access. Skip to 5.1.6 if holes cannot be drilled.
- 5.1.5 Drill a 12 to 13 mm hole centered on the marked locations.
Note: If the location of the crack tip is marked on both sides of a member with a through-thickness crack, the hole shall be drilled at the location furthest from the crack origin in the direction of crack propagation.
- 5.1.6 Clean the area around the crack. Contamination in the weld area will lead to poor weld quality and must be removed prior to welding using solvents. It is sometimes useful to spray on a vegetable oil solvent such as WD-40[®] and preheat to at least 120 degrees C to burn off moisture and contaminants.
- 5.1.7 Air-arc gouge out the crack between the holes or marked points to $\frac{3}{4}$ the thickness of the member. The root opening and groove angle should be in accordance with the welding procedure specification (WPS). See Figure 13.

Note: Make sure to remove all of the crack for a partial-thickness crack. Often the crack can be seen by the gouger or welder and may appear to propagate during gouging or welding. Gouger and welder should be trained to report this and to take appropriate measures to locate the ends of the crack again and increase the extent of the repair if necessary.

5.1.8 Clean and remove slag from the vee-gouged area.

5.1.9 Fill the gouged area with small stringer weld beads. This completes the repair for a partial-thickness repair. See Figure 14.

Note: Make sure to fill in the whole area of the vee-gouge.

5.1.10 Clean around the crack on the opposite side of the member.

5.1.11 Air-arc gouge out the crack between the holes or marked points to $\frac{1}{2}$ the thickness of the member.

Note: Make sure to remove the entire crack when air-arc gouging.

5.1.12 Repeat steps 5.1.7 and 5.1.8 to complete repair. See Figure 15.



Figure 13: Gouge and access hole at attachment detail



Figure 14: Weld repair of crack not yet through-thickness without termination holes.



Figure 15: Weld repair of typical through-thickness crack with termination holes drilled to larger diameter after the weld is complete.

5.2 Hole Drilling

- 5.2.1 Hole drilling should not be performed on cracks located in inner or outer hull plates or in bulkheads where leakage would be unacceptable.
- 5.2.2 Measure the length of the crack in millimeters. Locate the approximate crack tip and mark with a steel punch. For two-ended cracks, do this for each crack tip.
- 5.2.3 Choose a minimum hole size based on the following equation:

$$D \geq \frac{S_R^2 a}{18\sigma_y} \quad \text{A-2}$$

D = hole diameter (mm)

S_R = approximate stress range at the crack location. If this is unknown, 150 MPa may be used.

a = crack length measured in 5.2.2 for one-ended cracks. For two-ended cracks, divide the measured length by 2 and use that value for a.

σ_y = yield strength of the steel containing the crack (MPa)

- 5.2.4 Clean the area around and ahead of the crack tip, removing as much corrosion product as possible.
- 5.2.5 Position the drill bit or hole saw such that the visually detected crack tip is located at the perimeter of the hole to be cut. See Figure 16.
- 5.2.6 Drill using appropriate coolant in accordance with manufacturer's recommendations. See Figure 17.



Figure 16: Drilling a stop hole using a magnetic base drill

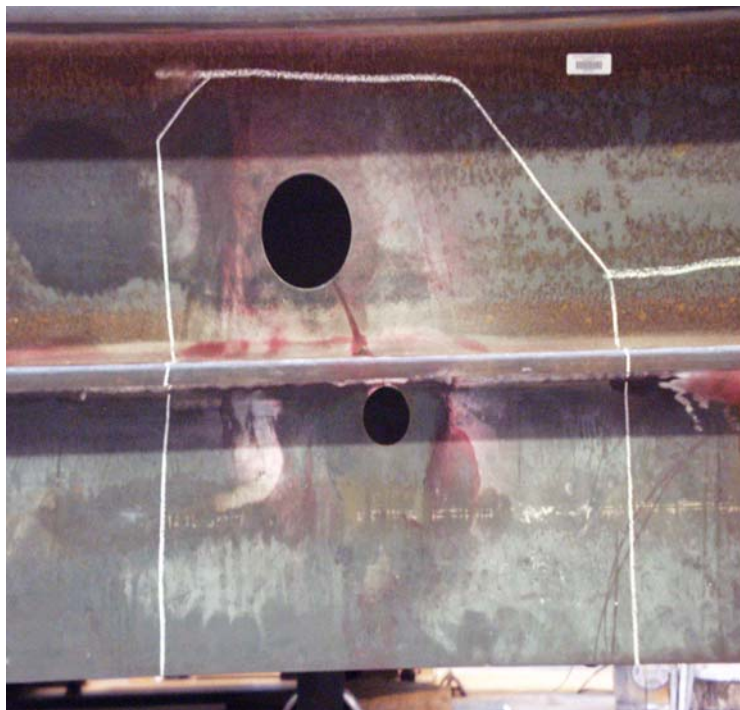


Figure 17: Stop holes at a cracked stiffener detail

5.3 Hammer Peening

- 5.3.1 Determine if the crack is through-thickness. If so, hammer peening should not be used.
- 5.3.2 Position the tool directly over the crack and apply heavy pressure. Peen along the entire length of the crack and at least 10 mm beyond each tip, moving the tool slowly. Repeat 3 times. See Figures 18-20.

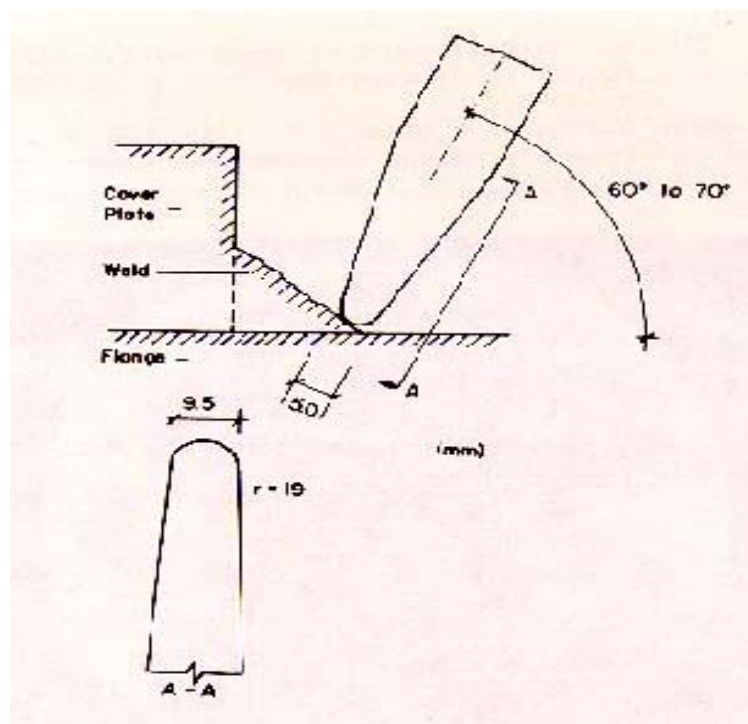


Figure 18: Schematic of peening tool applied to toe of transverse fillet weld

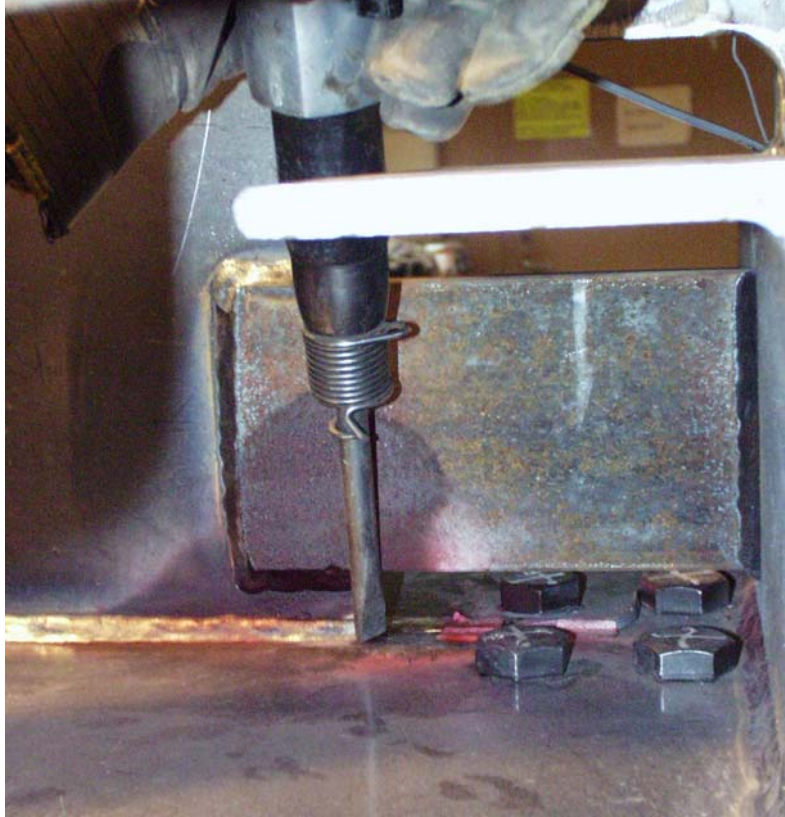


Figure 19: Photo of hammer peening operation



Figure 20: Hammer peened toe of a fillet weld

5.4 Detail Modifications

5.4.1 Detail Modifications can vary greatly between situations. General guidelines given here for typical modifications. See Appendix B for further guidance.

5.4.2 Doubler Plates

All doubler plate repair designs should be in accordance with ABS rules.

5.4.2.1 Bolted: Select plate dimensions to cover the crack plus clearance for bolts. Bolt spacing should be 75 mm with 40 mm edge distance. Position bolts at least 40 mm from crack edge. Select a plate thickness greater than or equal to the thickness of the cracked plate. Select bolt sizes based on strength requirements of the cracked section. See Figure 21.



Figure 21: Bolted doubler plate

5.4.2.2 Welded: Drill holes at crack tips in accordance with section 5.2. Select plate dimensions to cover the crack plus at least 50 mm edge distance on all sides of the crack. Weld to cracked plate using 8 mm fillet welds on all

sides. Weld in accordance with procedures in 5.1. Hammer peen the toes of these fillet welds for improved fatigue strength as per 5.3. See Figure 22.



Figure 22: Welded doubler plate

5.4.3 Radius Corners:

At the intersection of 90 degree inside corners, fatigue strength can be improved by welding on a rounded bracket. The bracket should not be thicker than the connected parts. The radius on the bracket must be at least 51 mm, and preferably at least 153 mm. Attach using full penetration groove welds.

5.5 Re-inspection

5.5.1 All repairs must be re-inspected and effectiveness re-evaluated on a regular basis.

APPENDIX B

DESIGN EXAMPLES

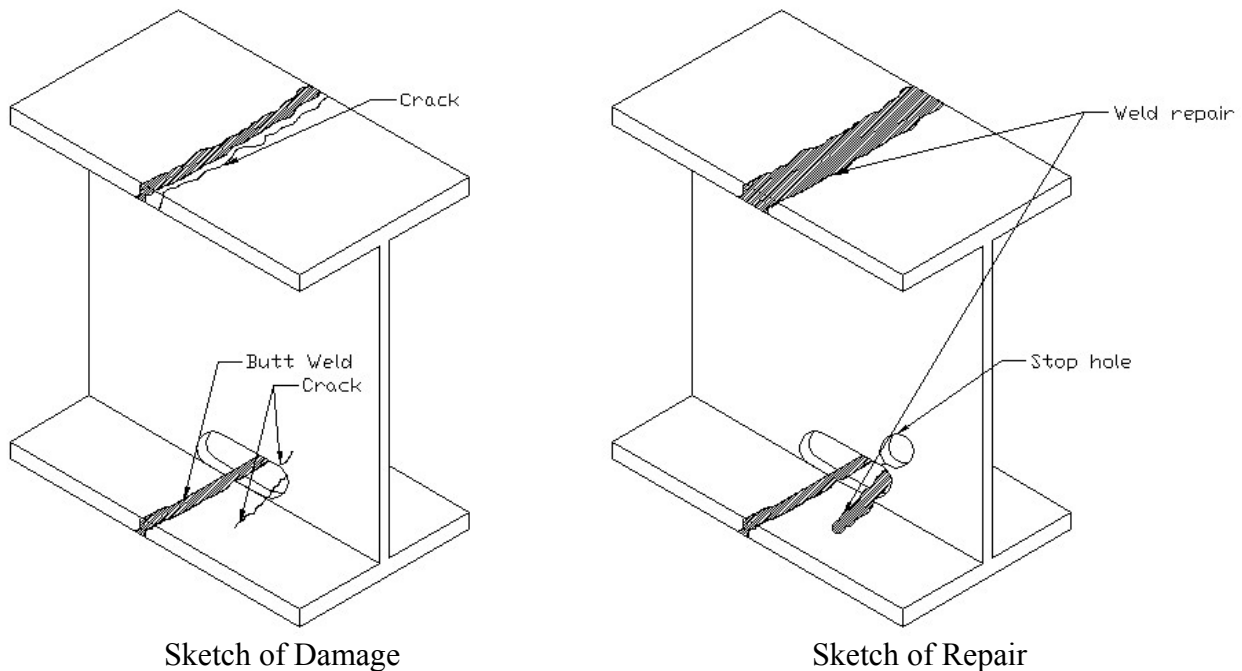
This appendix contains eight detailed examples of repair designs and procedures for typical cracks occurring in:

- A) Butt welds and weld access holes
- B) Fillet-welded attachments
- C) Bracket details
- D) Connections between longitudinal stiffeners and transverse web frames

These examples can be used along with procedures given in Appendix A to determine the optimum repair strategy for a given crack. The examples also include a simple method for calculating the expected life of the repair, to aid in inspection and maintenance scheduling.

Repair Design Example #1

Cracks at butt welds and weld access holes in longitudinal stiffeners and girders.



Repair:

1. Locate crack tips using dye penetrant testing. Mark 6 mm past the crack tips using a permanent marker or paint stick.
2. Clean the area around the crack, especially at tips, removing as much corrosion product as possible.
3. If the crack is less than 3 mm deep, hammer peen the crack along its length and 10 mm beyond each crack tip.
4. If the crack is greater than 3 mm deep, air-arc gouge out the entire crack using a 3 to 6 mm copper gouging rod and extending between the two marks from step 1.
5. Chip out slag and clean gouged area of debris.
6. Fill the vee-gouged area with stringer welds, using either the shielded metal arc welding (SMAW) or flux-core arc welding (FCAW) processes with a low hydrogen all position fill material.
7. For cracks in the web coming out of the access hole, drill a stop hole sized according to equation A-1.

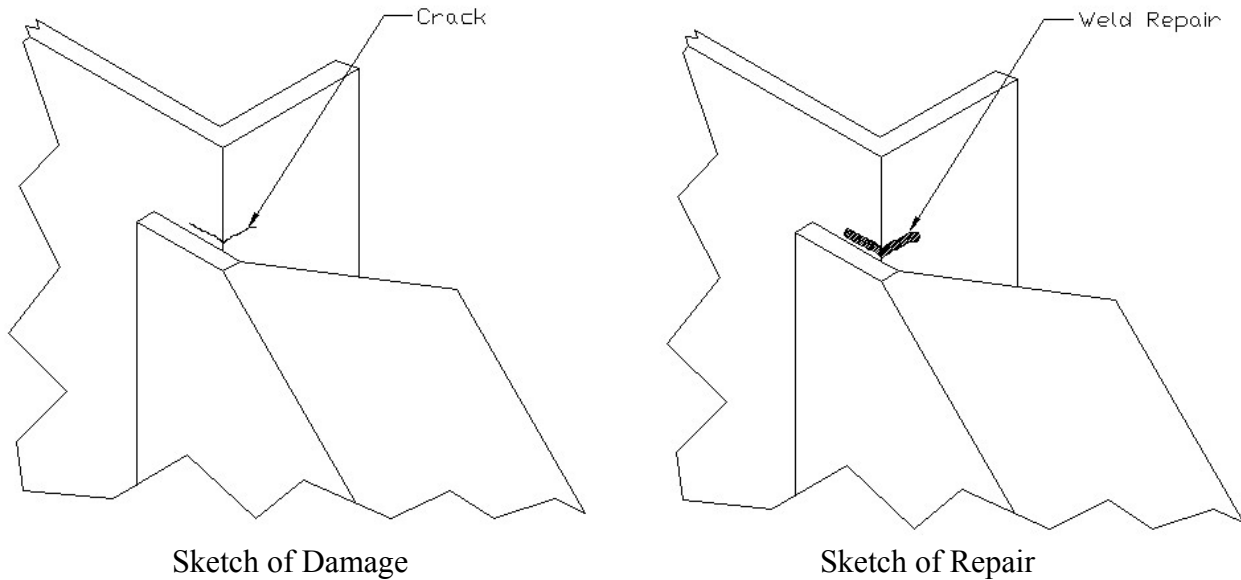
Residual life calculation:

1. The original detail can be considered Category D, regardless of the type of complete joint penetration weld detail. Access holes and drain holes are also Category D. A successful hammer peening repair can be considered Category C. The weld repaired detail can be considered Category D. The stop hole repair can be considered Category C.
2. Expected ratio of fatigue strength of repair to fatigue strength of original detail is:
 - a. Hammer peening repair: 2.0
 - b. Gouge and weld repair: 1.0
 - c. Stop hole repair in web: 2.0
3. Expected ratio of life of repaired detail to life of original detail is:
 - a. Hammer peening repair: 8.0
 - b. Gouge and weld repair: 1.0
 - c. Stop hole repair in web: 8.0

These repairs probably can be considered permanent.

Repair Design Example #2

Cracks initiate from the weld toe at the end of a bracket and propagated into girders and web frames. They are repaired before they reach through thickness.



Repair:

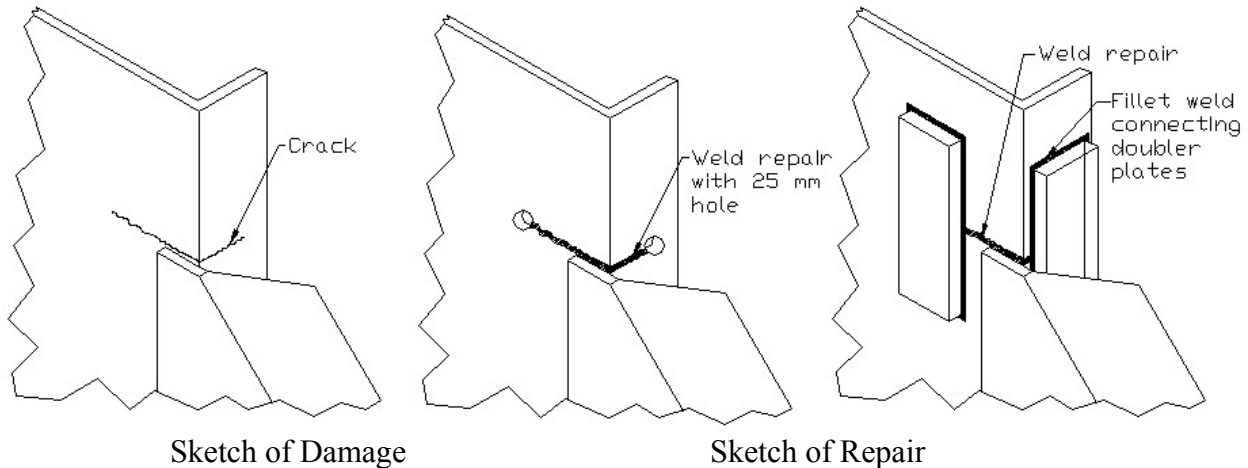
8. Locate crack tips using dye penetrant testing. Mark 6 mm past the crack tips using a permanent marker or paint stick.
9. Clean the area around the crack, especially at tips, removing as much corrosion product as possible.
10. Air-arc gouge out the entire crack using a 3 to 6 mm copper gouging rod and extending between the two marks from step 1.
11. Chip out slag and clean gouged area of debris.
12. Fill the vee-gouged area with stringer welds, using either the shielded metal arc welding (SMAW) or flux-core arc welding (FCAW) processes with a low hydrogen all position fill material.

Residual life calculation:

4. The original detail can be considered an AASHTO Category E'. The repaired detail can be considered lower than an AASHTO Category E'.
5. Expected ratio of fatigue strength of repair to fatigue strength of original detail is 0.661.
6. Expected ratio of life of repaired detail to life of original detail is $(0.661)^3 = 0.289$. This repair probably cannot be considered permanent.
7. This is the quickest repair to do and may prove to be cost effective.

Repair Design Example #3

Cracks occur at the weld toe connecting a bracket to a girder or web frame. The crack has propagated to a through-thickness crack that extends away from the bracket into the girder or web frame.



Repair:

1. Locate crack tips using dye penetrant testing. Mark about 6 mm past the crack tips using a steel punch.
2. Clean the area around the crack, especially at tips, removing as much corrosion product as possible.
3. Drill a 12 mm diameter hole centered on each punch mark.
4. On one side of the member air-arc gouge out the crack between the holes to $\frac{3}{4}$ of the thickness of cracked plate.
5. Chip out slag and clean gouged area of debris.
6. Fill the vee-gouged area and holes with stringer welds, using either the shielded metal arc welding (SMAW) or flux-core arc welding (FCAW) processes with a low hydrogen all position fill material.
7. Clean the other side of the cracked member as done in step 2.
8. On the cracked side of the member air-arc gouge out the crack and weld root to $\frac{1}{2}$ of the thickness of the cracked section.
9. Repeat steps 5 and 6 for this side of the repair.
10. Grind the last 50 to 80 mm of the weld at each end, on each side flush with the base metal.
11. Mark the ends of the welded area with a steel punch and drill 25 mm diameter holes at the marks.
12. Grind a notch for the bracket into one doubler plate of about the same thickness as the cracked section, and at least 75 mm wide by 225 mm tall. Make sure that the bracket

does not touch the plate when place on the flange of the girder or web frame over the weld repair termination hole.

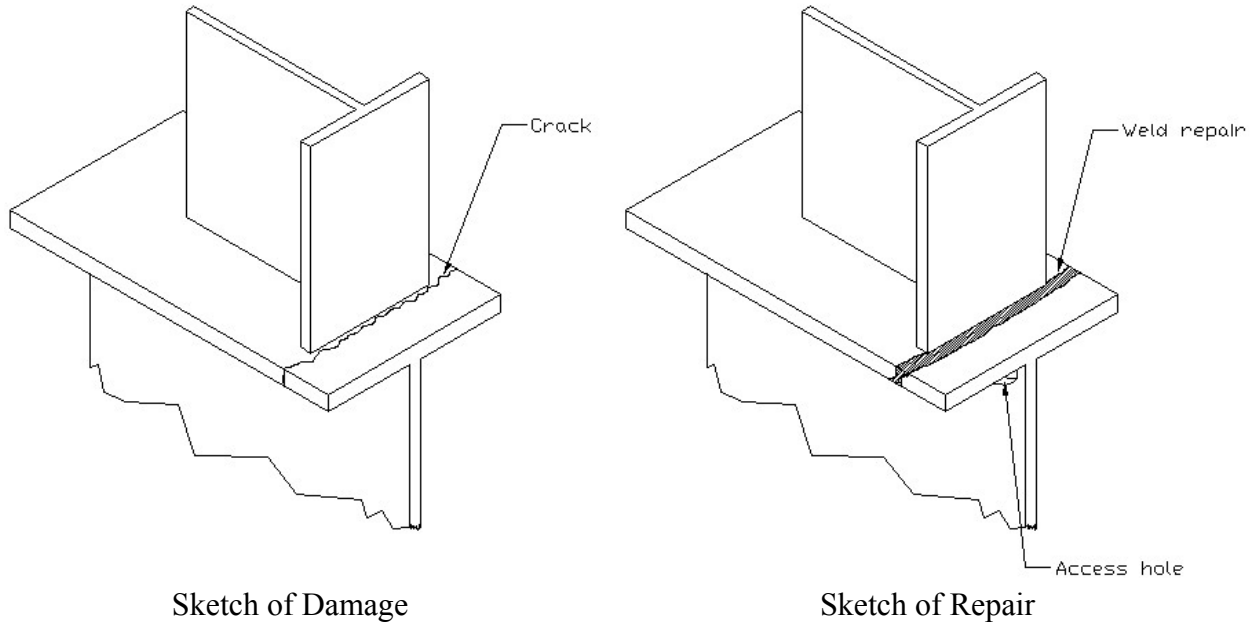
13. Weld the doubler plate to the flange using the same welding process as in step 6. The weld will run all of the way around the doubler except for half of one the long sides where the bracket is in the way.
14. Weld the second doubler plate to the web in the same manor, but weld all of the way around this one if possible.

Residual life calculation:

1. The original detail can be considered an AASHTO Category E'. Repaired detail can also be considered an AASHTO Category E'.
2. Expected ratio of fatigue strength of repair to fatigue strength of original detail is 0.997.
3. Expected ratio of life of repaired detail to life of original detail is $(0.997)^3 = 0.992$. This repair can probably be considered permanent.
4. These repairs never cracked so the life was cut short by other repairs failing. They can probably be considered to have at least equal life if not better due to the increase in cross-sectional area and the reduced stress at the critical area.

Repair Design Example #4

Cracks occur at the weld toe connecting an attachment to a girder or web frame. The crack has propagated to a through thickness crack that extends through the flange and into the web.



Repair:

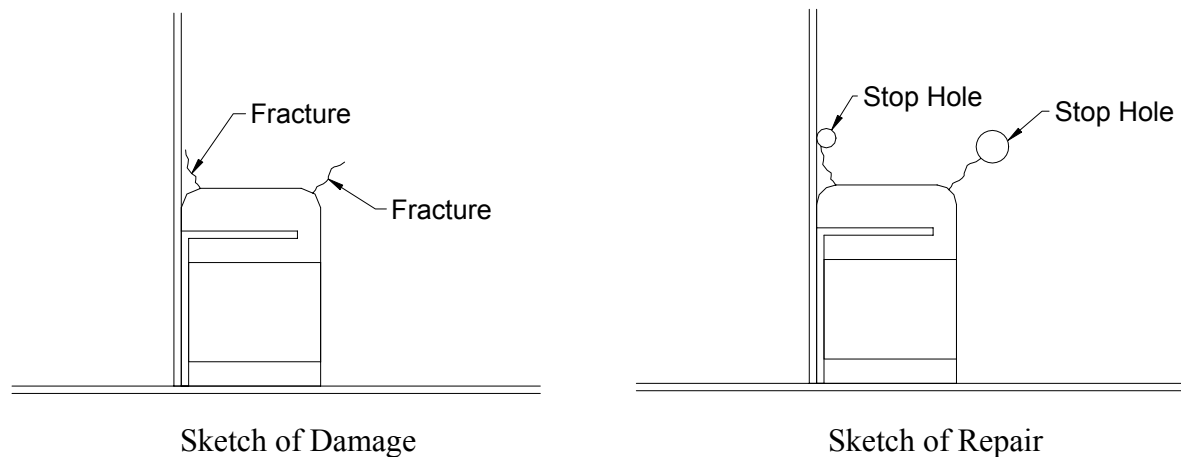
1. Locate crack tips using dye penetrant testing. Mark 6 mm past the crack tips using a permanent marker or paint stick.
2. Clean the area around the crack, especially at the tips, removing as much corrosion product as possible.
3. Mark 6 mm past the crack tip in web with a steel punch, and drill a 12 mm diameter hole at this mark.
4. Gouge out an adequate oval access hole using an air-arc gouger and hole at the crack tip as a start point.
5. Air-arc gouge out the crack on one side of the flange to $\frac{3}{4}$ of the flange thickness. The marks from step 1 mark to the start and stop points for gouging.
6. Chip out slag and clean vee-gouged area.
7. Fill the vee-gouged area with stringer welds, using either the shielded metal arc welding (SMAW) or flux-core arc welding (FCAW) processes with a low hydrogen all position weld material.
8. Air-arc gouge out the crack and weld toe from the other side of the flange to about $\frac{1}{2}$ of the flange thickness. Again using the marks from step 1 as boundaries.
9. Repeat steps 6 and 7 for this side of the crack.

Residual life calculation:

1. The original detail can be considered an AASHTO Category E detail, while the repair can be considered an AASHTO Category E' detail.
2. Expected ratio of fatigue strength of repair to fatigue strength of original detail is 1.05.
3. Expected ratio of life of repaired detail to life of original detail is $(1.05)^3 = 1.16$. This repair can probably be considered permanent.
4. This repair can be improved by hammer peening the repair, making the expected ratio of life 2.0. The life for the hammer peened repairs were all runouts in the test, so this should have a longer life yet and can probably be considered permanent.

Repair Design Example #5

Fractures in way of a cutout for the passage of a longitudinal through a transverse primary member. These may occur at connections to the inner or outer bottom or side shells.



Repair:

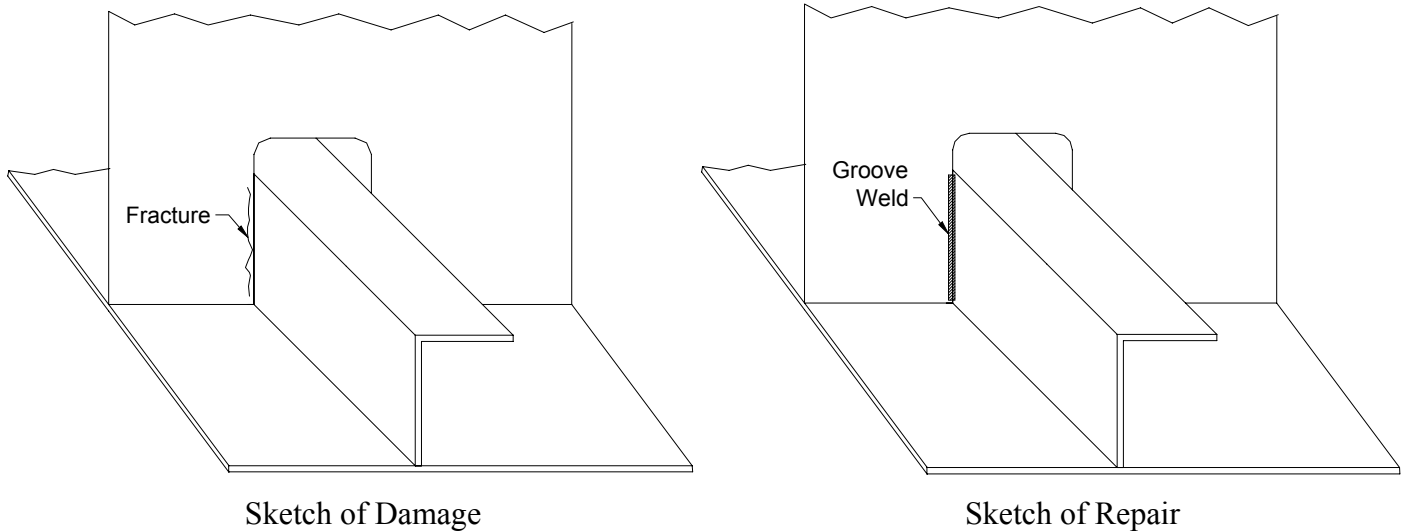
5. Locate crack tip using dye penetrant testing. Mark the crack tip using a steel punch.
6. Clean the area around the crack, especially at tip, removing as much corrosion product as possible.
7. Measure crack length and determine diameter of hole to drill using equation A-1.
8. Drill hole such that visible crack tip is located at the edge of the stop hole.

Residual life calculation:

9. Original detail can be considered BS 7608 Category F2. Repaired detail can be considered BS 7608 Category D.
10. Expected ratio of fatigue strength of repair to fatigue strength of original detail is 1.43.
11. Expected ratio of life of repaired detail to life of original detail is $(1.43)^3 = 2.92$. This repair can probably be considered permanent.

Repair Design Example #6

Fractures at the passage of a longitudinal through a transverse primary member. Fracture occurs at the root of the weld connecting the longitudinal to the transverse member. These may occur at connections to the inner or outer bottoms or side shells.



Repair:

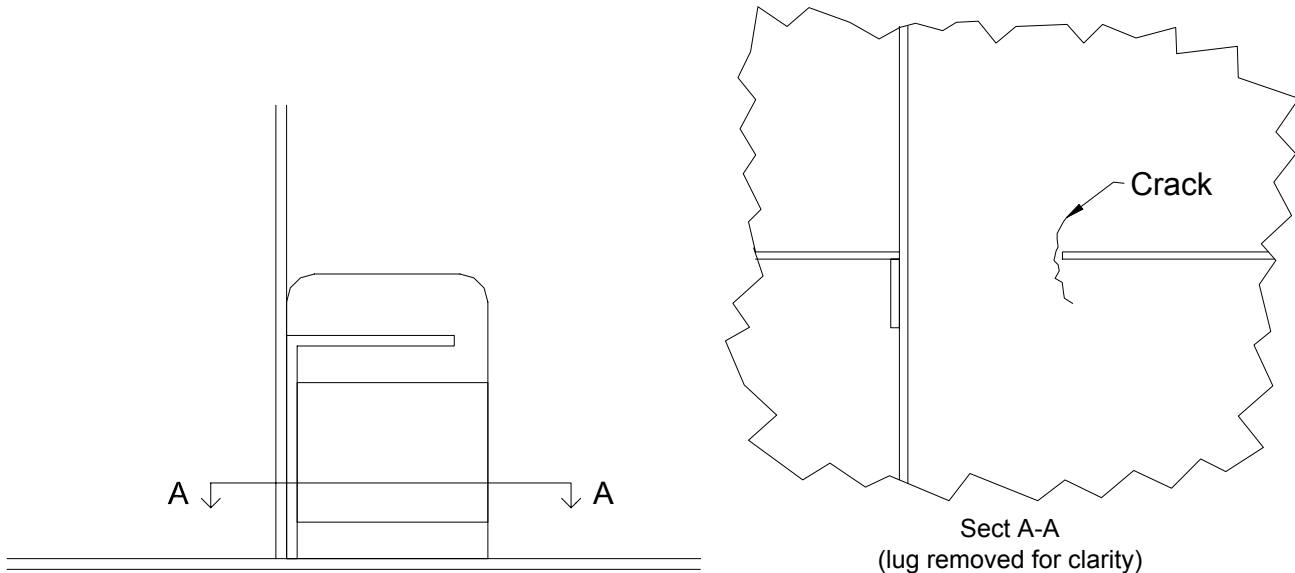
1. Locate entire length of crack using dye penetrant testing.
2. Clean the area around the crack removing as much corrosion product as possible.
3. Using an air arc-gouger, cut away the weld and base metal in the web frame along the entire length of the crack, and beyond each crack tip approximately 10 mm. Cut so that a vee-shaped edge preparation is achieved in the transverse member where it connects to the longitudinal. Clean out any slag with a chipping hammer.
4. Groove weld the transverse member to the longitudinal using SMAW or FCAW and low hydrogen, all-position fill material. Fill the edge preparation and add a few extra passes of fillet weld on top of the groove weld for reinforcement.
5. Hammer peen the toes of the repair weld in accordance with procedures given in 5.3.

Residual Life Calculation:

1. Original detail can be considered BS 7608 Category F2. Repaired detail can be considered BS 7608 Category D.
2. Expected ratio of fatigue strength of repair to fatigue strength of original detail is 1.43.
3. Expected ratio of life of repaired detail to life of original detail is $(1.43)^3 = 2.92$. This repair can probably be considered permanent.

Repair Design Example #7

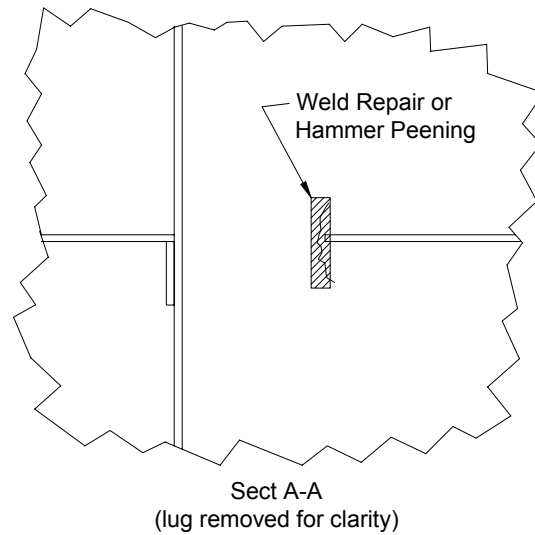
Fractures occurring in inner or outer bottom or sideshell at a cutout in a transverse web frame where a longitudinal passes through.



Sketch of Damage

Repair:

1. Clean the area around the crack, removing as much corrosion product as possible.
2. Locate the entire crack length using dye penetrant testing.
3. If the crack is not through-thickness and 3 mm deep or less, perform hammer peening along the entire length of the crack. Use at least four (4) passes.
4. For through-thickness cracks and partial thickness cracks deeper than 3 mm, perform a one-sided weld repair without a backing bar as described below.
 - a. Air arc-gouge a vee-shaped groove along the length of the crack and approximately 10 mm beyond each crack tip. The depth of the vee-shaped groove should be approximately 90 percent of the plate thickness.
 - b. Remove any slag with a chipping hammer.
 - c. Weld the gouged area using SMAW or FCAW with low hydrogen all position fill material. Use sufficient voltage to penetrate the last 10 percent of the plate thickness. Use enough passes to provide reinforcement above the plate surface.
 - d. Hammer peen the toes of the repair weld using at least four passes.



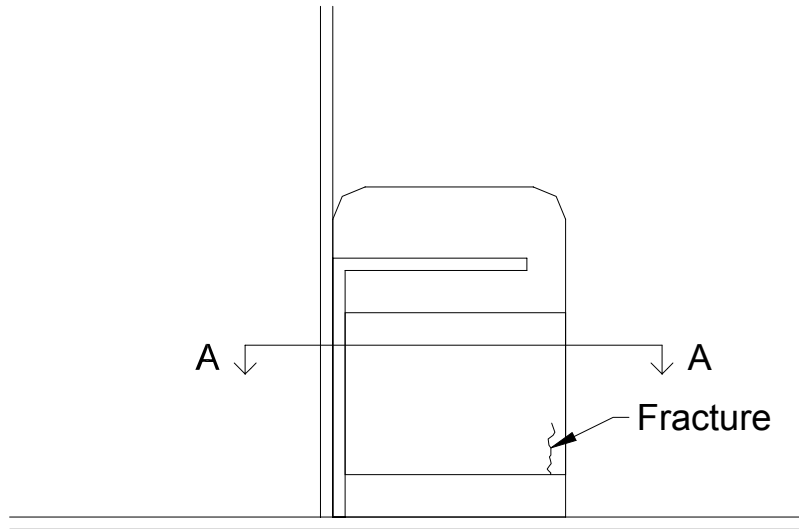
Sketch of Repair

Residual Life Calculation:

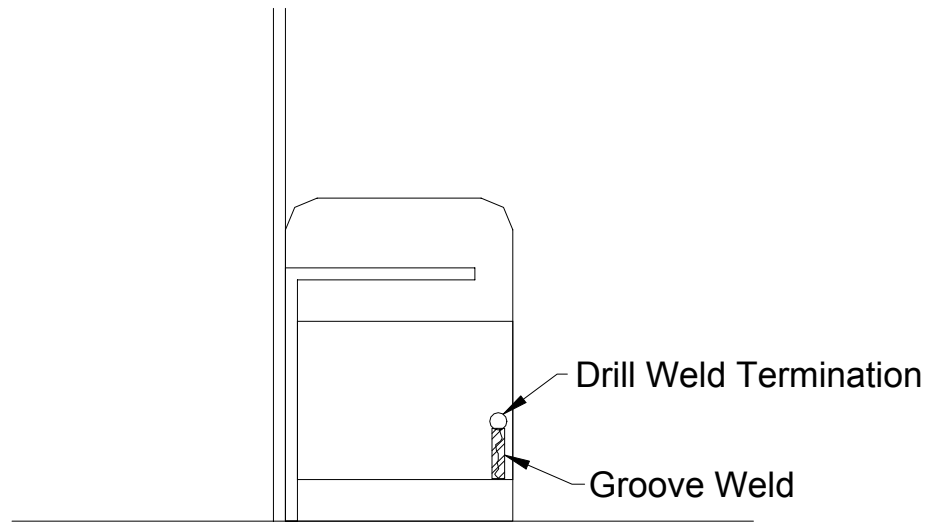
1. The original detail can be considered BS 7608 Category F2. For the surface crack, the hammer peening repair can be expected to be BS 7608 Category F. For the through-thickness crack, the one-sided weld repair without a backing bar and with hammer peening can be expected to be BS 7608 Category D.
2. The ratio of the fatigue strength of the repaired to original detail is 1.13 for hammer-peened surface cracks. For weld-repaired cracks with hammer peening, this ratio is 1.43.
3. For hammer-peened surface cracks, the ratio of the remaining life of the repaired vs. original detail is $(1.13)^3 = 1.44$. For weld-repaired cracks, this ratio is $(1.43)^3 = 2.92$. Both repairs, if executed properly, can be considered to be permanent.

Repair Design Example #8

Fracture in a lug plate at the connection between transverse web frames and longitudinals.



Sketch of Damage



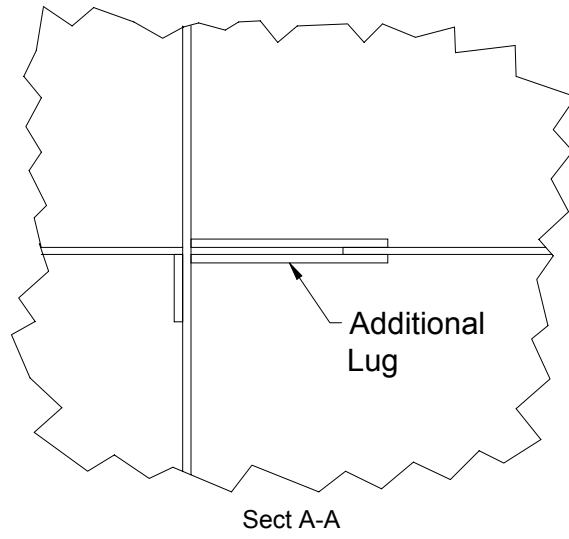
Sketch of Repair

Repair 1:

1. Clean the area around the crack, removing as much corrosion product as possible.
2. Locate the entire crack length using dye penetrant testing.
3. Repair using a two-sided weld repair as follows:
 - a. Air arc-gouge a vee-shaped groove along the length of the crack and approximately 10 mm beyond each crack tip. The depth of the vee-shaped groove should be approximately 75 percent of the plate thickness.
 - b. Remove any slag with a chipping hammer.
 - c. Weld the gouged area using SMAW or FCAW with low hydrogen all position fill material. Use enough passes to provide reinforcement above the plate surface.
 - d. Back-gouge a vee-shaped groove along the other side of the crack, penetrating deep enough to reach the first repair weld and completely remove the crack.
 - e. Weld this second groove in the same manner.
 - f. Grind the weld termination area smooth and drill a 19 mm diameter hole to remove weld termination defects.
 - g. Hammer peen the toes of the repair weld using at least four passes.
4. (Optional) The fatigue strength can be improved by modifying the detail and adding a second lug plate on the opposite side of the transverse web frame. This would cut the stress range at this location in half, thus giving an increase in life by a factor of eight compared to the original. The second lug should be fillet-welded to the web frame and groove welded to the longitudinal. (See below.)

Residual Life Calculation:

1. The original detail can be considered BS 7608 Category F2. The two-sided weld repair with hammer peening can be expected to be Category W. Adding a second lug restores the detail to Category F2, but cuts the stress range in half.
2. The ratio of the fatigue strength of the repaired to original detail is 0.57 for the weld repair alone. For the modified detail this ratio is 2.0.
3. The ratio of the remaining life of the repaired vs. original detail is $(0.57)^3 = 0.19$ for the weld repair plus hammer peening. This detail will likely need to be reinspected frequently if this repair strategy is used. If the detail is modified as described above, the ratio becomes $(2.0)^3 = 8.0$, and the repair can be considered permanent.



Sketch of Modified Detail

APPENDIX C

REFERENCES

1. Maddox, S.J., Fatigue Strength of Welded Structures, Second Edition, Abington Publishing, Cambridge, UK, 1991.
2. AASHTO, AASHTO LRFD Bridge Design Specifications, Second Edition, The American Association of State Highway and Transportation Officials, Washington, D.C., 1998.
3. American Institute of Steel Construction, Load and Resistance Factor Design Specification for Structural Steel Buildings, Third Edition, American Institute of Steel Construction (AISC), Chicago, 1999.
4. AREMA, AREMA Manual for Railway Engineering, Chapter 15: Steel Structures, American Railway Engineering Association, 2002.
5. AWS, Structural Welding Code – Steel, ANSI/AWS D1.1-02, American Welding Society, Miami, 2002.
6. BS 7608, Code of Practice for Fatigue Design and Assessment of Steel Structures, British Standards Institute, London, 1994.
7. ENV 1993-1-1, Eurocode 3: Design of Steel Structures – Part 1.1: General Rules and Rules for Buildings, European committee for Standardization (CEN), Brussels, April, 1992.
8. Petershagen, H., “Fatigue Problems in Ship Structures,” Advances in Marine Structures, Elsevier Applied Science, London, pp. 281-304, 1986.
9. Malakhoff, A., Packard, W.T., Engle, A.H., and Sielski, R.A., “Towards Rational Surface Ship Structural Design Criteria,” Advances in Marine Structures-2, C.S. Smith and R.S. Dow, (eds), Elsevier Applied Science, London, pp. 495-528, 1991.

10. Liu, D., and Thayamballi, A., "Local Cracking in Ships – Causes, Consequences, and Control," Proceedings: Workshop and Symposium on the Prevention of Fracture in Ship Structure, March 30-31, 1995, Washington, D.C., Marine Board, Committee on Marine Structures, National Research Council, 1996.
11. Jordan, C.R. and Krumpfen, R.P., Jr., Design Guide for Ship Structural Details, SSC-331, Ship Structure Committee, Washington D.C., 1985.
12. Antoniou, A.C., A Survey of Cracks in Tankers under Repair, PRADS-International Symposium on Practical Design in Shipbuilding, Tokyo, October 1977.
13. White, G.J. and Ayyub, B.M., "Reliability-Based Fatigue Design for Ship Structures," Naval Engineers Journal, pp. 135-149, May 1987.
14. Jordan, C.R. and Krumpfen, R.P., Jr., "Performance of Ship Structural Details," Welding Journal, pp. 18-28, January, 1984.
15. Clarke, J.D., "Fatigue Crack Initiation and Propagation in Warship Hulls," Advances in Marine Structures – 2, C.S. Smith and R.S. Dow, (eds), Elsevier Applied Science, London, pp. 42-60, 1991.
16. Rolfe, S.T., Hays, K.T., and Henn, A.E., "Fracture Mechanics Methodology for Fracture Control in VLCC's," Ship Structures Symposium '93, November 16-17, 1993, Arlington, VA, available from SNAME, Jersey City, NJ, 1993.
17. Radaj, D., Design and Analysis of Fatigue Resistant Welded Structures, Halsted Press, New York, 1990.
18. Dexter, R.J., and Pilarski, P.J., Effect of Welded Stiffeners on Fatigue Crack Growth Rate, SSC-413, Ship Structure Committee Report, Washington, D.C., 2000.

19. Dexter, R.J., and Pilarski, P.J., “Growth and Instability of Large Cracks in Redundant Structures,” Proceedings, 12th Engineering Mechanics Conference, ASCE, 17-20 May 1998, La Jolla, CA, ASCE, 1998.
20. Fisher, J.W., Frank, K.H., Hirt, M.A., and McNamee, B.M., Effect of Weldment on the Fatigue Strength of Steel Beams, National Cooperative Highway Research Program (NCHRP) Report 102, Highway Research Board, Washington, D.C., 1970.
21. Fisher, J.W., Albrecht, P.A., Yen, B.T., Klingerman, D.J., and McNamee, B.M., Fatigue Strength of Steel Beams with Welded Stiffeners and Attachments, National Cooperative Highway Research Program (NCHRP) Report 147, Transportation Research Board, Washington, D.C., 1974.
22. Petershagen, H., and Zwick, W., Fatigue Strength of Butt Welds Made by Different Welding Processes, IIW-Document XIII-1048-82, 1982.
23. Petershagen, H., “The Influence of Undercut on the Fatigue Strength of Welds – A Literature Survey,” Welding in the World, Vol. 28, No. 7/8, pp. 29-36, 1990.
24. Roberts, R. et al, Corrosion Fatigue of Bridge Steels, Vol. 1-3, Reports FHWA/RD-86/165, 166, and 167, Federal Highway Administration, Washington, D.C., May 1986.
25. Outt, J.M.M., Fisher, J.W., and Yen, B.T., Fatigue strength of weathered and deteriorated riveted members, Report DOT/OST/P-34/85/016, Department of Transportation, Federal Highway Administration, Washington D.C., October 1984.
26. Albrecht, P., and Shabshab, C., “Fatigue strength of weathered rolled beam made of A588 steel,” Journal of Materials in Civil Engineering, Vol 6, No. 3, pp. 407-428, 1994.

27. ABS, Guide for Fatigue Strength Assessment of Tankers, American Bureau of Shipping, New York, June 1992.
28. UK Health & Safety Executive (formerly the UK Department of Energy), Fatigue Design Guidance for Steel Welded Joints in Offshore Structures, H.M.S.O., London, 1984.
29. Haagensen, P. J., "Weld Improvement Methods for Increased Fatigue Strength," Proceedings International Conference Engineering Design in Welded Constructions, Madrid, Spain, September 1992, pp.73-92.
30. Tveiten, B.W. and Moan, T., "Determination of Structural Stress for Fatigue Assessment of Welded Aluminum Ship Details," Marine Structures, Vol 13, pp. 189-212, 2000.
31. Fisher, J. W., et. al., Development of Advanced Double Hull Concepts, Phase I.3a, Structural Failure Modes: Fatigue, Final Report for Cooperative Agreement N00014-91-CA-0001, Vol.3a, TDL 91-01, Lehigh University, Bethlehem, PA, March 1993.
32. Dexter, R.J., Tarquinio, J.E., and Fisher, J.W., "Application of Hot-Spot Stress Fatigue Analysis to Attachments on Flexible Plate," Proceedings of the 13th International conference on Offshore Mechanics and Arctic Engineering Conference (OMAE), 27 February-3 March 1994, Salama et al (eds.), ASME, Vol. III, Materials Engineering, pp. 85-92, 1994.
33. Fisher, J.W., et. al, Resistance of Welded Details Under Variable Amplitude Long-Life Fatigue Loading, National Cooperative Highway Research Program (NCHRP) Report 354, Transportation Research Board, Washington, D.C., 1993.
34. ABS, Rules for Building and Classing Steel Vessels, American Bureau of Shipping, Houston, 2001.
35. Chen, H.H., H.Y. Jan, J.F. Conlon, and D. Liu., "A New Approach for the Design and Evaluation of Double-Hull Tanker Structures," SNAME Annual Transactions, 1993.

36. Munse, W.H., et. al., Fatigue Characterization of Fabricated Ship Details for Design, SSC-318, Ship Structure Committee, Washington, D.C., 1982.
37. Kelly, B. A., and Dexter, R.J., “Fatigue Performance of Repair Welds” ATLSS Report No. 97-09, Final Report Submitted to Edison Welding Institute for Ship Structure Committee Project SR-1376, Lehigh University, Bethlehem, PA, 1997, also published as Adequacy of Weld Repairs for Ships, SSC-424, Ship Structure Committee, Washington, D.C., 2003.
38. Ship Maintenance Project: Phases II and III, Volume 2, Study of Fatigue of Proposed Critical Structural Details in Double Hull Tankers, SSC-395, Ship Structure Committee, Washington, D.C., 1997.
39. Ship Maintenance Project: Phase I, Volume 4, Design and Maintenance Procedures and Advancements in Tankship Internal Structural Inspections Techniques, Ship Structure Committee Report SSC-386, Washington, D.C., 1995.
40. ANSI/AWS D3.5-85, Guide for Steel Hull Welding, American Welding Society, Miami, 1985.
41. Guidance Manual for the Inspection and Condition Assessment of Tanker Structures, issued by: International Chamber of Shipping and Oil Companies International Marine Forum, on behalf of Tanker Structure Co-operative Forum, published by Witherby & Co. Ltd., London, England, 1986.
42. Condition Evaluation and Maintenance of Tanker Structures, Tanker Structure Co-operative Forum, published by Witherby & Co. Ltd., London, England, 1992.
43. Guidelines for the Inspection and Maintenance of Double Hull Tanker Structures, issued by: Tanker Structure Co-operative Forum, published by Witherby & Co. Ltd., London, England, 1995.

44. Kirkhope, K.J., Bell, R., Caron, L., and Basu, R.I., Weld Detail Fatigue Life Improvement Techniques, SSC-400, Ship Structure Committee, Washington, D.C., 1996.
45. Fisher, J.W., and Dexter, R.J., "Weld Improvement for Fatigue Life Extension," AWS/WIC International Conference on Fatigue, Toronto, 9-10 May, pp. 82-87, 1994.
46. Booth, G.S., "A Review of Fatigue Strength Improvement Techniques," Improving the Fatigue Performance of Welded Joints, Welding Institute, pp. 5-10.
47. Haagensen, P.J., "Effectiveness of Grinding and Peening Techniques for Fatigue Life Extension of Welded Joints," Proceedings of 12th International Conference on Offshore Mechanics and Arctic Engineering, OMAE 1993, Glasgow, Scotland, June 20-24, 1993.
48. Fisher, J.W., Hausammann, H., Sullivan, M.D., and Pense, A.W., Detection and Repair of Fatigue Damage in Welded Highway Bridges, National Cooperative Highway Research Program Report 206, Transportation Research Board, June 1979.
49. Graf, O., "Versuche uber das Verhalten von Genietten und Geschweissten Stossen in Tragern I30 ASW ST37 bei oftmals Wiederholter Belastung," Der Stahlbau, Berlin-Wilmersdorf, Germany, January 1977.
50. Yamada, K. And Albrecht, P., "Fatigue Behavior of Two Flange Details," Journal of the Structural Division, American Society of Civil Engineers, Vol. 103, No. ST4, April 1977.
51. Takamori, H., and Fisher, J.W., "Tests of Large Girders Treated to Enhance Fatigue Strength," Transportation Research Record 1696, Vol. 1, pp. 93-99, 2000.
52. Hausammann, H., Fisher, J.W., and Yen, B.T., "Effect of Peening on Fatigue Life of Welded Details," ASCE Proceedings, W. H. Munse Symposium on Behavior of Metal Structures - Research to Practice, 1983.

53. Braid, J., Bell, R., and Militaru, D., "Fatigue Life of As-Welded, Repaired, and Hammer-Peened Joints in High-Strength Structural Steel," Welding in the World, Vol. 39, No. 5, pp. 248-261, 1998.
54. Harrison, J.D., "Further Techniques for Improving the Fatigue Strength of Welded Joints," British Welding Journal, Volume 13, No. 11, 1966.
55. Roy, S., Fisher, J.W., and Yen, B.T., Fatigue Resistance of Welded Details Enhanced by Ultrasonic Impact Treatment (UIT), Proceedings, 11th International Society of Offshore and Polar Engineering Conference, Stavanger, Norway, 2001.
56. Trufyakov, V.I., et al., "Ultrasonic Impact Peening Treatment of Welds and its Effect on Fatigue Resistance in Air and Seawater," Proceedings, 25th Offshore Technology Conference, Houston, 1993.
57. Wylde, J.G., "The Fatigue Performance of Repaired Fillet Welds", The Welding Institute, Abington, Cambridge, England, May 1983.
58. Gregory, E.N., Slater, G., and Woodley, C.C., Welded Repair of Cracks in Steel Bridge Members, National Cooperative Highway Research Program Report 321, Transportation Research Board, October 1989.
59. Caramelli, S., Croce, P., Froli, M., and Sanpaolesi, L., "Repair Techniques for the Rehabilitation of Fatigue Cracked Orthotropic Steel Bridges," Proceedings IABSE Workshop: Evaluation of Existing Steel and Composite Bridges, Lausanne, pp. 161-169, 1997.
60. Dexter, R.J., et al., "Fatigue Strength and Adequacy of Fatigue Crack Repairs," Interim Report Project SR-1398, submitted to Ship Structure Committee, University of Minnesota, February 2001.

61. Fisher, J.W., Barthelemy, B.M., Mertz, D.R., and Edinger, J.A., Fatigue Behavior of Full Scale Welded Bridge Attachments, Transportation Research Board, NCHRP 227, 1980.
62. Fisher, J.W., and Mertz, D.R., “Hundreds of Bridges, Thousands of Cracks”, Civil Engineering, ASCE, Vol. 5, No. 4, 1985.
63. Sielski, R.A., and Dexter, R. J. et al., “Effectiveness of Doubler Plates as a Permanent Repair Under Cyclic Loads in a Highly Corrosive Environment,” Small Business Innovative Research Topic Number N01-057 Final Report, Palm Desert, CA, December 2001.
64. Sielski, R.A., “Design of Test Specimens for Fatigue Strength and Adequacy of Weld Repairs Project,” Interim Report Project SR-1398, submitted to Ship Structure Committee, Gibbs & Cox, Inc., September 2000.
65. Picture Repository, USAshipbuilding.com website, Pennsylvania State University, 2001.
66. Cheung, M.C., and Slaughter, S.B., “Innerbottom Design Problems in Double-Hull Tankers,” Marine Technology, SNAME, Vol. 35, No. 2, pp. 65-73, April 1998.
67. Bulk Carriers, Guidelines for Assessment and Repair of Hull Structure, Witherby & Co. Ltd, London, 1995.
68. Lotsberg, I, et al., “Full Scale Fatigue Testing of Side Longitudinals in FPSO’s,” Proceedings, 11th International Society of Offshore and Polar Engineering Conference, Stavanger, Norway, 2001.
69. Ulleland, T., and Svensson, M., et al., “Stress Concentration Factors in Side Shell Longitudinals Connected to Transverse Webframes,” Proceedings, 11th International Society of Offshore and Polar Engineering Conference, Stavanger, Norway, 2001.

70. Andersen, M.R., "Fatigue Crack Initiation and Growth in Ship Structures," PhD Dissertation, Technical University of Denmark, January 1998.
71. Kaczinski, M.R, et al, "Williamsburg Bridge Orthotropic Deck Fatigue Test," ATLSS Report No. 97-04, Lehigh University, December 1997.
72. Knight, J.W., "Improving the Fatigue Strength of Fillet Welded Joints by Grinding and Peening," Welding Research International, Vol. 8, No. 6, 1978.
73. Kelly, B. A., and Dexter, R.J., "Restored Fatigue Life with Repair Welds," The Proceeding of the Seventh (1997) International Offshore and Polar Engineering Conference, Volume IV, Honolulu, Hawaii, May 25-30, 1997, International Society of Offshore and Polar Engineers, Golden, Colorado, pp 572- 577.
74. Dexter, R.J., and Kelly, B. A., "Research on Repair and Improvement Methods", *International Conference on Performance of Dynamically Loaded Welded Structures*, Proceedings of the IIW 50th Annual Assembly Conference, San Francisco, California, July 13-19, 1997, Welding Research Council, Inc., New York, pp. 273-285.
75. Kober, R.J. Dexter, E.J. Kaufmann, B.T. Yen, and J.W. Fisher, "The Effect of Welding Discontinuities on the Variability of Fatigue Life", *Fracture Mechanics, Twenty-Fifth Volume*, ASTM STP 1220, F. Erdogan and Ronald J. Hartranft, Eds., American Society for Testing and Materials, Philadelphia 1994

SHIP STRUCTURE COMMITTEE PARTNERS AND LIAISON MEMBERS

PARTNERS

The Society of Naval Architects and Marine Engineers

Mr. Joe Cuneo
President,
Society of Naval Architects and Marine Engineers

Dr. John Daidola
Chairman,
SNAME Technical & Research Steering
Committee

The Gulf Coast Region Maritime Technology Center

Dr. John Crisp
Executive Director,
Gulf Coast Maritime Technology Center

Dr. Bill Vorus
Site Director,
Gulf Coast Maritime Technology Center

LIAISON MEMBERS

American Iron and Steel Institute
American Society for Testing & Materials
American Society of Naval Engineers
American Welding Society
Bethlehem Steel Corporation
Canada Center for Minerals & Energy Technology
Colorado School of Mines
Edison Welding Institute
International Maritime Organization
International Ship and Offshore Structure Congress
INTERTANKO
Massachusetts Institute of Technology
Memorial University of Newfoundland
National Cargo Bureau
Office of Naval Research
Oil Companies International Maritime Forum
Tanker Structure Cooperative Forum
Technical University of Nova Scotia
United States Coast Guard Academy
United States Merchant Marine Academy
United States Naval Academy
University of British Columbia
University of California Berkeley
University of Houston - Composites Eng & Appl.
University of Maryland
University of Michigan
University of Waterloo
Virginia Polytechnic and State Institute
Webb Institute
Welding Research Council
Worcester Polytechnic Institute
World Maritime Consulting, INC

Mr. Alexander Wilson
Captain Charles Piersall (Ret.)
Captain Dennis K. Kruse (USN Ret.)
Mr. Richard Frank
Dr. Harold Reemsnyder
Dr. William R. Tyson
Dr. Stephen Liu
Mr. Dave Edmonds
Mr. Tom Allen
Dr. Alaa Mansour
Mr. Dragos Rauta
Mr. Dave Burke / Captain Chip McCord
Dr. M. R. Haddara
Captain Jim McNamara
Dr. Yapa Rajapaksie
Mr. Phillip Murphy
Mr. Rong Huang
Dr. C. Hsiung
Commander Kurt Colella
Dr. C. B. Kim
Dr. Ramswar Bhattacharyya
Dr. S. Calisal
Dr. Robert Bea
Dr. Jerry Williams
Dr. Bilal Ayyub
Dr. Michael Bernitsas
Dr. J. Roorda
Dr. Alan Brown
Dr. Kirsi Tikka
Dr. Martin Prager
Dr. Nick Dembsey
VADM Gene Henn, USCG Ret.

RECENT SHIP STRUCTURE COMMITTEE PUBLICATIONS

Ship Structure Committee Publications on the Web - All reports from SSC 392 and forward are available to be downloaded from the Ship Structure Committee Web Site at URL:

<http://www.shipstructure.org>

SSC 391 and below are available on the SSC CD-ROM Library. Visit the National Technical Information Service (NTIS) Web Site for ordering information at URL:

<http://www.ntis.gov/fcpc/cpn7833.htm>

SSC Report Number	Report Bibliography
SSC 424	<u>Evaluation of Accidental Oil Spills from Bunker Tanks (Phase I)</u> T. McAllister, C. Rekart, K. Michel 2003
SSC 423	<u>Green Water Loading on Ship Deck Structures</u> M. Meinhold, D. Liut, K. Weems, T. Treakle, Woe-Min Lin 2003
SSC 422	<u>Modeling Structural Damage in Ship Collisions</u> Dr. A.J. Brown 2003
SSC 421	<u>Risk Informed Inspection of Marine Vessels</u> Dr. B.M. Ayyub, U.O. Akpan, P.A. Rushton, T.S. Koko, J. Ross, J. Lua 2003
SSC 420	<u>Failure Definition for Structural Reliability Assessment</u> Dr. B. M. Ayyub, P.E. Hess III, D.E. Knight 2002
SSC 419	<u>Supplemental Commercial Design Guidance for Fatigue</u> R.A. Sielski, J. R. Wilkins, J.A. Hultz 2001
SSC 418	<u>Compensation for Openings in Primary Ship Structure</u> J.J. Hopkinson, M. Gupta, P. Sefcsik 2002
SSC 417	<u>Prediction of Structural Response in Grounding Application to Structural Design</u> K.K. Tikka 2001
SSC 416	<u>Risk Based Life Cycle Management of Ship Structure</u> Dr. B.M. Ayyub, U.O. Akpan, G. F. DeSouza, T. S. Koko, X. Luo 2001
SSC 415	<u>Crack Arrest Toughness of Steel Weldments</u> Dr. L.N. Pussegoda, Dr. L. Malik, B.A. Graville, Y. Han, and Dr. S. J. Kennedy, 2000
SSC 414	<u>Probability Based Design (Phase 4) Synthesis of the Reliability Thrust Area</u> P.A. Frieze 2000
SSC-413	<u>Effect of Welded Stiffeners on Crack Growth Rate</u> R. J. Dexter, P. J. Pilarski 2000
SSC 412	<u>Interactive Nature of Cathodic Polarization and Fatigue</u> C. Jaske 2000